T.C.
MANİSA CELAL BAYAR ÜNİVERSİTESİ
LİSANSÜSTÜ EĞİTİM ENSTİTÜSÜ



YÜKSEK LİSANS TEZİ
BİYOMÜHENDİSLİK ANABİLİM DALI
TEZLİ YÜKSEK LİSANS PROGRAMI

ASSESSMENT OF PRIME EDITING IN GRAPEVINE PROTOPLASTS

Ad SOYAD
Gülşen KOLAŞİNLİLER

Danışman
Dr. Öğr. Üyesi Hilal Betül KAYA AKKALE

MANİSA–2024

TAAHHÜTNAME

Bu tezin Manisa Celal Bayar Üniversitesi Lisansüstü Eğitim Enstitüsü Biyomühendislik Ana Bilim Dalında akademik ve etik kurallara uygun olarak yazıldığını ve kullanılan tüm literatür bilgilerinin referans gösterilerek tezde yer aldığını, tamamen kendi çalışmam olduğunu, her alıntıya kaynak gösterdiğimi, tezin yazımında akademik ve etik kurallara aykırı herhangi bir yapay zeka ve program kullanmadığımı beyan ederim.

Gülşen KOLAŞİNLİLER

ÖZET

Yüksek Lisans Tezi

Gülşen KOLAŞİNLİLER
Manisa Celal Bayar Üniversitesi
Lisansüstü Eğitim Enstitüsü
Biyomühendislik Anabilim Dalı

Danışman: Dr. Öğr. Üyesi Hilal Betül KAYA AKKALE

İkinci Danışman: Dr. Cengiz AKKALE

Asma hem ülkemiz hem de dünyada çok geniş bir alanda yetiştiriciliği yapılan kültürel ve ekonomik açıdan en önemli bitkilerden bir tanesidir. Asma yetiştiriciliğinde *Uncinula necator* mantarı sebep olduğu külleme hastalığı nedeni ile ciddi verim kaybına ve ekonomik zarara yol açmaktadır. Artan dünya nüfusu ve iklim değişikliğine bağlı olarak, geleneksel bitki ıslahı yöntemlerinin, insan beslenmesi için gereken tarımsal ürünlerin yetiştirilmesinde yetersiz kalacağı öngörülmektedir. Bu sebeple klasik ıslah tekniklerine alternatif olarak transgen içermeyen ve nükleazları kullanarak genomda hedeflenen değişiklikleri yapabilen CRISPR gibi genom düzenleme araçlarının kullanılmasının tarımsal üretimde önemi artmaktadır. CRISPR-Cas9 sisteminin yeni bir adaptasyonu olan prime düzenleme ve bu tekniğin bitkilerde daha başarılı sonuç vermesini sağlayan dual-epegRNA yaklaşımı ile bitkilerde genom düzenleme çalışmaları hızlı bir şekilde ilerlemektedir. Bitkilerde genom düzenleme çalışmalarının en uzun süren ve maliyetli basamağı bitki doku kültürü uygulamalarıdır. Bu nedenle, genom düzenleme bileşenlerinin bitki protoplastlarında test edilmesi ve doğrulanması büyük önem taşımaktadır.

Bu tez çalışmasında, külleme hastalığına dayanıklılık ile ilişkili *pLL3* ve *pLL13,* pektat liyaz benzeri genler, ile *PDS* geni hedef alınarak prime düzenleme ve dual-epegRNA yaklaşımı kullanılarak elde edilen DNA konstrüktleri Chardonnay protoplastlarında test edilmiş ve düzenleme verimlilikleri karşılaştırılmıştır.

Tez çalışması kapsamında, Chardonnay yapraklarından optimize edilmiş protoplast izolasyon protokolü ile en yüksek $75x10^6$/g yaprak protoplast verimi elde edilmiş, protoplast canlılığı ise %91 olarak belirlenmiştir. Optimizasyonu gerçekleştirilen PEG aracılı protoplast transformasyon metodu kullanılarak, GK plazmidleri için ortalama transformasyon verimliliği %20,25-%27,79 aralığında elde edilmiştir. Transformasyon sonrasında, protoplast DNA'ları amplikon sekanslama ile analiz edilmiş ve çalışma kapsamında elde edilen konstrüktlerin genom düzenleme verimliliği %0.16-%0.76 aralığında bulunmuştur. Kullanılan genom düzenleme tekniğinin asma protoplastlarında başarılı bir şekilde çalıştığı ve hedef mutasyonları gerçekleştirebildiği doğrulanmıştır. Çalışma kapsamında optimize edilen protoplast izolasyonu ve transformasyonu protokollerinin, bu alanda çalışan araştırmacılar için önemli bir kaynak olabileceği düşünülmektedir.

Anahtar Kelimeler: Asma (*V. vinifera* L.), Chardonnay, *pLL* genleri, prime düzenleme, dual-epeg, protoplast izolasyonu, geçici gen ekspresyonu

2024, 90 sayfa

ABSTRACT

M.Sc. Thesis

Gülşen KOLAŞİNLİLER
Manisa Celal Bayar University
Graduate School of Education
Department of Bioengineering

Supervisor: Assist. Prof. Dr. Hilal Betül KAYA AKKALE

Co-Supervisor: Dr. Cengiz AKKALE

Grapevine is one of the most culturally and economically significant plants cultivated over a vast area both in our country and around the world. In grapevine cultivation, the powdery mildew disease caused by the fungus *Uncinula necator* leads to significant yield loss and economic damage. With the increasing world population and climate change, it is predicted that traditional plant breeding methods will be insufficient for growing agricultural products needed for human nutrition. Therefore, the use of genome editing tools like CRISPR, which can make targeted changes in the genome using nucleases without incorporating transgenes, is becoming increasingly important in agricultural production as an alternative to classical breeding techniques. Genome editing studies in plants are progressing rapidly with prime editing, a new adaptation of the CRISPR-Cas9 system, and the dual-epegRNA approach, which allows for more successful results in plants. The longest and most expensive step in genome editing studies in plants is plant tissue culture applications. Therefore, testing and verifying genome editing components in plant protoplasts is of great importance.

In this thesis, DNA constructs obtained using prime editing and the dual-epegRNA approach, targeting *pLL3* and *pLL13*, pectate lyase-like genes, and the PDS gene related to resistance to powdery mildew disease, were tested in Chardonnay protoplasts, and their editing efficiencies were compared.

Within the scope of the thesis, the highest protoplast yield of $75x10^6$/g leaf was obtained using the optimized protoplast isolation protocol from Chardonnay leaves, and protoplast viability was determined to be 91%. Using the optimized PEG-mediated protoplast transformation method, the average transformation efficiency for prime editing constructs was obtained in the range of 20.25%-27.79%. After transformation, protoplast DNAs were analyzed by amplicon sequencing, and the genome editing efficiencies of the constructs obtained within the scope of the study were found to be in the range of 0.16-0.76%. It was confirmed that the genome editing technique used worked successfully in grapevine protoplasts and could achieve the target mutations. The protoplast isolation and transformation protocols optimized within the scope of the study are considered to be an important resource for researchers working in this field.

Keywords: Chardonnay, grapevine (*V. vinifera* L.), *pLL* genes, prime editing, dual-epeg, protoplast isolation, transient gene expression.

2024, 90 pages

ÖNSÖZ VE TEŞEKKÜR

Bu tez, Literatür araştırmaları, Giriş, Gereç ve Yöntem, Bulgular ve Tartışma, Sonuç ve Öneriler olmak üzere 4 ana bölümden oluşmaktadır. Bu çalışma kapsamında, protoplast izolasyonu ve protoplast transformasyonu protokolleri Chardonnay Asma çeşidi için optimize edilerek diğer bitki türlerinde de uygulanabilmesi için farklı bakış açıları sağlayabilmektedir.

Tezin özgünlüğü, genom düzenleme çalışmalarında yaygın olarak kullanılan CRISPR teknolojisinin yeni ve umut vaat eden bir versiyonu olan Prime Düzenlemenin ilk kez asma protoplastlarında uygulanmış ve değerlendirilmiş olmasıdır. Bu tez doğrultusunda elde edilen sonuçlar literatürde genom düzenleme çalışmalarına ışık tutacak potansiyeldedir.

Yoğun emek, moral ve motivasyon gerektiren bu çalışma serüvenim boyunca benden desteklerini hiçbir zaman esirgemeyen, karşılaştığım her zorlukta bana rehberlik eden çok değerli danışman hocalarım Dr. Öğr. Üyesi Hilal Betül KAYA AKKALE ve Dr. Cengiz AKKALE' ye gönülden teşekkürlerimi sunarım.

Çok kıymetli yorumları ile tezimin değerlendirilmesinde katkı sağlayan ve değerli tavsiyeleriyle yol gösterici olan tez savunma jürilerim Doç. Dr. Tuğba KESKİN GÜNDOĞDU ve Dr. Öğr. Üyesi Tülay ÖNCÜ ÖNER'e teşekkürlerimi sunarım.

3501 numaralı program, 122O004 numaralı proje kapsamında destek veren ve bana burs imkanı sağlayan TÜBİTAK'a bizzat teşekkür ederim. Bu proje çerçevesinde ayrıca danışmanlık eden ve çok değerli katkılarıyla gelişmemde rol oynayan Cornell Üniversitesi'nde görevli Prof. Dr. Adam Bogdanove ve Dr. Lance Cadle-Davidson'a teşekkürü borç bilirim.

Tez materyallerinin sağlanmasında katkı sağlayan Kavaklıdere Şarapçılık A.Ş ve Manisa Bağcılık Araştırma Enstitüsü'ne, çalışmaların gerçekleştirildiği ve gerekli imkanların sağlandığı Manisa Celal Bayar Üniversitesi Biyomühendislik Bölümü'ne ve tüm değerli bölüm hocalarıma teşekkür ederim.

Manevi destekleriyle her zaman yanımda olan, bana cesaret veren sevgili Moleküler Genetik Laboratuvarı arkadaşlarıma çok teşekkür ederim.

Maddi ve manevi desteklerini hiçbir zaman esirgemeyen ve bana her zaman güvenen canım ailem size sonsuz teşekkür ederim.

Son olarak, "Vatanını en çok seven görevini en iyi yapandır" sözü başta olmak üzere sayısız birçok sözüyle hayatıma ışık tutan, bana pes etmemeyi ve her zorluğun üstesinden gelebileceğimi öğreten Ulu Önderimiz Gazi Mustafa Kemal Atatürk'e saygı, sevgi ve minnetle.

Gülşen KOLAŞİNLİLER
Manisa, 2024

ABBREVIATIONS

aa. Amino acid

BSA. Bovine Serum Albumin

Cas9. CRISPR Associated Protein 9

CRISPR. Clustered regularly interspaced short palindromic repeats

ddH_2O. double distilled water

DNA. Deoxyribonucleic acid

epeg-RNA. Engineered prime editing guide RNA

FDA. Fluorescein Diacetate

FW. Fresh weight

GFP. Green Fluorescent Protein

HDR. Homology Directed Repair

NHEJ. Non- Homologous End Joining

PAM. Protospacer Adjacent Motif

PBS. Primer Binding Site

PDS. Phytoene Desaturase

PCR. Polymerase Chain Reaction

PE. Prime Editing

PEG. Polyethylene glycol

peg-RNA. Prime editing guide RNA

pLL genes. pectate lyase-like genes

R genes. Resistance genes

RNA. Ribonucleic acid

RNP. Ribonucleoprotein

RT. Reverse transcriptase6

S genes Susceptible genes

sgRNA. Single guide RNA

UV. Ultraviolet

TABLE OF FIGURES

Figure 1. Grape producing countries in the world and grape production amount (FAOSTAT, 2021) 2
Figure 2. Top 10 grape producing countries in the world (FAOSTAT, 2024) 2
Figure 3. Symptoms of powdery mildew on grapevine leaves and fruit (Source: https://agric.wa.gov.au/n/2449) 4
Figure 4. The CRISPR-Cas9 mechanism (Ren et al., 2022). 8
Figure 5. General workflow diagram of the CRISPR-Cas9 application (Biorender). 8
Figure 6. Prime editing mechanism (Kaya, 2024). 14
Figure 7. pegRNA and epegRNA (Nelson et al., 2022) 15
Figure 8. Dual-pegRNA approach (Lin et al., 2021) 16
Figure 9. Multiple alignment result, brown; Ca+2 binding site, blue; substrate binding site, green; catalysis, pink; disulfide binding site 25
Figure 10. Designing of dual-pegRNAs for the R218K mutation in the PLL3 gene 26
Figure 11. Parameters which were used in the designing of dual-pegRNAs for the R218K target mutation in the PLL3 gene. 27
Figure 12. Dual-pegRNA sequences obtained by using of PlantPegDesigner web application for target genes. 27
Figure 13. Obtainment of linker sequence for R218K target mutation in PLL3 gene by pegLIT application 28
Figure 14. Schematic representation of the designed dual-epegRNA 29
Figure 15. Dual-epegRNA sequence designed for the PLL3-D131A target gene. ... 29
Figure 16. Dual-epegRNA sequence designed for the PLL13-D131A target gene. . 30
Figure 17. Dual-epegRNA sequence designed for the PLL3-R218K target gene. ... 30
Figure 18. Dual-epegRNA sequence designed for the PLL13-R218K target gene. . 30
Figure 19. Dual-epegRNA sequence designed for the PDS1 target gene. 31
Figure 20. Detailed gene map of pLW14 (PLL3_R218K) plasmid 33
Figure 21. Detailed gene map of pLW15 (PLL13_R218K) plasmid 34
Figure 22. Detailed gene map of pLW16 (PLL3_D131A) plasmid 34
Figure 23. Detailed gene map of pLW17 (PLL13_D131A) plasmid 35
Figure 24. Detailed gene map of pLW18 (PDS1) plasmid 35
Figure 25. Liquid culture of modular plasmids which is integrated into E. coli in the shaker for over-night incubation. 37
Figure 26. Schematic representation of the strategy applied to obtain the final constructs (Cermak et al., 2017). 39
Figure 27. Obtained single colonies of GKs plasmids after E. coli transformation. . 40
Figure 28. Plasmid map of GK1 41
Figure 29. Plasmid map of GK2 41
Figure 30. Plasmid map of GK3 42
Figure 31. Plasmid map of GK4 42
Figure 32. Plasmid map of GK5 43
Figure 33. Large-scale liquid cultures of GK samples in 100 mL 43
Figure 34. Planting of Chardonnay cultivars 45
Figure 35. Chardonnay cultivars in a growth chamber 46
Figure 36. Leaf samples used for protoplast isolation (*: young leaves which are used in the optimized protoplast isolation protocol. *: mature leaf tissue). 48
Figure 37. Different cutting styles of leaves which are performed in this study. a) random cutting style, b) tape-sandwich method, and c) strip cutting (petiole part is indicated by red color). 49

Figure 38. Workflow of optimized protoplast isolation protocol..... 50
Figure 39. Workflow of applied protoplast transformation protocol (Biorender) 53
Figure 40. Virtual digest of GK plasmids by SacI enzyme..... 59
Figure 41. 1% agarose gel images of GK plasmids in terms of restriction digestion60
Figure 42. Effects of leaf amount of grapevine on protoplast isolation a) Protoplasts obtained with 20 mg of young leaves b) Protoplasts obtained with 40 mg of young leaves..... 62
Figure 43. Imaging of protoplasts under the bright- field microscope by the implementation of different cutting styles. a) microscopic imaging of protoplast by application of random cutting, b) microscopic imaging of protoplast by application of tape-sandwich method, c) microscopic imaging of protoplast by application of strip cutting..... 63
Figure 44. Comparison of protoplast yield depend on a) pretreatment, and b) different digestion time..... 66
Figure 45. Visualization of obtained protoplasts under the inverted bright field microscope after different digestion time a) after 4 hours, b) after 8 hours, c) 16 hours, and d) after 20 hours. 67
Figure 46. Phase separation after sucrose cushion method..... 68
Figure 47. Images of protoplasts in different areas under the inverted bright field microscope 69
Figure 48. Imaging of viable protoplasts under the bright field and Fluorescence microscope 70
Figure 49. Microscopic imaging of transformed protoplasts under the bright field and fluorescence microscope a) $2.5x10^5$ protoplast number, b) $5x10^5$ protoplast number, c) $1x10^6$ protoplast number, d) $2x10^6$ protoplast number..... 72
Figure 50. Comparison of transformation efficiency depend on a) protoplast number, and b) PEG incubation time..... 73
Figure 51. Microscopic images of transformed protoplasts with GK1 plasmids under the bright field and fluorescence microscope a) images from first replication, b) images from second replication, c) images from third replication..... 76
Figure 52. Microscopic images of transformed protoplasts with GK2 plasmids under the bright field and fluorescence microscope a) images from first replication, b) images from second replication, c) images from third replication..... 77
Figure 53. Microscopic images of transformed protoplasts with GK3 plasmids under the bright field and fluorescence microscope a) images from first replication, b) images from second replication, c) images from third replication..... 78
Figure 54. Microscopic images of transformed protoplasts with GK4 plasmids under the bright field and fluorescence microscope a) images from first replication, b) images from second replication, c) images from third replication..... 79
Figure 55. Microscopic images of transformed protoplasts with GK5 plasmids under the bright field and fluorescence microscope a) images from first replication, b) images from second replication, c) images from third replication..... 80
Figure 56. Microscopic images of transformed protoplasts a) (+) control, b) (-) control 80
Figure 57. Obtained gel image of protoplast GK samples as a result of PCR. 81
Figure 58. Obtained gel image of protoplast samples as a result of PCR with pMODC-3001 and non-transformed. 81
Figure 59. Amplicon sequencing results of GK1 construct. a) first replication of GK1, b) second replication of GK1, c) third replication of GK1, d) (-) control of GK1 82

Figure 60. Amplicon sequencing results of GK2 construct. a) first replication of GK2, b) second replication of GK2, c) third replication of GK2, d) (-) control of GK2 83
Figure 61. Amplicon sequencing results of GK3 construct. a) first replication of GK3, b) second replication of GK3, c) third replication of GK3, d) (-) control of GK3 84
Figure 62. Amplicon sequencing results of GK4 construct. a) first replication of GK4, b) second replication of GK4, c) third replication of GK4, d) (-) control of GK4 85
Figure 63. Amplicon sequencing results of GK5 construct. a) first replication of GK5, b) second replication of GK5, c) third replication of GK5, d) (-) control of GK4 86

TABLE INDEXES

Table 1. Application of CRISPR-Cas9 mediated genome editing in plants 9
Table 2. Application of CRISPR-Cas9 mediated genom editing in grapevine 11
Table 3. Target genes and their ID numbers in databases 24
Table 4. Target gene and target mutation which were caused by desired editing. 25
Table 5. Linker sequences obtained in the pegLIT web application for target genes and target mutations. 28
Table 6. Reaction components and their amounts which were used in transferring of dual-epegRNAs into Module B plasmid by Golden gate assembly. 31
Table 7. Temperatures and durations which were applied in the transfer of pegRNAs to the Module B plasmid. 32
Table 8. Obtained module B plasmids after insertion of dual-epegRNAs. 33
Table 9. DNA concentration of modular plasmids which are used in assembly. 37
Table 10. Modular system plasmids 38
Table 11. Components and their amount for Golden gate assembly reaction 38
Table 12. Reaction temperatures, duration and cycle for obtaining the final constructs by Golden gate assembly. 38
Table 13. Reaction components and their amount in the restriction digestion 40
Table 14. DNA concentration of final plasmids which are used in protoplast transformation. 45
Table 15. Implemented optimization parameters in protoplast isolation. 46
Table 16. Content of enzyme solution and their concentration 49
Table 17. Content of W5 buffer and their concentration 49
Table 18. Content of MMG buffer and their concentration 50
Table 19. Implemented optimization parameters in protoplast transformation. 51
Table 20. Used plasmid DNA amount in transformation of protoplasts. 52
Table 21. Content of PEG solution 53
Table 22. Primer information designed for amplicon sequencing of GK plasmids. . 55
Table 23. Reaction components and quantities used in PCR for amplicon sequencing 56
Table 24. Temperature, time, and number of cycles applied in the first PCR round for amplicon sequencing. 57
Table 25. Selected application for optimized protoplast isolation protocol 69
Table 26. Selected application for optimized protoplast transformation protocol 75
Table 27. Comparison of transformation efficiencies of prime editing constructs ... 79
Table 28. Editing efficiencies (%) of GK plasmids. 86

CONTENT

ÖZET I
ABSTRACT III
ÖNSÖZ VE TEŞEKKÜR IV
ABBREVIATIONS V
TABLE OF FIGURES VI
TABLE INDEXES IX
CONTENT X
SECTION ONE 1
INTRODUCTION 1
1.1. Literature Research 1
1.1.1. The Importance of Grapevine in Türkiye and Worldwide 1
1.1.2. Powdery Mildew Disease of Grapevine and Powdery Mildew Resistance Mechanism 3
1.1.3. Genome Editing in Plants 5
1.1.4 CRISPR-Cas9 Mediated Genome Editing in Plants 5
1.1.5. CRISPR-Cas9-Mediated Genome Editing in Grapevine 10
1.1.6. A New Adaptation of CRISPR-Cas9 “Prime Editing” 13
1.1.7. Resistance (R) And Susceptibility (S) Genes of Plants 17
1.1.8. Resistance (R) and Susceptible (S) Genes related to Powdery Mildew 18
1.1.9. Plant Tissue Culture in Genome Editing 19
1.1.10. Plant Protoplasts in Genome Editing Studies 20
SECTION TWO 24
MATERIALS AND METHODS 24
2.1. Determination of mutation in target genes, and designing of dual epeg-RNAs 24
2.2. Assembly of dual-epegRNAs into Module B Plasmids 31
2.3. Assembly of A, B, C module plasmids into transformation backbone 35
2.4. Obtainment of Chardonnay grapevine plants 45
2.5. Protoplast Isolation 46
2.6. PEG mediated transformation for protoplasts 51
2.7. Amplicon Sequencing for transformed protoplast samples 54
RESULTS AND DISCUSSION 59
3.1. Confirmation of Prime Editing Designed Constructs 59
3.2. A Highly Efficient Protoplast Isolation from Chardonnay leaves 60
3.2.1. Effect of explant tissue and tissue age in protoplast isolation 60

3.2.2. Effect of surface sterilization of leaves in protoplast isolation 62
3.2.3. Effect of Cutting style in protoplast isolation 63
3.2.4. Effect of pretreatment in protoplast isolation..... 64
3.2.5. Effect of different digestion time in protoplast isolation 65
3.2.6. Separation of protoplasts from enzymatic solution and after washing with W5 buffer 67
3.2.7. Protoplast yield and viability 69
3.3. Transformation efficiency in protoplasts 71
3.3.1. Effect of protoplast number in transformation efficiencies 71
3.3.2. Effect of different PEG incubation time in transformation efficiency 73
3.3.3. Effect of incubation time and incubation buffer after transformation 74
3.4. Transformation efficiencies of GK plasmids on Chardonnay mesophyll protoplasts 75
3.5. The PCR analysis for Amplicon sequencing of the prime editing constructs 81
3.6. The Amplicon sequencing analysis of prime editing constructs..... 82
CONCLUSION & RECOMMENDATIONS 89
REFERENCES..... 91

SECTION ONE

INTRODUCTION

1.1. Literature Research

1.1.1. The Importance of Grapevine in Türkiye and Worldwide

The grapevine (*Vitis vinifera* L.) is one of the most important fruit trees with a historical value dating from the past to the present. Geological and archaeological studies show that grapevines have been produced in many parts of the world since millions of years ago (Saglam, 2018). The most important reason for the widespread production of grapes around the world is that the vine requires non-selective climate and soil conditions. It is also known to be the plant species with the highest number of varieties compared to other fruits because it has a historical value, and it is widely produced around the world. It is estimated that there are more than 10000 grapevine varieties in the world (Semerci et al., 2015).

Grapevine has become one of the most widely cultivated and one of the most economically and culturally important horticultural crops in the world, with 7.6 million hectares of production and an annual market value of ~$3.6 billion in wine export markets alone (Wan et al., 2020). In our country, grapevine trees are mostly grown for the production of table grapes (52%), raisins (38%), fruit juice and wine (10%), while wine production (90%) is by far the leading production in European countries (Gökhan Söylemezoglu, 2016). The fact that grapes and grapevine leaves are rich in secondary metabolites has led to their widespread use in the food and beverage, cosmetic and pharmaceutical industries. The beneficial effects of these metabolites on various diseases have been proven by different studies, which has increased the interest in vine-derived metabolites and led to increased investments and research in the viticulture sector (Tyagi et al., 2003; Tenkumo et al., 2020).

In the world, countries such as the USA, France, Italy and Spain, especially China, lead the viticulture sector (Kaya et al., 2023). According to the World Food and Agriculture Organization (FAO) data for the 2022, grape production amounts by

country in the world (Figure 1) are shown (FAOSTAT, 2024). Turkey ranks 6th in grape production in the world with 4165000/ton grape production, indicating that it plays a critical role in the viticulture sector (Figure 2).

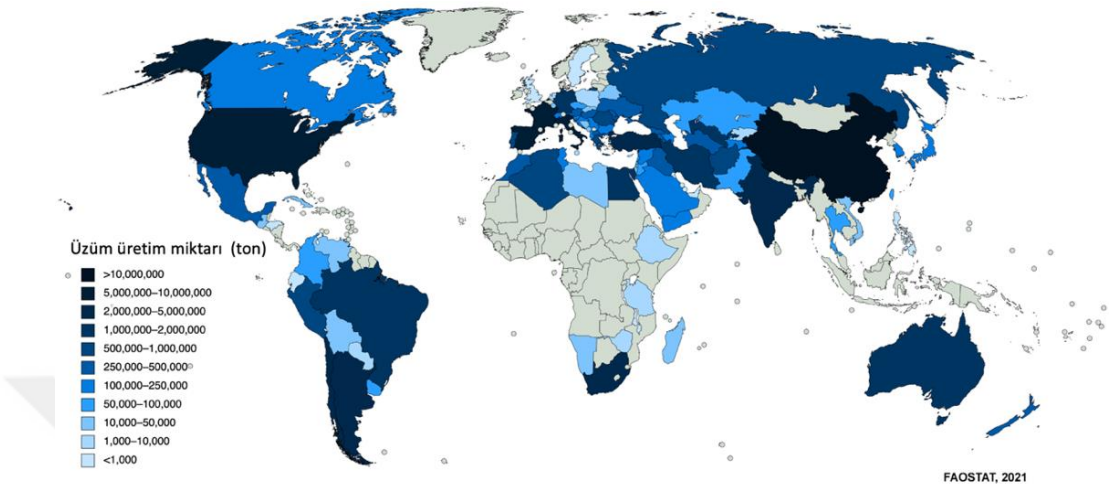


Figure 1. Grape producing countries in the world and grape production amount (FAOSTAT, 2021)

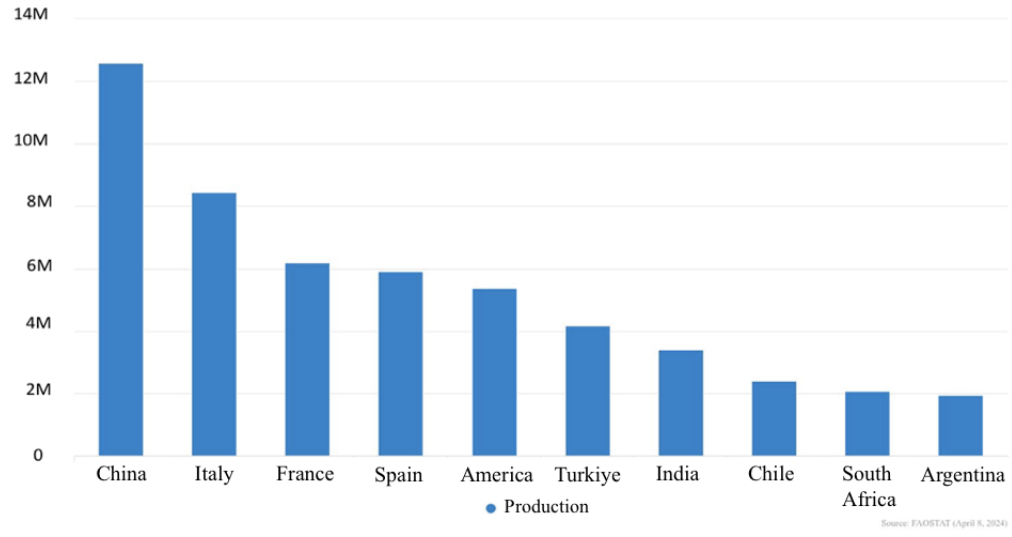


Figure 2. Top 10 grape producing countries in the world (FAOSTAT, 2024)

In addition, Turkey contributed significantly to the country's agricultural economy by earning 176538/1000 USD with 223370/ton grape exports in 2022

(FAOSTAT, 2024). Thanks to the import and export of grape production, Turkey plays a key role in the viticulture sector both globally and nationwide, while providing livelihoods for many producers.

1.1.2. Powdery Mildew Disease of Grapevine and Powdery Mildew Resistance Mechanism

Powdery mildew, caused by the fungus *Uncinula necator*, is one of the most important problems in the viticulture sector worldwide (Kunova et al., 2021). Along with grapevine, this fungus causes disease in many other economically important plant species (Vogel, 2000). This pathogen, which can infect more than 650 monocotyledonous and 9000 dicotyledonous species, is among the most common phytopathogenic fungi (Glawe, 2008). *Uncinula necator* is an obligate biotrophic pathogen that requires a living plant host for growth and reproduction. The pathogen ensures its life cycle by growing and reproducing with spores (conidium). These spores exert effective pressure to break the cell wall and form an infection structure called appressorium to penetrate the host cell. As the fungus penetrates the plant cell, it invades the cell membrane of the host by forming a multi-lobed structure called haustorium at the site of infection (Qiu et al., 2015). Thanks to this structure, the pathogen obtains the nutrients it needs from the plant and ensures the continuity of its life cycle. This pathogen, which causes powdery mildew disease, can infect all green tissues of the plant, including leaves, shoots, flowers and clusters. The pathogen spreads from these infected tissues and causes symptoms like white spots on tissues such as vines and leaves (Figure 3).

The most important economic damage is caused by flower and fruit infections. Infection causes a decrease in both photosynthesis and the sugar and anthocyanin content in the fruit, significantly reducing fruit quality (Kunova et al., 2021). Wine and table grape varieties are highly susceptible to powdery mildew disease because they do not contain a genetic defense mechanism against *Uncinula necator*, which negatively affects the production of functional products (Armijo et al., 2016). This disease, which causes yield and quality loss especially in humid regions, causes serious product loss in the viticulture sector. According to the data of the General Directorate

of Agricultural Research and Policies, powdery mildew disease, which is reported to be seen in every region of our country, causes up to 90% crop loss in the absence of spraying (Ministry of Agriculture, 1995).



Figure 3. Symptoms of powdery mildew on grapevine leaves and fruit (Source: https://agric.wa.gov.au/n/2449)

Chemical pesticide applications are among the most effective methods to combat powdery mildew (Armijo et al., 2016). Sulfur-based pesticides are especially preferred in powdery mildew. On average, 35% of all pesticides produced worldwide are used in viticulture (Tanabe et al., 2023). Powdery mildew can be controlled to a certain extent with the use of pesticides. However, unconscious and intensive use of pesticides increases production costs and threatens human and environmental health. The unconscious use of pesticides causes an increase in carbon emissions and causes great damage to the environment (Brookes and Barfoot, 2020). Therefore, reducing the use of pesticides is becoming an important issue to increase the sustainability of agriculture (Fouillet et al., 2022). In the Green Deal Action Plan, which our country has also signed, one of the targets set under the title of Sustainable Agriculture is to reduce the use of pesticides. In line with this goal, it is of great importance to apply alternative technologies to avoid yield loss. It is reported that the cost of pesticides used in viticulture reaches approximately 20% of the total production cost, which negatively affects producers. In addition, the rapid emergence of resistant strains of the pathogen causes existing chemicals to become ineffective, necessitating the development of alternative approaches instead of chemical use (Tucker et al., 2022).

1.1.3. Genome Editing in Plants

The discovery of programmable nucleases such Mega nucleases, Zinc Finger Nucleases (ZFNs), and Transcription Activator-such Effector Nucleases (TALENs) has greatly advanced plant genome editing. Plant genomes can be precisely modified with these methods to improve desired features. Targeted mutations have been successfully performed in various crops like rice and wheat using TALENs, which are designed to recognize certain DNA sequences. These tools provide certain modifications in plant genomes to enhance desirable traits (Christian et al., 2010; Zhang et al., 2013). ZFNs, which are made up of nuclease-fused zinc finger domains that bind DNA, have been used to modify the genes of plants such as tobacco and maize, showing promise in the development of herbicide-resistant cultivars. (Gao et al., 2010; Ainley et al., 2013). Meganucleases are highly selective enzymes that can detect lengthy DNA sequences. They have been used for targeted gene integration and trait enhancement in crops including soybean and grapevine (Grizot et al., 2009; Gao et al., 2014). These nuclease-based editing methods have opened the door to more accurate and effective plant breeding, tackling issues with sustainability and global food security by producing crops with improved nutritional profiles and increased resistance to environmental pressures. (Voytas & Gao, 2014; Čermák et al., 2015).

Plant genome editing has transformed agricultural biotechnology by providing accurate and effective techniques for crop enhancement. One of the most well-known methods for editing plant genomes is CRISPR-Cas9, which enables precise changes to be made to plant genomes, improving characteristics like disease resistance, drought tolerance, and nutritional value. (Zhang et. al. 2018; Gao et al. 2020).

1.1.4 CRISPR-Cas9 Mediated Genome Editing in Plants

It is predicted that classical plant breeding methods will be insufficient to grow agricultural products needed for human nutrition in the world based on the increasing world population and climate change (Bailey-Serres et al., 2019; Zhang et al., 2021). The world population is estimated to reach 10 billion by 2050. Accordingly, global food demand is said to increase by 25%-70% above current production levels (El-Mounadi et al., 2020). Therefore, plant breeding techniques are being applied to meet

the increasing demand for food and reduce the use of harmful chemicals such as pesticides.

Although traditional plant breeding techniques are widely and effectively applied in agriculture, the fact that they take a long time, require a large area, high cost and labor force limits product development through classical breeding in plants with unlimited genetic diversity. This situation necessitates the use of alternative techniques in plant breeding (Bailey-Serres et al., 2019). Although transgenic plants offer a solution to the limitations of conventional plant breeding, the use, import and export of transgenic crops are subject to strict regulations. Today, although there are other countries, notably the USA, who advocate the use of transgenic crops and allow their production, there are serious restrictions in many countries, including Turkey. For this reason, various genome editing technologies are being applied to provide faster, more predictable and widely species-adaptable alternatives to traditional plant breeding techniques (El-Mounadi et al., 2020; Najafi et al., 2023).

The development and application of genome editing tools such as CRISPR-Cas9, which do not contain transgenes and can make targeted changes in the desired region of the genome using site-specific nucleases, is of great importance for agricultural production. CRISPR-Cas9 is one of the most common genomes editing tools that offer alternative solutions to plant breeding. In 2020, the CRISPR-Cas9 genome editing technique (Jiang and Doudna, 2017), which won the Nobel Prize in Chemistry for the researchers who invented the technique, offers a fast, precise, cost-effective and easy-to-apply method for the development of plants and agricultural products (Wada et al., 2020). The CRISPR system is basically a type of adaptive immunity in bacteria. First discovered as a defense mechanism in bacteria, it is now being applied as a groundbreaking system in plant biotechnology.

CRISPR-Cas9 creates a double-chain break in the target genome region, allowing the desired modification and editing (insertion, deletion, substitution) in this region. The most important components of the CRISPR-Cas9 system consist of Cas9 enzyme, guide RNA (sgRNA) and PAM sequence (protospacer adjacent motif) (Gaj

et al., 2016). The ~20 base pairs long sgRNA sequence designed according to the target region combines with the Cas9 enzyme to form a protein-RNA complex. The 'NGG' sequence, called PAM, located at the 3' end of the target site enables the target site to be recognized by the protein-RNA complex. With the protein-RNA complex that recognizes the target site due to the PAM, the Cas9 enzyme cuts the target site from the 3' end to the 5' end of the target region to form a double chain break (Jiang and Doudna, 2017; Wada et al., 2020). These double-stranded breaks are repaired by repair mechanisms called non-homologous end-joining (NHEJ) or homologous directed repair (HDR), resulting in target insertion, deletion (indel) and substitution (Jiang and Doudna, 2017; Ren et al., 2022). The working principle of the mentioned CRISPR-Cas9 mechanism is shown in Figure 4. These edits performed by the CRISPR-Cas9 mechanism cause changes in the activation of the target gene. Thus, it is aimed to transfer the targeted feature to new generations of the plant with the modifications made (Jaiswal et al., 2019; Wada et al., 2020; Saini et al., 2023).

CRISPR-Cas9-mediated genome editing technology was first tested in Arabidopsis, tobacco, rice and wheat in 2013 and has since been applied in many different plant varieties to improve agronomically important traits, determine gene function, develop methods and prove the success of the method (Yin et al., 2017; Wada et al., 2020). The basic steps used in the application of CRISPR-Cas9 technology in plants are shown in Figure 5.

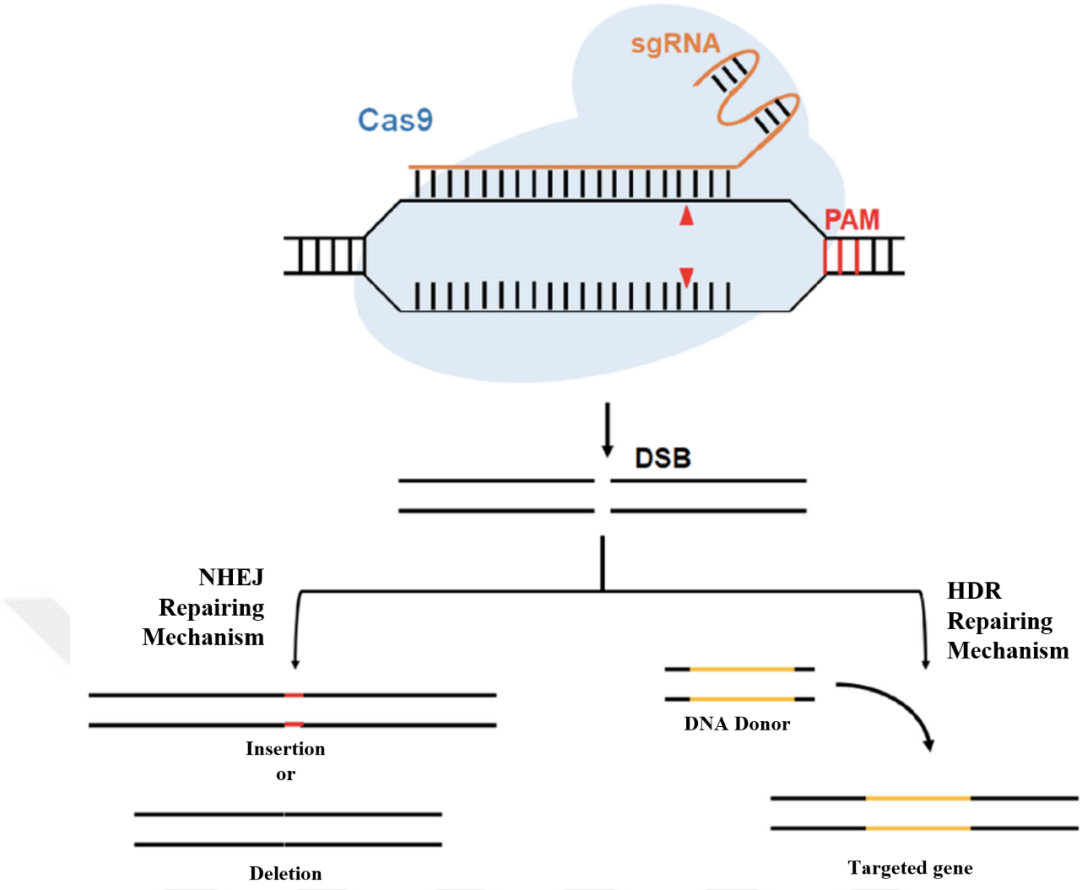


Figure 4. The CRISPR-Cas9 mechanism (Ren et al., 2022).

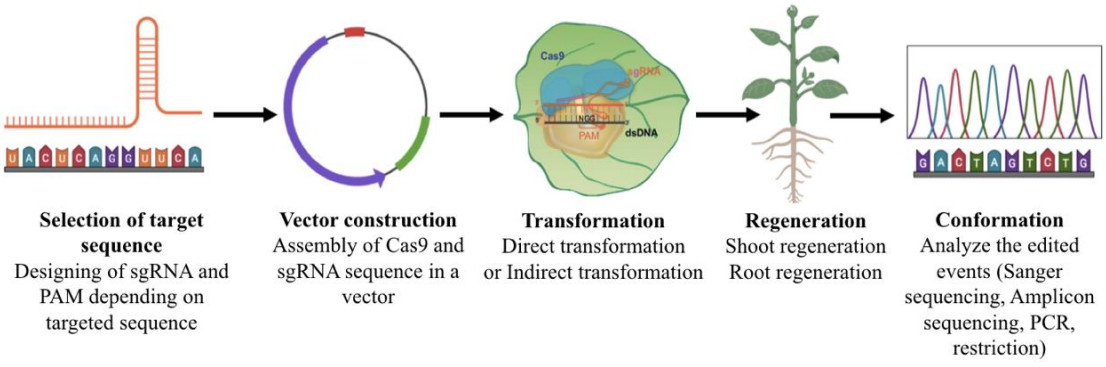


Figure 5. General workflow diagram of the CRISPR-Cas9 application (Biorender).

Genome editing studies in plants have been applied for different purposes in different plants such as obtaining resistant varieties against biotic and abiotic stresses and extending the shelf life of some plants or reducing harmful metabolites. CRISPR-Cas9 genome editing studies applied in some plants are given in Table 1.

Table 1. Application of CRISPR-Cas9 mediated genome editing in plants

Plant	Desired gene	Purpose	Reference
Maize	*ZmTMS5*	Generation of thermosensitive male-sterile maize	(Li et al., 2017)
Sorghum	*k1C*	High Lysine content	(Li et al., 2018)
Wheat	*TaEDR1*	Enhance powdery mildew resistance	(Zhang et al., 2017)
Wheat	*TaGW2-A1*, *-B1* ve *-D1*	Increase wheat grain weight and protein content	(Zhang et al., 2018)
Wheat	*Ms1*	Male-sterile hexaploid wheat lines	(Okada et al., 2019)
Rice	*OsRR22*	Increase salinity tolerance	(Zhang et al., 2019)
Rice	*CaO1* and *LAZY1*	Synthesis of chlorophyll-b	(Miao et al., 2013)
Rice	*SBEl* and *SBEllb*	Generation of High-Amylose	(Sun et al., 2017)
Rice	*Gn1a*, *DEP1*, *GS3* and *lPA1*	Increase grain size and number	(Li et al., 2016)
Rice	*OsERF922*	Enhance Rice Blast Resistance	(Wang et al., 2016)
Rice	*OsSWEET13*	Enhance Bacterial Blight resistance	(Zhou et al., 2015)
Rice	*OsMATL*	Induces haploid seed formation	(Yao et al., 2018)
Rice	*ALS*	Enhance herbicide resistance	(Endo et al., 2016)
Rice	*ALS*	Enhance herbicide resistance	(Sun et al., 2016)
Rice	*TMS5*	Thermo-sensitive Genic Male Sterile Rice	(Zhou et al., 2016)
Banana	*PDS*	Obtain phytoene desaturase alleles	(Naim et al., 2018)
Camelina sativa	*FAD2*	Enhance oleic acid content of seed	(Jiang et al., 2017)
Arabidopsis	*FWA* and *SUPERMAN* promoter	Targeted gene activation and DNA methylation	(Papikian et al., 2019)
Arabidopsis	*CBF*	Enhance cold tolerance	(Jia et al., 2016)
Tomato	*SlJAZ2*	Enhance Bacterial Speck resistance	(Ortigosa et al., 2019)
Tomato	*SlMlo1*	Enhance powdery mildew resistance	(Nekrasov et al., 2017)
Tomato	*SP5G*	Fast flowering	(Soyk et al., 2017)

Tomato	*SlAGL6*	Seedless fruit formation	(Klap et al., 2017)
Tomato	*SllA9*	Seedless fruit formation	(Ueta et al., 2017)
Tomato	*CrtR-b2* ve *Psy1*	Alteration in carotenoid content	(D'Ambrosio et al., 2018)
Potato	*GBSS*	Increase amylopectin content	(Andersson et al., 2017)
Cucumber	*elF4E*	Enhance viral diseases resistance	(Chandrasekaran et al., 2016)
Soya bean	*GmFT2a*	Late flowering	(Cai et al., 2018)
Orange	*CsLOB1*	Enhance Canker resistance	(Peng et al., 2017)
Citrus	*CsLOB1*	Enhance Canker resistance	(Jia et al., 2017)

1.1.5. CRISPR-Cas9-Mediated Genome Editing in Grapevine

The fact that grapevine is a perennial plant with a heterozygous genome makes the genetic transformation step of genome editing long and challenging. To date, CRISPR-Cas9-mediated genome editing has been demonstrated in a limited number of studies in grapevines. Ren et al. (2016) used CRISPR-Cas9 in Chardonnay suspension cells to disrupt the function of the tartaric acid-related L-idonate dehydrogenase (IdnDH) gene and a mutation frequency of 100% was obtained in the edited cells (Ren et al., 2016). In another study, they observed biallelic mutations in 15 plants and monoallelic mutations in 7 plants using CRISPR-Cas9 in Thompson Seedless cultivar to show that the transcription factor gene VvWRKY52 is required for susceptibility to Botrytis cinerea (Wang et al., 2018). In previous work to test the applicability of CRISPR-Cas9 method in grapevine, albino plants were obtained by silencing the phytoene desaturase (*VvPDS*) gene (Nakajima et al., 2017). In previous study targeting the *VvPDS* gene, the relationship between gene editing efficiency and the GC content of sgRNA, the types of materials used for genetic modification and the expression level of SpCas9 was investigated (Ren et al., 2019). As a result of this study, it was determined that sgRNA with a GC content of 65% had the highest CRISPR-Cas9 editing efficiency and they stated that editing success varied in varieties. Ren et al. (2020) successfully silenced the VvCCD8 gene by CRISPR-Cas9 application to demonstrate the applicability of the method, determine gene function and increase shoot branching (Ren et al., 2020). To increase the efficiency of CRISPR-Cas9-mediated genome editing in grapevine, the effect of GC content of sgRNA, Cas9

expression level and grapevine genotypes on grapevine genome editing was investigated. According to the results obtained, CRISPR-Cas9 editing efficiency was increased as the increasing of sgRNA GC content. In addition, it was concluded that the expression level of Cas9 and grapevine genotypes were also effective on editing efficiency (Ren et al., 2019). In a study, isolated grapevine U3/U6 and ubiquitin (UBQ) promoters were used to drive sgRNA and Cas9 expression during genome editing in grapevine instead of *Arabidopsis* U6 (*At*U6) and CaMV35 promoters, respectively. The use of grapevine promoters was found to significantly improve editing efficiency by increasing sgRNA and Cas9 expression (Ren et al., 2021a). In another study, a single point mutation was performed with prime editing in the VvDXS1 gene region in order to impart the specific flavor of Muscat grape to the Scarlet royal grapevine variety (Yang et al., 2024). Genome editing studies in grapevine are summarized in Table 2.

Table 2. Application of CRISPR-Cas9 mediated genome editing in grapevine

Target gene(s)	**Purpose**	**Transformation method/ Type of explant**	**Editing type**	**Cultivar**	**Reference**
MLO7	Method development	PEG-mediated transformation, Protoplast, callus	Gene knocking-out	Chardonnay	(Malnoy et al., 2016)
IdnDH	Proof of principle, reduction of tartaric acid content	*Agrobacterium*-mediated transformation, embryogenic cells	Gene knocking-out	Chardonnay	(Ren et al., 2016)
PDS	Proof of principle, obtainment of albino phenotype	*Agrobacterium* mediated transformation, Embryogenic callus	Gene knocking-out	Neo Muscat	(Nakajima et al., 2017)
WRKY52	Gene functional analysis, development of resistant cultivars against to	*Agrobacterium* mediated transformation, Proembryonal callus	Gene knocking-out	Thompson Seedless	(Wang et al., 2018)

	gray mold disease				
MLO3, MLO4	Development of resistant cultivars against to powdery mildew	*Agrobacterium* mediated transformation, Embryogenic callus	Gene knocking-out	Thompson Seedless	(Wan et al., 2020)
CCD7, CCD8	Proof of principle, gene functional analysis and increasing of shoot branching	*Agrobacterium* mediated transformation, Embryogenic callus	Gene knocking-out	41B rootstock (*Vitis vinifera* cv. *Chasselas* × *Vitis berlandieri*)	(Ren et al., 2020)
MLO7, DMR6 and DLO	Development of resistant cultivars against to powdery mildew and downy mildew	*Agrobacterium* mediated transformation, Embryogenic callus	Gene knocking-out	N/A	(Giacomelli et al., 2023)
PDS, GAI	Proof of principle, obtainment of Albino and chunky phenotype	PEG-mediated transformation, Protoplast	Gene knocking-out	Chardonnay, Colombard, Merlot, Cabernet Sauvignon, Thompson Seedless, Pixie	(Tricoli and Debernardi, 2024)
DMR6-1	Development of resistant cultivars against to downy mildew	*Agrobacterium* mediated transformation, Embryogenic callus	Gene knocking-out	N/A	(Djennane et al., 2024)
VvDXS 1	Creation of Muscat flavor	*Agrobacterium* mediated transformation, Embryogenic callus	Changing of amino acid sequence by point mutation	Scarlet royal	(Yang et al., 2024)

1.1.6. A New Adaptation of CRISPR-Cas9 "Prime Editing"

Double-stranded DNA breaks which are induced by are CRISPR-Cas9-mediated genome editing are repaired by cellular repair mechanisms (Jiang and Doudna, 2017). To prevent the occurrence of off-target mutations and eliminate the error-proneness of repair mechanisms, prime editing, a new adaptation of the CRISPR-Cas9 system, has been developed in which target modification can be performed without the need for double-strand breaks and any donor. Prime editing can perform any desired base transformation, small deletions and insertions (Anzalone et al., 2019; Wada et al., 2020; Li et al., 2023). Published in Nature in 2019 by David Liu from Harvard University and his research group, the prime editing technique was tested for the first time in yeast and animal cells, and genome editing was successfully performed without the double strand break (DSB) required for genome editing through HDR (homology directed repair), one of the cell repair mechanisms, or without using a donor DNA template. In this study, prime editing was used to repair genetic variations that cause sickle cell anemia and Tay-Sachs disease in humans and was reported to have the potential to correct the target region by 89% (Anzalone et al., 2019).

Prime editing consists of a prime regulatory protein and a prime regulatory guide RNA (pegRNA). The prime regulatory protein is a fusion of an engineered reverse transcriptase (RT) and the Cas9 nickase (H840A) (Petrova and Smirnikhina, 2023). The target-specifically designed pegRNA consists of a reverse transcriptase (RT) template containing a complementary sequence (spacer), a primer binding sequence (PBS) (~8-16 nt) and the desired editing sequence, which is complementary to the DNA strand where a single strand break occurs (Figure 6).

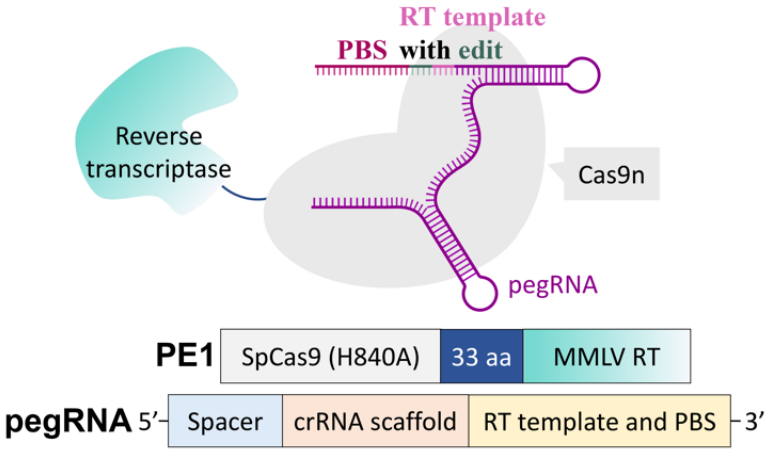


Figure 6. Prime editing mechanism (Kaya, 2024).

The modified Cas9 enzyme, which performs single-strand breaks, recognizes the target DNA sequence via pegRNA and cuts the DNA chain containing PAM. The 3' end of the cut DNA chain initiates reverse transcription of the edited sequence on the pegRNA by reverse transcriptase and realizes the desired change. Thus, the newly synthesized 3' strand containing the edited sequence replaces the unedited 5' strand and the broken strand is repaired by the cell's repair mechanism (Anzalone et al., 2019; Lu et al., 2022; Petrova and Smirnikhina, 2023). Compared to CRISPR-Cas9-mediated genome editing based solely on target DNA-gRNA hybridization, prime editing shows lower off-target editing with two hybridization steps (target DNA-pegRNA PBS and target DNA- reverse transcriptase). In 2021, another study published in Nature Biotechnology by David Liu and his group concluded that the 3' end of pegRNA, which contains the RT template and PBS region, can degrade during prime editing and that this degradation will affect the efficiency of prime editing (Nelson et al., 2022). By adding an RNA motif to the 3' end of pegRNA, they were able to prevent degradation by increasing the stability of pegRNA (Figure 7). They named their newly developed pegRNA containing this RNA motif as epegRNA (engineered-pegRNA). They developed a web-based software (pegLIT) to design the appropriate RNA motif and the linker sequence (Nelson et al., 2022).

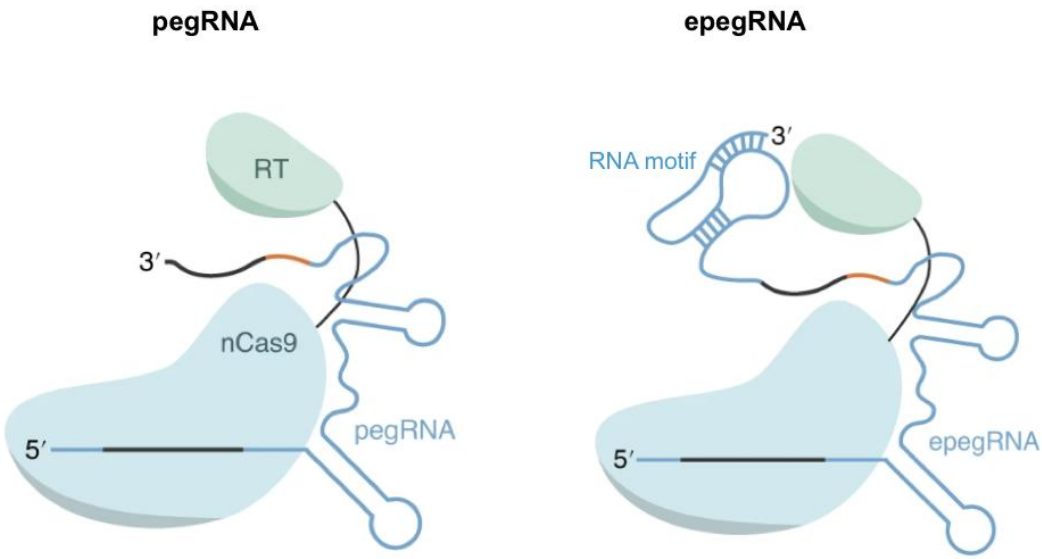


Figure 7. pegRNA and epegRNA (Nelson et al., 2022)

The successful results obtained in prime editing studies led to the testing of the technique on plants. Prime editing technique was first applied in rice and wheat (Lin et al., 2020). Subsequently, different research groups applied the prime editing technique in rice (Butt et al., 2020; Hua et al., 2020; Li et al., 2020; Wang et al., 2021), tomato (Lu et al., 2021), potato (Perroud et al., 2022), maize (Jiang et al., 2020), *Arabidopsis* (Wang et al., 2021) and *Nicotiana benthamiana* (Wang et al., 2021).

So far, the longest insertion by prime editing (66 bp) was performed in *Arabidopsis* (Wang et al., 2021). Prime editing in grapevine was first reported in 2024 by Yingzhen Yang et al. (2024). This study is shown as the first study in which prime arrangement was applied in woody plants. In this study, Lysine was converted to Asparagine (AAG=>AAC) by prime editing in the *Vv*DXS1 gene region, a grape aroma gene, to produce high-level monoterpenes that give Muscat grape aroma in the Scarlet royal grapevine variety (Yang et al., 2024). In this study, it was reported that the mutation was made by prime editing in the *Vv*DXS1 gene did not create too many indels or unwanted point mutations in the target region. It was also observed that <2.3% of the transgenic plants obtained had an editing efficiency above 45%.

Various optimization studies have been carried out to increase the applicability and efficiency of the prime editing technique in plants. In addition, various web applications have been developed to design gene cassettes and facilitate the acquisition of constructs (Huang and Puchta, 2021; Lin et al., 2021). Another research group aimed to increase the efficiency of prime editing has succeeded in increasing the efficiency of prime editing in plants between 2.9 and 17.4-fold by using a dual-pegRNA strategy, which places the same edit on different DNA strands and optimizing the binding temperatures of PBS and RT template (Lin et al., 2021) (Figure 8).

To increase the applicability of the dual-pegRNA strategy and shorten the design time, a web application called "PlantPegDesigner" was developed (Lin et al., 2021). Another research group tested an analog of the dual-pegRNA strategy on animal cells and concluded that the use of dual-pegRNA increased the efficiency of prime editing and reduced the off-target effect (Zhuang et al., 2022). In another study, Zhen Liang and colleagues used dual-pegRNA to increase the efficiency of prime editing in rice (Liang et al., 2023).

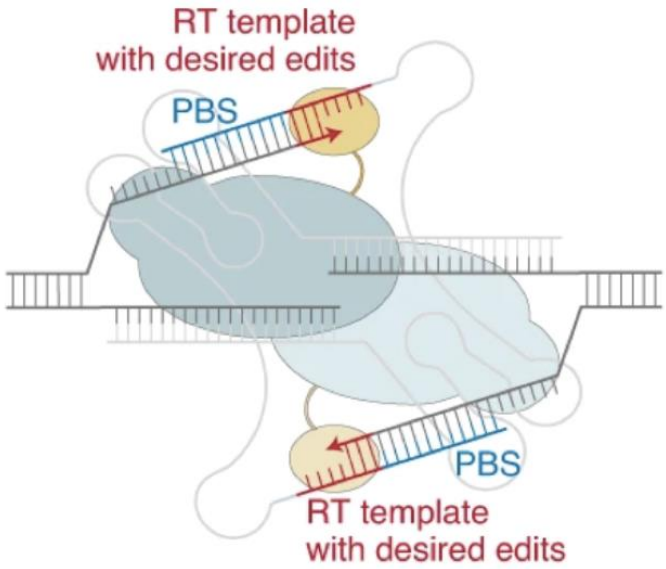


Figure 8. Dual-pegRNA approach (Lin et al., 2021)

1.1.7. Resistance (R) And Susceptibility (S) Genes of Plants

Over the past 25 years, extensive work has been done on investigating the plant immune system, leading to a better understanding of the molecular basis of plant disease resistance. The first line of defense against many biotrophic pathogens is provided by the plant (host) resistance (R)-genes. The plant will be resistant to the pathogen if it carries resistance (R) genes against specific avirulence genes of the pathogen. The avirulence genes in the pathogen activate the plant's defense mechanism by encoding proteins that are recognized by receptor proteins encoded by the plant's resistance (R) genes. Once the host is successfully protected from the pathogen, the pathogen is subject to natural selection and tries to develop new mechanisms to cause disease. Plant susceptibility (S) genes are genes that encode plant phenotypes that are sensitive to attack by plant pathogens. These genes control the molecular responses that cause plants to show signs of infection when the plant is attacked by the pathogen (Garcia-Ruiz et al., 2021; Bishnoi et al., 2023).

While the transfer of resistance (R) genes to elite varieties through classical breeding leads to the development of new disease-resistant varieties, recessive mutations in susceptibility (S) genes owned by the host also provide resistance in plants. While plant susceptibility (S) genes cause pathogen infection, disruption of susceptibility genes can render plants resistant to pathogens (Takken, 2014). While dominant R genes inactivate pathogen effectors, S genes are essential for the emergence of disease in the plant. When S genes are inactivated by mutation, recessive inherited resistance emerges. R genes are usually specific to a particular pathogen strain and can be easily inactivated by rapidly mutating pathogens, while S genes generally offer more durable resistance and a broader spectrum (Jorgensen, 1992). R-gene-induced defense responses can often result in localized cell death or a hypersensitivity response (hypersensitive reaction, HR) (Dangl, 2001). In contrast, loss of S genes (gene silencing), which are essential for the pathogen to successfully infect the plant, may not show strong defense mechanisms. For example, silencing of S-genes such as PMR5 (Vogel et al., 2004), DMR6 (Paula de Toledo Thomazella et al., 2016), LOB1 (Peng et al., 2017) and SWEET14 (Li et al., 2012; Char et al., 2017) has conferred broad-spectrum disease resistance in several economically important plant species (Takken, 2014).

The most common application for obtaining disease-resistant plants is to silence S genes, resulting in loss of gene function. However, since S genes are often involved in multiple pathways, including plant development, loss of function in these genes can lead to different undesirable pleiotropic effects (one gene affecting more than one phenotypic trait), such as reduced fitness (Feng et al., 2016), impaired interactions with beneficial microbes (Garcia-Ruiz, 2018) or susceptibility to other pathogens (Garcia-Ruiz et al., 2021). To prevent pleiotropic effects caused by the silencing of S-genes, research on partial silencing of the gene, rather than complete gene silencing, has gained great momentum.

1.1.8. Resistance (R) and Susceptible (S) Genes related to Powdery Mildew

MLO, one of the most well-known susceptibility genes in plants, is a successful example of achieving permanent resistance to powdery mildew disease (Kusch and Panstruga, 2017). In a study conducted many years ago, it was reported that a mutation in the MLO gene in barley conferred powdery mildew resistance to the plant and the resulting mutant maintained powdery mildew resistance in plants. It has been determined that there are 17 different members of the MLO gene family in grapevine and silencing of a specific group of these genes by RNAi (RNA interference) has been shown to provide partial resistance to the powdery mildew pathogen, *Uncinula necator* (Pessina et al., 2016). MLO genes, which have been identified as susceptibility genes in grapevine powdery mildew disease, have been knocked out by CRISPR-Cas9 technology and their association with powdery mildew has been confirmed, but it has not yet been possible to develop resistant varieties against the disease. Furthermore, silencing of the MLO gene(s) has revealed similar pleiotropic effects on grapevine growth and development as observed in barley and *Arabidopsis* MLO mutants (Feechan et al., 2009). The occurrence of similar pleiotropic effects on grapevine leaves may not directly affect grape production but indirectly limit plant growth (Feechan et al., 2009). Therefore, silencing of the S gene(s) is of great importance in conferring beneficial resistance traits by minimizing pleiotropic effects (Garcia-Ruiz et al., 2021).

Pectins are a class of polysaccharide polymers characterized by a linear structure of α-1,4 galacturonic acid (GalA) residues. Pectins, one of the most important components of the cell wall of plants, form a matrix structure with cellulose and hemicellulose network within the cell wall (Caffall and Mohnen, 2009). Pectate lyase catalyzes the elimination cleavage of de-esterified pectin, an important component of primary cell walls in many higher plants. Pectate lyase enzymes cause maceration of plant tissues and can also activate plant defense systems. Pectate lyase-like (*PLL*) genes have been identified in several plant species and have been implicated in a wide range of physiological processes linked to pectin degradation. Plant *PLL* genes encode proteins with strong amino acid sequence homology to the PelC isoform of bacterial pectate lyases and have been found to exist as extended families in the plants studied. Broad-spectrum resistance to powdery mildew disease has been obtained by silencing the pectate lyase-like gene *AtPMR6* in the model plant *Arabidopsis* (Vogel et al., 2002), and partial resistance has been reported by silencing its two orthologs in grapevine (*VvPLL3* and *VvPLL13*) with artificial microRNA, with promising results (Raj Majumdar 2015). Silencing of *PLL* genes for pathogen resistance can lead to different pleiotropic effects (Kusch and Panstruga, 2017; Garcia-Ruiz et al., 2021). These effects can cause undesirable trait changes in grapevines. For this reason, instead of silencing the gene completely, it is thought that by disrupting the catalytic activity of this gene without changing its binding activity, it is possible to both provide resistance to the pathogen and prevent pleiotropic effects that may occur. Studies have confirmed that the pectate lyase C (PelC) conserved regions in *PLL* genes contain Ca+ binding sites responsible for the catalytic activity of the enzyme (Herron et al., 2000; Herron et al., 2003). In this case, it is thought that instead of silencing *PLL* susceptibility genes completely, resistance to powdery mildew can be obtained by minimizing pleiotropic effects by modifying the Ca+ binding sites that enable the enzyme to show catalytic activity in the conserved PelC regions in these genes.

1.1.9. Plant Tissue Culture in Genome Editing

Plant tissue culture is based on the *in vitro* growth of parts (explants) taken from plant organs such as roots, stems, leaves or tissues called apical and meristems (Kayin and Turan, 2023). In CRISPR-Cas9-mediated genome editing applications in plants, the transfer of genome editing components such as Cas9 and sgRNA to cultured

plant explants and the subsequent differentiation of the transferred cells into a whole plant through various plant hormones are achieved by sterile plant tissue culture techniques (Custodio et al., 2022).

Plant tissue culture techniques require a long time with the involving of regeneration process and this regeneration process may lead to unwanted somoclonal variations in mutant plants (Laforest and Nadakuduti, 2022). In addition, plant tissue culture, which requires high cost, can only be applied on a limited number of plants and requires different applications in different plants (Wada et al., 2020). Plant tissue culture techniques, which are also used in different fields such as disease elimination, plant breeding and production of secondary metabolites, limit genome editing studies in plants due to their long time, high cost and specific application to each variety (Zhang et al., 2021). It is of great importance to develop alternative techniques that do not require plant tissue culture techniques to implement CRISPR-Cas9-mediated genome editing studies in plants more quickly, effectively and efficiently. Genome editing tools have made great progress since their first application, but the same progress has not been realized since the first application of plant tissue culture techniques applied in plant regeneration and transformation stages. This rapid development in genome editing tools has increased the need for the development of innovative approaches in tissue culture applications, which is the most costly and long-lasting step in genome editing studies in plants (Custodio et al., 2022; Laforest and Nadakuduti, 2022; Kocsisova and Coneva, 2023).

1.1.10. Plant Protoplasts in Genome Editing Studies

Tissue culture is the most challenging step in genome editing studies because of its time-consuming, labor intensive, and genotype dependent properties (Wada et al., 2020; Son and Park, 2022). Plant protoplasts provide an alternative and rapid strategy to assess multiple genome editing reagents rapidly such as, sgRNAs, Cas proteins, and promoters, instead of implementing CRISPR reagents directly to the plants (Nadakuduti et al., 2019; Yue et al., 2021). Protoplasts, plant cells without typical polysaccharide wall, surrounded only by the plasma membrane. These cells provide convenient platform, and they are widely used in various biotechnological

applications in plants, such as gene functional analysis, validation of genome editing components, evaluation of protein localization, DNA-protein interaction, protein-protein interaction (Jung et al., 2015; Gilliard et al., 2021; Yue et al., 2021). In addition, transient gene expression in protoplasts provides a rapid and high-throughput analysis for gene function without more time-consuming process for plant transformation (Zhao et al., 2015). Additionally, with the aim of enabling DNA-free genome editing, protoplasts supply an alternative strategy by having a capability of regeneration (Scintilla et al., 2022).

Protoplasts have been successfully isolated from many types of crops such as *Arabidopsis*, tobacco, rice, wheat, maize, lettuce, carrot, and tomato (Lin et al., 2018; Jiang et al., 2021). Even though protoplast has been isolated from woody plant crops such as, citrus, apricot, peach, tea plants, and grapevine, protoplast isolation is more challenging in these plants (Li et al., 2022). Protoplast isolation activity not only varies between different plant types, but also differs among different cultivars of the same plant type. Even different explant types of same cultivars can affect the protoplast yield and viability (Ren et al., 2021b). Until now, different explant types such as, berries (Fontes et al., 2010), leaves (Zhao et al., 2015), and callus tissues (Malnoy et al., 2016) were used in protoplast isolation from grapevine. Though efforts of grapevine-derived protoplast research had been started in 1985, it is still challenging to protoplast isolation, transformation and regeneration of whole plant from protoplasts (Bertini et al., 2019; Yue et al., 2021). The reason for the limitation in application of cutting-edge technologies of grapevine is that recalcitrance feature of the *Vitis* genus. *In vitro* grapevine experiments like embryogenesis and protoplast regeneration are affected by this feature. Therefore, regeneration of grapevines is challenging besides isolation of regenerative protoplasts from grapevine (Derman and Vivier, 2022). Protocol optimizations are continuing to depend on different varieties of grapevine in order to obtain regenerative and viable protoplasts. Optimization of parameters which affect protoplast isolation is essential to obtain a high number of healthy protoplasts. There are multiple parameters that affect the protoplast viability and yield such as, type and amount of explant, cutting style, content of enzymatic buffer, digestion time, osmotic status of protoplasts, filtering, and separation of protoplast from debris (Xu et al., 2021; Derman and Vivier, 2022).

Polyethylene glycol (PEG) is the most common transformation method in protoplasts (Adedeji et al., 2022). While large-scale isolation of viable grapevine protoplast is demanding, obtaining of stable, high viability, and quantity protoplasts is one of the most essential stages for efficient transient gene expression in protoplasts (Zhao et al., 2015; Adedeji et al., 2022). However, fragility of protoplasts is the most common limitation for their isolation and highly skilled operators are needed to handle them (Derman and Vivier, 2022). Also, ruptured protoplasts accumulate abundant calcium oxalate crystals which are another limiting factor to cause bursting of other viable protoplasts (Ren et al., 2021b). Also, there are various parameters that affect the transformation efficiency such as protoplast number, DNA concentration, PEG concentration, and PEG incubation time (Adedeji et al., 2022).

In grapevine genome editing studies, Barbier and Bessis (1990) were used leaf of Chardonnay cultivar of grapevine as an explant material for protoplast isolation. It was aimed that obtainment of high yield protoplasts from *in vitro* regenerated grapevine plants (Bessis, 1990). In another study, Mliki et al. (2003) were used leaf of *in vitro* regenerated grapevine plant as an explant for protoplast isolation. They selected Tunisian Sakasly and Muscat d'Alexandrie grape varieties for regeneration of plant (A. Mliki, 2003). In recent studies, Malnoy et al. (2016) were used grapevine mesophyll tissue as an explant in addition to embryogenic callus for protoplast isolation. *MLO*-7 gene was targeted to increase resistance of Chardonnay cultivar of grapevine against powdery mildew. They used protoplasts to aim that direct delivery of CRISPR-Cas9 ribonucleoproteins (RNPs) (Malnoy et al., 2016). In another study, Zhao et al. (2015) were used mesophyll tissue of Rizamat and the wild Chinese cultivars of grapevine for protoplast isolation. They were targeted *RPW8.2* gene expression for downy mildew disease. Tricoli et al. (2024) were obtained protoplasts from embryogenic callus of Chardonnay, Colombard, Merlot, Cabernet Sauvignon, and Pixie cultivars of grapevine to regenerate genome edited plants (Tricoli and Debernardi, 2024).

In this study, the constructs which were designed by prime editing approach were assessed in grapevine (cv. Chardonnay) protoplasts. The enzyme catalytic activity of *pLL3* and *pLL13* susceptible genes were blocked by the point mutation due

to the prime editing plasmids which were designed by dual-epeg approach. The obtained plasmids which are labelled as GK1-GK2-GK3-GK4-GK5 were transformed into grapevine Chardonnay cv. protoplasts. The presence of GK plasmids in protoplasts has been proven by the transient gene expression of the GFP. The highest transformation efficiency was achieved by GK4 plasmid as 27.79%. The working of prime editing constructs was also proven in grapevine protoplasts by amplicon sequencing. The highest editing efficiency was achieved with GK1 plasmid as 0.76 %. In addition, this study provided originality in the literature as the first study of prime editing assessment in grapevine protoplasts.

As part of the study, protoplast isolation from leaf mesophyll tissue of grapevine was optimized before the assessment of prime editing reagents directly in plant protoplasts with investigation of various significant parameters (e.g. leaf age, leaf amount, sterilization of leaves, cutting style, mannitol implementation for pre-treatment, different digestion time (4h, 8h, 16h, and 20h), filtration by different pore sizes, separation of protoplasts by sucrose gradient and ice incubation). The highest protoplast yield was obtained as $75x10^6$/g leaf weight. In addition, transformation protocol was also optimized by evaluation of different parameters such as protoplast number, PEG incubation time, and incubation duration and buffer after transformation.

SECTION TWO

MATERIALS AND METHODS

2.1. Determination of mutation in target genes, and designing of dual epeg-RNAs

DNA and protein sequences of *VvPLL3* and *VvPLL13* target gene regions were downloaded from "EnsemblPlants" and "Genoscope" databases to determine the location of the PelC conserved region on *VvPLL3* and *VvPLL13* target genes and "*Vitis vinifera* cv. Chardonnay cl. 04" was verified by alignment with genome assembly results (http://169.237.73.197/Chardonnay04/downloads.html). *PDS1* gene was also used as a control in the study. DNA and protein sequence information for *PDS1* gene was downloaded from "EnsemblPlants" and "Genoscope" databases and verified with the results of "*Vitis vinifera* cv. Chardonnay cl. 04". Identification (ID) numbers of the sequences in the respective databases for *VvPLL3*, *VvPLL13* and *PDS1* genes was shown in Table 3.

Table 3. Target genes and their ID numbers in databases

Targeted gene	EnsemblPlants ID numbers	Genoscope ID numbers
VvPLL3	VIT_08s0007g04820	GSVIVT00000608001
VvPLL13	VIT_13s0019g04900	GSVIVT00018134001
PDS1	VIT_09s0002g00100	GSVIVT01016650001

To detect the PelC conserved region on *VvPLL3* and *VvPLL13* genes, the sequence information of the PelC conserved region was downloaded from the NCBI database. Subsequently, multiple sequence alignment was performed to identify the PelC conserved region on *PLL3* and *PLL13* genes. The result of multiple alignment including this region is shown in Figure 9. Within these regions, 2 of the Ca+ binding and substrate binding sites associated with catalytic activity were selected and these specific amino acids were identified as target regulation sites for grapevine *PLL3* and *PLL13* genes. With a single nucleotide change in these amino acids on PelC, it is planned to block catalytic activity without silencing the genes completely.

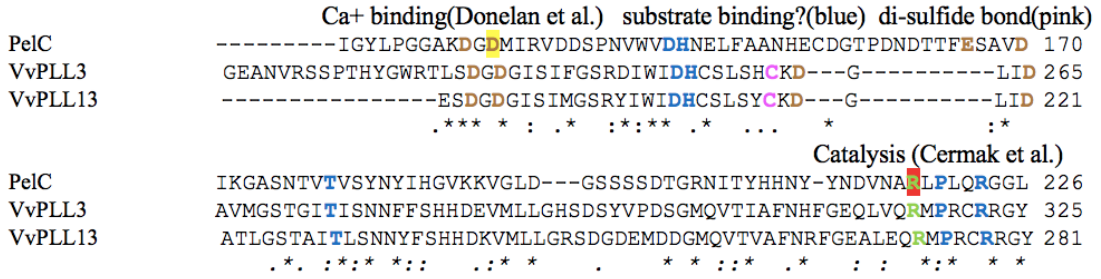


Figure 9. Multiple alignment result, brown; Ca+2 binding site, blue; substrate binding site, green; catalysis, pink; disulfide binding site

The planned target modifications to the *VvPLL3* and *VvPLL13* target genes are described below.

1. D131A (conversion of the amino acid aspartic acid (D) to alanine (A), the 131st amino acid on PelC): The amino acid aspartic acid is the amino acid involved in Ca+ binding required for substrate binding (highlighted in yellow on Figure 9). A mutation in this amino acid is thought to cause the mutant not to bind to the substrate.

2. R218K (conversion of the amino acid arginine (R) to lysine (K), the 218th amino acid on PelC): The amino acid arginine is the amino acid responsible for catalytic activity (highlighted in red on Figure 9). A mutation in this amino acid will not affect the binding of the substrate but will prevent the enzyme from working.

It was planned to completely block the activity of the gene by adding a stop codon to the 5' end of the gene to silence the *PDS1* gene. The arrangements to be made to provide target changes in *VvPLL3*, *VvPLL13* and *PDS1* genes are given in Table 4.

Table 4. Target gene and target mutation which were caused by desired editing.

Target gene and mutation	Target editing
D131A mutation in *VvPLL3* gene	GAT => GCT
R218K mutation in *VvPLL3* gene	CGG => AAG
D131A mutation in *VvPLL13* gene	GAT => GCT
R218K mutation in *VvPLL13* gene	AGG => AAG

Addition of stop codon in *PDS1* gene	TGG => TGA

Prime editing and dual-pegRNA strategy were used to achieve the targeted modification. Using the PlantPegDesigner web application, gRNAs and pegRNA sequences including primer binding site (PBS) and reverse transcriptase sites (RT template) were determined. After the dual-pegRNAs were designed, the pegLIT web application was used to add the appropriate motif and linker sequence to the 3' end of the pegRNAs and sequences for dual-epegRNAs were obtained. The use of PlantPegDesigner web application for target genes is described step by step (Figure 10-Figure 11). First, the sequence containing the target mutation in the target gene was pasted into the relevant box on the web page. Figure 10 shows an example of a dual-pegRNA design with R218K modification in the *PLL3* gene. The relevant sequence region for the conversion of "cg" bases to "aa" for the R218K change in the *PLL3* gene was pasted into the box. The desired editing is shown in parentheses with the original sequence written at first and the mutation performed afterwards.

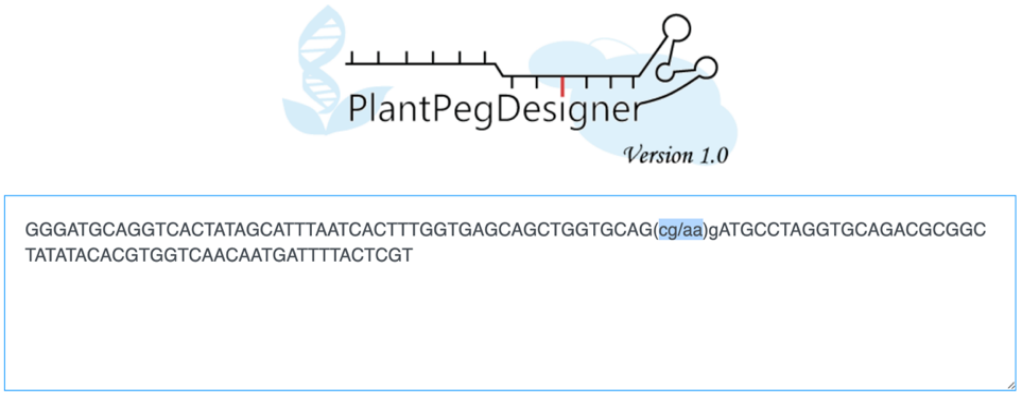


Figure 10. Designing of dual-pegRNAs for the R218K mutation in the *PLL3* gene

The parameters which were used in the dual-pegRNA design were selected as shown in Figure 11. After data was entered into the PlantPegDesigner web application, the gRNA spacer sequence, PBS sequence and RT sequences for forward and reverse sequences for the dual-pegRNA strategy were determined by the program and the most optimal ones were obtained. The dual-pegRNA sequences obtained with the PlantPegDesigner web application for the target genes are shown in detail in Figure

12. The pegRNA generated for the forward sequence is shown as NGG-pegRNA and the pegRNA generated for the reverse sequence is shown as CCN-pegRNA.

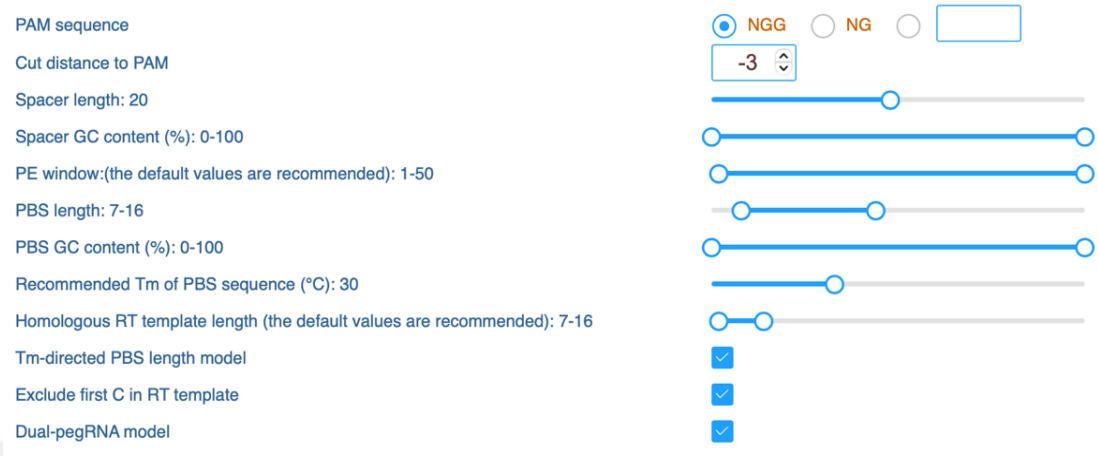


Figure 11. Parameters which were used in the designing of dual-pegRNAs for the R218K target mutation in the *PLL3* gene.

NGG pegRNA (5'-3')	gRNA spacer	CGCACACTGTC GGACGGTGA	ttggtgagca gctggtgcag	cctcggaatc ggacggtgAt	ggccttcaat cgcttcggtg	ttcagaactc ccaatgtacc
	PBS	ccgtccgac	caccagctg	accgtccga	cgaagcgatt	acattgggag
	RT template	atcgatattcc aGca	acctaggcat cTTctg	tggatatccc aGc	accttggcat cTtctgctcc agcgcctcac	taaagatgtc tTcaggt
CNN pegRNA (5'-3')	gRNA spacer	TACAATGGGAC AACGAACAG	atatagccgc gtctgcacct	gatgtacctt gaccccatga	aagtaccccc gccggcacct	atcaatataa agatgtctCc
	PBS	ttcgttgtcc	tgcagacgc	tggggtcaag	tgccggcg	gacatcttta ta
	RT template	gtcggacggtg Ctggaatatcg atattcggatc acgagacatat ggatcgaccac tg	agctggtgca gAAgatgcct agg	atcggacggt gCtgggatat ccatca	gctggagcag aAgatgccaa gg	atgtacctgA a

Figure 12. Dual-pegRNA sequences obtained by using of PlantPegDesigner web application for target genes.

After the sequences shown in detail in Figure 12 were determined for each target gene, pegLIT web application was used to add the appropriate motif and linker sequence to the 3' end of the pegRNAs and sequences for dual-epegRNAs were obtained. Using the pegLIT application, the linker sequence for the selected motif (tevopreQ1) was obtained by pasting the gRNA spacer sequence, PBS sequence and RT template sequence into the relevant boxes for the R218K target mutation in the

PLL3 gene (Figure 13). The linker sequences obtained for the tevopreQ1 motif sequence using the pegLIT program for all target genes are given in Table 5.

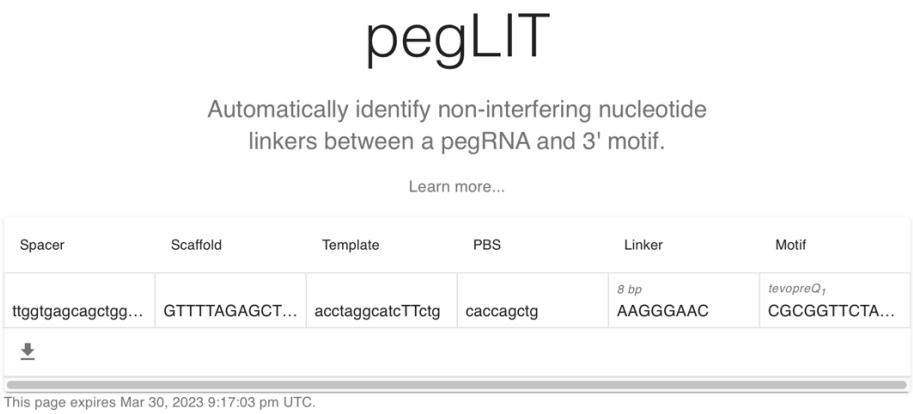


Figure 13. Obtainment of linker sequence for R218K target mutation in *PLL3* gene by pegLIT application

Table 5. Linker sequences obtained in the pegLIT web application for target genes and target mutations.

Target gene and target mutation	**pegRNA**	**linker sequence**	**tevopreQ1 motif sequence (5'-3')**
***PLL3*_D131A**	NGG_pegRNA	TACCATTA	CGCGGTTCTATCTAGTTACGCGTTAAACCAACTAGAA
	CNN_pegRNA	AGCTCTCT	
***PLL13*_D131A**	NGG_pegRNA	ATAAACTA	
	CNN_pegRNA	AATTTAGA	
***PLL3*_R218K**	NGG_pegRNA	AAGGGAAC	
	CNN_pegRNA	TCAGAACA	
***PLL13*_R218K**	NGG_pegRNA	GAAGTAAC	
	CNN_pegRNA	AACATTGT	
PDS1	NGG_pegRNA	AAGTAACG	
	CNN_pegRNA	AATTAGCT	

After the target gene regions were designed as dual-epegRNAs, tRNA sequence was added between the two pegRNAs so that each pegRNA could be expressed in the same vector (Cermak et al., 2017). For the integration of dual-epegRNAs into the vector, appropriate restriction enzyme sites were added to the 5' end and 3' end to obtain overhang regions compatible with the vector. The schematic representation of dual-epegRNAs is given in Figure 14.

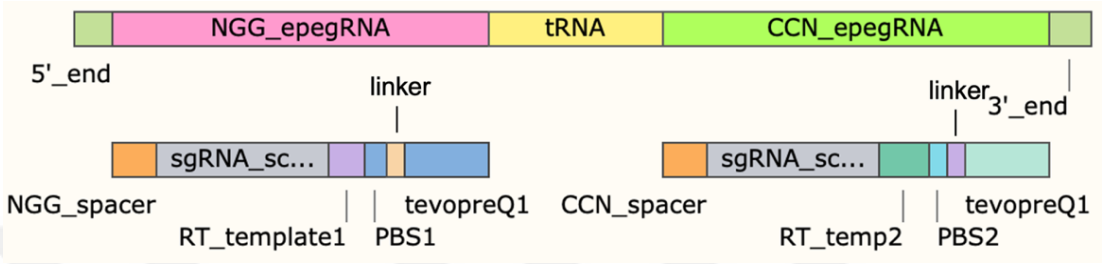


Figure 14. Schematic representation of the designed dual-epegRNA

The final sequences of the dual-epegRNAs designed for the target genes are given in Figure 15 to Figure 19.

PLL3-D131A

5'AAAAAACGTCTCAgattCGCACACTGTCGGACGGTGAgttttagagctagaaatagcaagttaaaataag
gctagtccgttatcaacttgaaaaagtggcaccgagtcggtgcatcgatattccaGcaccgtccgacTACCATTACGCGGTT
CTATCTAGTTACGCGTTAAACCAACTAGAAAACAAAGCACCAGTGGTCTAGTGGTA
GAATAGTACCCTGCCACGGTACAGACCCGGGTTCGATTCCCGGCTGGTGCATACAAT
GGGACAACGAACAGgttttagagctagaaatagcaagttaaaataaggctagtccgttatcaacttgaaaaagtggcaccgagt
cggtgcgtcggacggtgCtggaatatcgatattcggatcacgagacatatggatcgaccactgttcgttgtccAGCTCTCTCGCG
GTTCTATCTAGTTACGCGTTAAACCAACTAGAAGTTTaGAGACGAAAAAA3'

NNNN> NGG-epegRNA
NNNN> tRNA
NNNN> CCN-epegRNA

Figure 15. Dual-epegRNA sequence designed for the *PLL3*-D131A target gene.

PLL13-D131A

5’AAAAAACGTCTCAgattcctcggaatcggacggtgAtGTTTTAGAGCTAGAAATAGCAAGTTAA
AATAAGGCTAGTCCGTTATCAACTTGAAAAAGTGGCACCGAGTCGGTGCtggatatcccaG
caccgtccgaATAAACTACGCGGTTCTATCTAGTTACGCGTTAAACCAACTAGAAAACAA
AGCACCAGTGGTCTAGTGGTAGAATAGTACCCTGCCACGGTACAGACCCGGGTTCG
ATTCCCGGCTGGTGCAgatgtaccttgaccccatgaGTTTTAGAGCTAGAAATAGCAAGTTAAA
ATAAGGCTAGTCCGTTATCAACTTGAAAAAGTGGCACCGAGTCGGTGCatcggacggtgCt
gggatatccatcatggggtcaagAATTTAGACGCGGTTCTATCTAGTTACGCGTTAAACCAACTAG
AAGTTTaGAGACGAAAAAA3’

NNNN> NGG-epegRNA
NNNN> tRNA
NNNN> CCN-epegRNA

Figure 16. Dual-epegRNA sequence designed for the *PLL13*-D131A target gene.

PLL3-R218K

5’AAAAAACGTCTCAgattttggtgagcagctggtgcaggttttagagctagaaatagcaagttaaaataaggctagtccgttatc
aacttgaaaaagtggcaccgagtcggtgcacctaggcatcTTctgcaccagctgAAGGGAACCGCGGTTCTATCTA
GTTACGCGTTAAACCAACTAGAAAACAAAGCACCAGTGGTCTAGTGGTAGAATAGT
ACCCTGCCACGGTACAGACCCGGGTTCGATTCCCGGCTGGTGCAatatagccgcgtctgcacctg
ttttagagctagaaatagcaagttaaaataaggctagtccgttatcaacttgaaaaagtggcaccgagtcggtgcagctggtgcagAAgat
gcctaggtgcagacgcTCAGAACACGCGGTTCTATCTAGTTACGCGTTAAACCAACTAGAAG
TTTaGAGACGAAAAAA3’

NNNN> NGG-epegRNA
NNNN> tRNA
NNNN> CCN-epegRNA

Figure 17. Dual-epegRNA sequence designed for the *PLL3*-R218K target gene.

PLL13-R218K

5'AAAAAACGTCTCAgatttcggtgaggcgctggagcaggttttagagctagaaatagcaagttaaaataaggctagtccgttat
caacttgaaaaagtggcaccgagtcggtgcaccttggcatcTtctgctccagcgcGAAGTAACCGCGGTTCTATCTA
GTTACGCGTTAAACCAACTAGAAAACAAAGCACCAGTGGTCTAGTGGTAGAATAGT
ACCCTGCCACGGTACAGACCCGGGTTCGATTCCCGGCTGGTGCAaagtacccccgccggcacct
gttttagagctagaaatagcaagttaaaataaggctagtccgttatcaacttgaaaaagtggcaccgagtcggtgcgctggagcagaAgat
gccaaggtgccggcgAACATTGTCGCGGTTCTATCTAGTTACGCGTTAAACCAACTAGAAGT
TTaGAGACGAAAAAA3’

NNNN> NGG-epegRNA
NNNN> tRNA
NNNN> CCN-epegRNA

Figure 18. Dual-epegRNA sequence designed for the *PLL13*-R218K target gene.

PDS1

5'AAAAAACGTCTCAgatttcagaactcccaatgtaccgttttagagctagaaatagcaagttaaaataaggctagtccgttatc
aacttgaaaaagtggcaccgagtcggtgctaaagatgtctTcaggtacattgggagAAGTAACGCGCGGTTCTATCTA
GTTACGCGTTAAACCAACTAGAAAACAAAGCACCAGTGGTCTAGTGGTAGAATAGT
ACCCTGCCACGGTACAGACCCGGGTTCGATTCCCGGCTGGTGCAatcaatataaagatgtctCcgt
tttagagctagaaatagcaagttaaaataaggctagtccgttatcaacttgaaaaagtggcaccgagtcggtgcatgtacctgAagacatctt
tataAATTAGCTCGCGGTTCTATCTAGTTACGCGTTAAACCAACTAGAAGTTTaGAGAC
GAAAAAA3'

NNNN> NGG-epegRNA
NNNN> tRNA
NNNN> CCN-epegRNA

Figure 19. Dual-epegRNA sequence designed for the *PDS1* target gene.

2.2. Assembly of dual-epegRNAs into Module B Plasmids

To easily cloning of the dual-epegRNAs which were designed for *VvPLL3*, *VvPLL13* and *PDS1* into plasmid by Golden gate assembly method, the dual-epegRNAs were synthesized as gBlocks by the project advisor Prof. Dr. Adam Bogdanove through IDT company and sent to Manisa Celal Bayar University as lyophilized. Since the synthesis of dual-pegRNA sequences as a single fragment as gBlocks had a "high complexity score" value, they were synthesized by dividing into 2 parts to include complementary sequences suitable for assembly with the Golden gate assembly technique. DNA constructs were obtained by using of Golden gate assembly, as mentioned in Cermak et al. (2017). The dual-epegRNAs which were synthesized as gBlocks DNA fragments were first transferred into the Module B plasmid by Golden gate assembly. The reaction components and reaction conditions are shown in Table 6 and Table 7, respectively.

Table 6. Reaction components and their amounts which were used in transferring of dual-epegRNAs into Module B plasmid by Golden gate assembly.

Component	Amount
25 ng module B plasmid	2 µl
50 ng gBlocks DNA fragment	2 µl
BsaI enzyme	0.5 µl
10X T4 DNA ligase buffer	2 µl
T4 DNA ligase	1 µl
H_2O	12.5 µl

Table 7. Temperatures and durations which were applied in the transfer of pegRNAs to the Module B plasmid.

Temperature	Time
37ºC	5 minutes
16ºC	10 minutes
37ºC	15 minutes
80ºC	5 minutes

After the Golden gate assembly reaction was completed, 5 µl of the reaction mixture was taken and transformed into *E. coli* (DH5α). The steps for *E. coli* transformation are given below.

1. 25 µl of thermo-competent *E. coli* (DH5α) cells were thawed on ice and 100 ng of plasmid DNA was added and gently mixed.
2. The mixture was kept on ice for 20 minutes and then heat shocked by placing the cells in a water bath at 42^{o}C for 30 seconds.
3. The cells were then kept on ice for another 2 minutes and 300 µl of LB was added to the cells and incubated at 37^{o}C, 250 rpm for 1 hour in a shaker incubator.
4. After incubation, the cells were inoculated on LB+agar petri dish containing kanamycin by smear method and incubated at 37^{o}C for 1 night.

The colonies obtained and they were confirmed by Sanger sequencing. In this way, module B plasmids were obtained and confirmed by Institute of Biotechnology, Cornell University. Detailed plasmid maps of the obtained module B plasmids were created in Benchling application. Detailed information on the modified module B plasmids containing dual-epegRNAs is given in Table 8, while plasmid gene maps are given in Figure 20-Figure 24.

Table 8. Obtained module B plasmids after insertion of dual-epegRNAs.

Plasmids which were generated for the dual-pegRNA cloned into module B	Target gene and target mutation
pLW14	*PLL3*-R218K
pLW15	*PLL13*_R218K
pLW16	*PLL3*_D131A
pLW17	*PLL13*_D131A
pLW18	*PDS1*

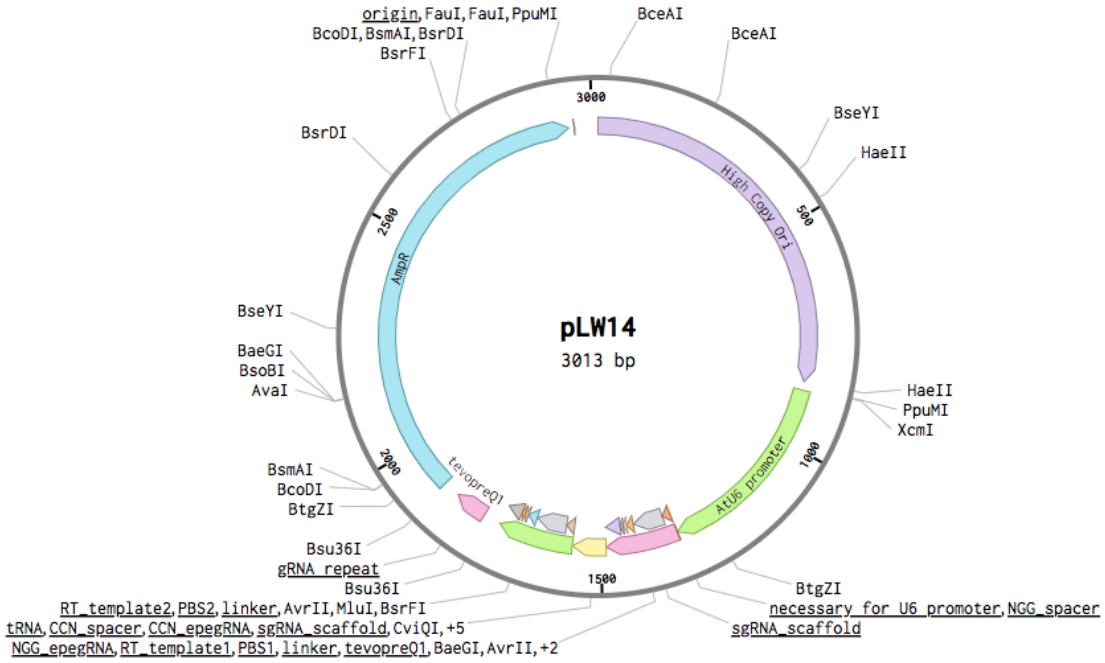


Figure 20. Detailed gene map of pLW14 (*PLL3*_R218K) plasmid

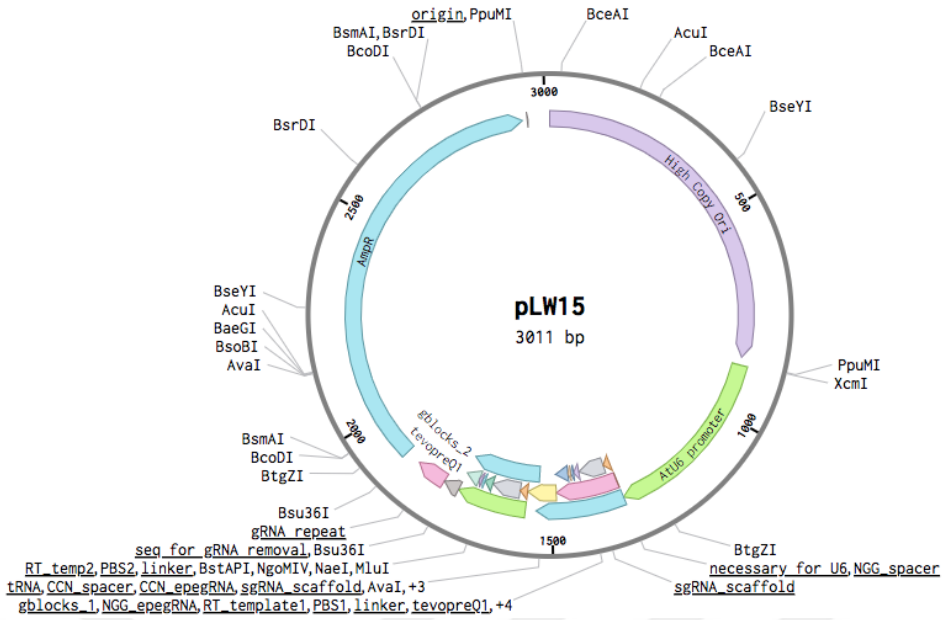


Figure 21. Detailed gene map of pLW15 (*PLL13*_R218K) plasmid

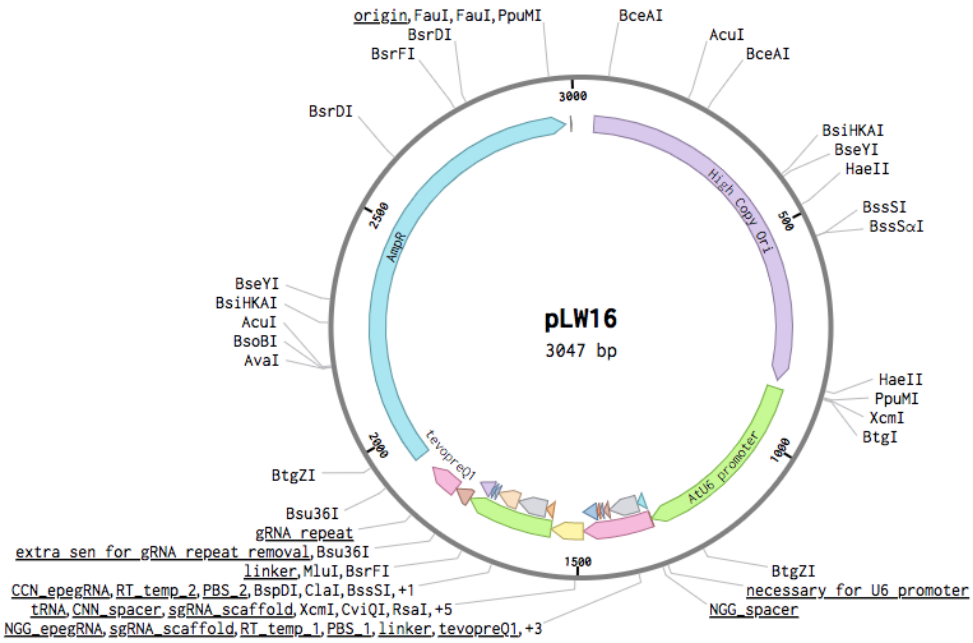


Figure 22. Detailed gene map of pLW16 (*PLL3*_D131A) plasmid

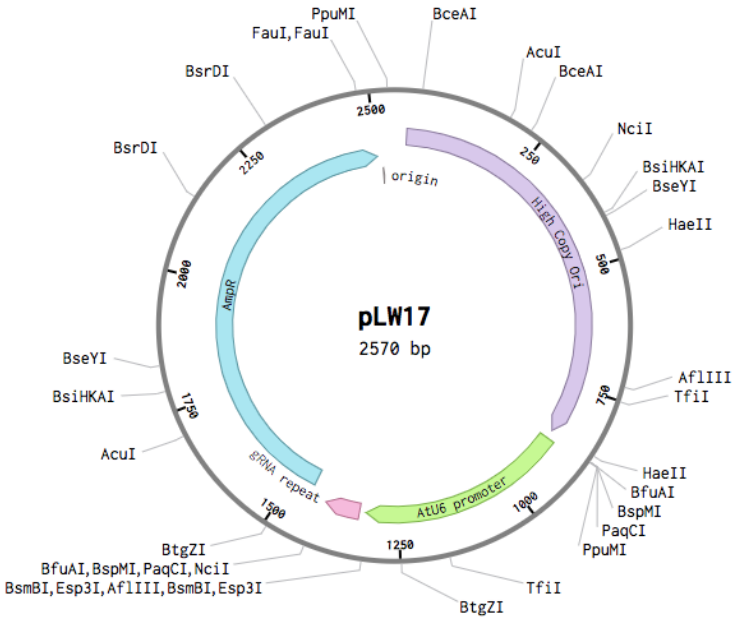


Figure 23. Detailed gene map of pLW17 (*PLL13*_D131A) plasmid

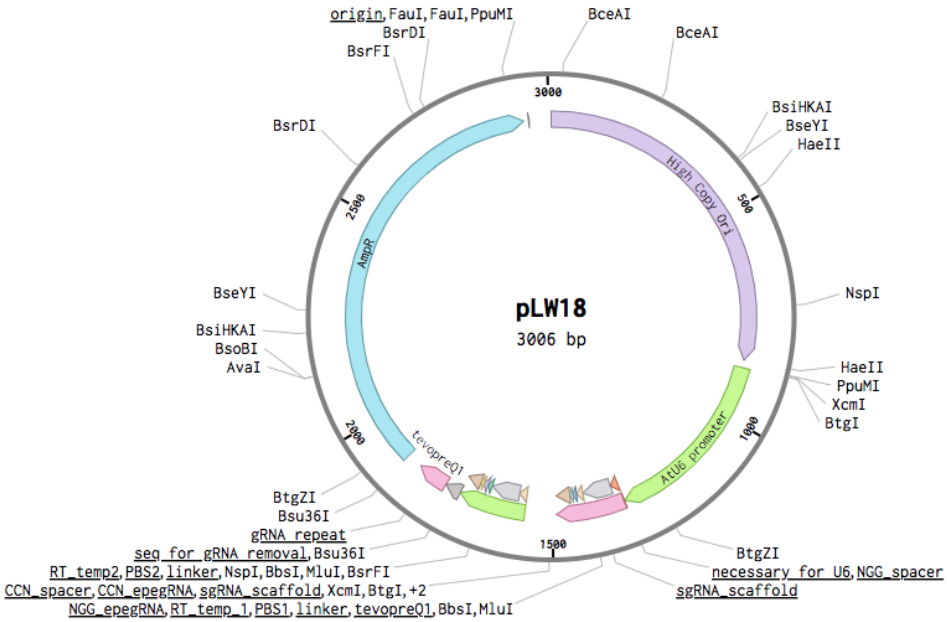


Figure 24. Detailed gene map of pLW18 (*PDS1*) plasmid

2.3. Assembly of A, B, C module plasmids into transformation backbone

After the obtainment of module B plasmids, DNA isolation of modular system plasmids (module A, module B, module C) was carried out. Module C (GFP) and

backbone plasmids were used from Webtools for the Voytas Lab Plant Genome Engineering Toolkit (Cermak et al., 2017). On the other hand, module A (Cas9) plasmid was not directly used from Voytas Lab Toolkit. Module A was redesigned with the removing of AarI restriction site by Li at Cornell University. All designed modular system plasmids (A, B, C and backbone plasmid) in *E. coli* as agar stock were sent from Cornell University to Manisa Celal Bayar University. Streak plate inoculation was made from the agar stocks for each plasmid with the presence of Kanamycin (Km). They were incubated at 37ºC in incubator. After over-night incubation, single colonies were obtained for each plasmid. Then, 3 mL liquid culture was started from single colonies of plasmids with the presence of 3 µL Kanamycin (Km) in shaker at 37ºC (Figure 25). After over-night incubation, DNA isolation was carried out from *E. coli* by using NEB Monarch Plasmid Miniprep DNA kit. DNA isolation protocol was applied as follows below.

1. Over-night grown 3 mL bacterial cell culture was harvested by centrifugation for 30 seconds at 16,000xg.
2. Pellet was resuspended in 200 µL plasmid resuspension buffer (B1) and they were vortexed until they completely resuspended.
3. After the cells were resuspended, 200 µL plasmid lysis buffer (B2) was added, and the tubes were gently inverted for 5-6 times, and they were incubated for 1 minute at room temperature. At the end of the incubation, the color of samples converted to dark pink.
4. 400 µL plasmid neutralization buffer (B3) was added to sample tubes, and they were gently inverted until they become neutralized, and color converted to yellow. Then, they were incubated for 2 minutes at room temperature.
5. Next, lysate was centrifuged for 5 minutes at 16,000xg. After, supernatant was transferred to spin column and they were centrifuged for 1 minute at 16,000xg. Then, the flow-through was discarded.
6. Column was re-inserted in the collection tube and 200 µL plasmid wash buffer 1 was added and they were centrifuged for 1 minute at 16,000xg. Flow-through was discarded. Then, second washing step was carried out by addition of 400 µL plasmid wash buffer 2 and they were centrifuged for 1 minute at 16,000xg.

7. Column was transferred to a clean Eppendorf and 100 µL elution buffer which was incubated at 50°C was added to column filter. They were incubated for 2 minutes and then, they were spin down for 1 minute to elute DNA.

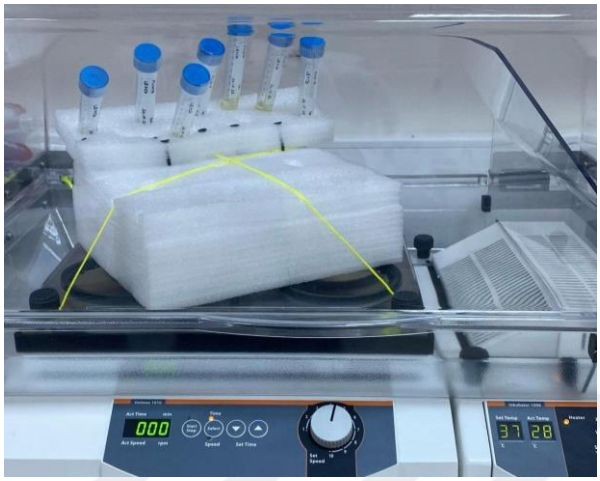


Figure 25. Liquid culture of modular plasmids which is integrated into *E. coli* in the shaker for over-night incubation.

After DNA isolation was made, DNA concentration of all plasmids was measured by Qubit. DNA concentration results are shown in Table 9. Modular system plasmids (module A, module B, module C) were transferred to the backbone plasmid (non-TDNA), which were used for transformation by a single golden gate reaction. The modular system plasmids which were used are shown in Table 10. The components and their amount which were used in Golden gate reaction to obtain an all-in-one plasmid (includes module A, module B, and module C) are shown in Table 11. Reaction conditions for assembly in terms of temperature and duration are shown in Table 12. Illustration to explain the principle of assembly of modular system plasmids by the Golden Gate reaction using the restriction enzyme AarI is shown in Figure 26.

Table 9. DNA concentration of modular plasmids which are used in assembly.

Targeted Plasmid	DNA concentration (ng/µL)
pLW13 (module A)	61.72 ng/µl
pLW14 (module B)	126 ng/µl

pLW15 (module B)	159 ng/µl
pLW16 (module B)	114 ng/µl
pLW17 (module B)	132 ng/µl
pLW18 (module B)	237 ng/µl
pMODC-3001 (module C)	83.2 ng/µl
pTRANS-100 (plasmid backbone)	24.05 ng/µl

Table 10. Modular system plasmids

Modul A (Cas9)	Modul B (e-peg RNA)	Modul C (GFP)	Transformation backbone plasmid
35S: AtCas9	AtU6: gRNA	35S: GFP	p-TRANS100 (non-T-DNA)

Table 11. Components and their amount for Golden gate assembly reaction

Components	**Amount**
Transformation backbone	75 ng
Module A plasmid	75 ng
Module B plasmid	75 ng
Module C plasmid	75 ng
AarI oligonucleotide	0.4 µL
AarI enzyme	0.5 µL
T4 DNA ligase enzyme	1 µL
10x T4 DNA ligase buffer	2 µL
H2O	Up to 20 µL

Table 12. Reaction temperatures, duration and cycle for obtaining the final constructs by Golden gate assembly.

Temperature	**Duration**	**Cycle**
37°C	5 minutes	10 times repeat
16°C	10 minutes	
37°C	15 minutes	-
80°C	5 minutes	-
+4°C	∞	-

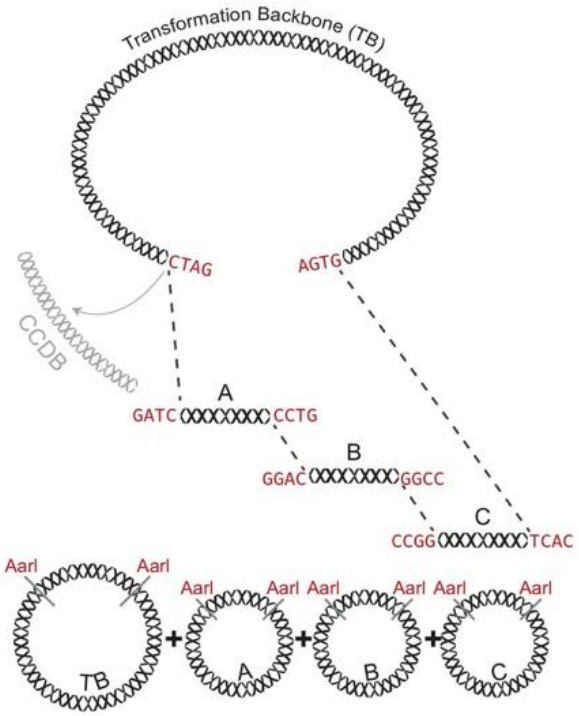


Figure 26. Schematic representation of the strategy applied to obtain the final constructs (Cermak et al., 2017).

After the Golden gate assembly reaction was completed, 5 µl of the reaction mixture was taken and transformed into *E. coli* (DH5α). The steps for *E. coli* transformation are given below.

1. 25 µl of thermo-competent *E. coli* (DH5α) cells were thawed on ice and 100 ng of plasmid DNA was added and gently mixed.
2. The mixture was kept on ice for 20 minutes and then heat shocked by placing the cells in a water bath at 42°C for 30 seconds.
3. The cells were then kept on ice for another 2 minutes and 300 µl of LB was added to the cells and incubated at 37°C, 250 rpm for 1 hour in a shaker incubator.
4. After incubation, the cells were inoculated on LB+agar petri dish containing kanamycin by smear method and incubated at 37°C for 1 night.

After over-night incubation, obtained single colonies (Figure 27) were confirmed by restriction digestion by using of *Sac*I enzyme. The components of restriction and their quantities which were used in the restriction confirmation are detailed shown in Table 13. The samples were incubated at 37°C for 30 minutes in a

Thermal Cycler. According to the confirmation, targeted plasmids which were named GK1, GK2, GK3, GK4, and GK5 were obtained. Plasmid maps of GKs which were obtained by using Benchling webtool are shown in Figure 28- Figure 32 in respectively.

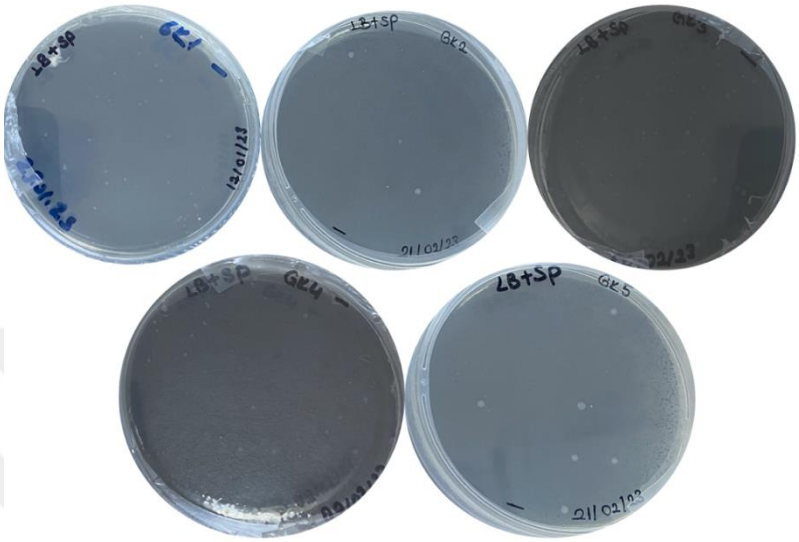


Figure 27. Obtained single colonies of GKs plasmids after *E. coli* transformation.

Table 13. Reaction components and their amount in the restriction digestion

Components of Restriction	**Amount**
Buffer	1.5 µl
SacI enzyme	0.2 µl
DNA	2 µl
H_2O	11.3 µl
Total volume: 15 µl	

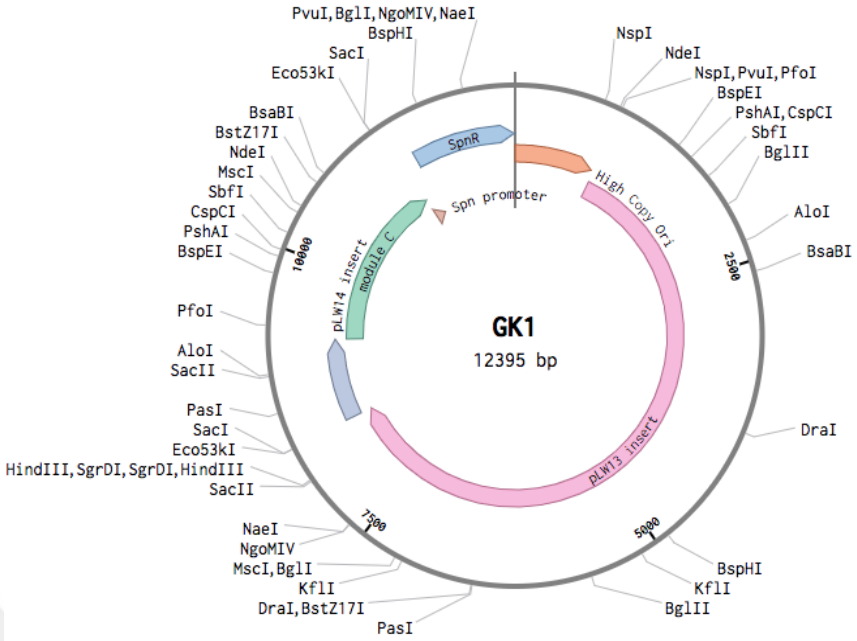


Figure 28. Plasmid map of GK1

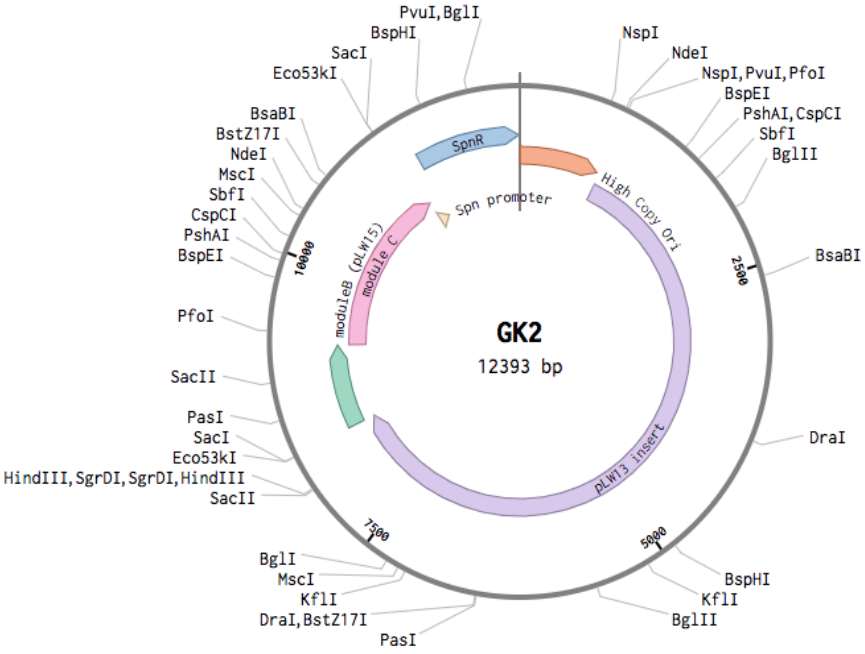


Figure 29. Plasmid map of GK2

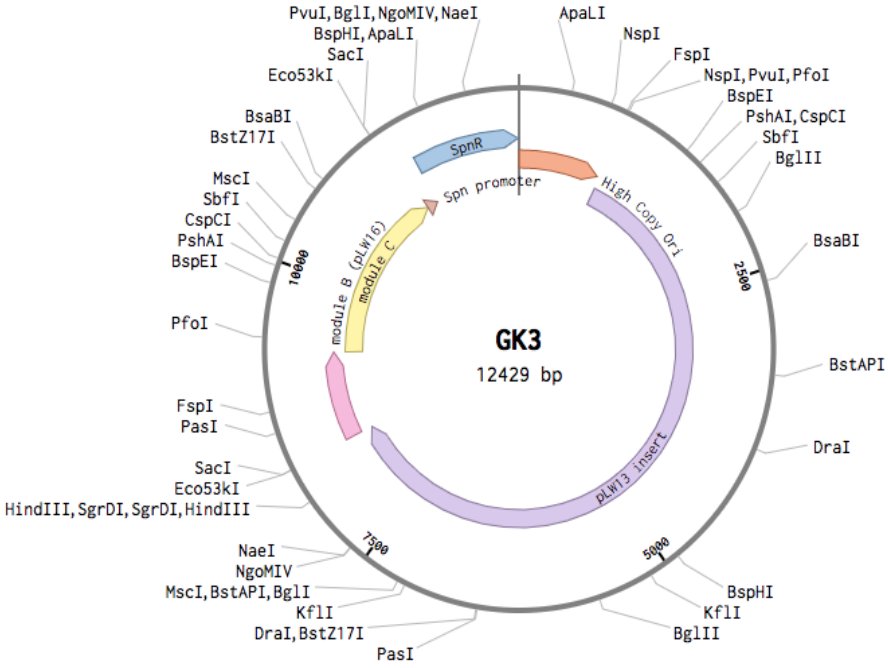


Figure 30. Plasmid map of GK3

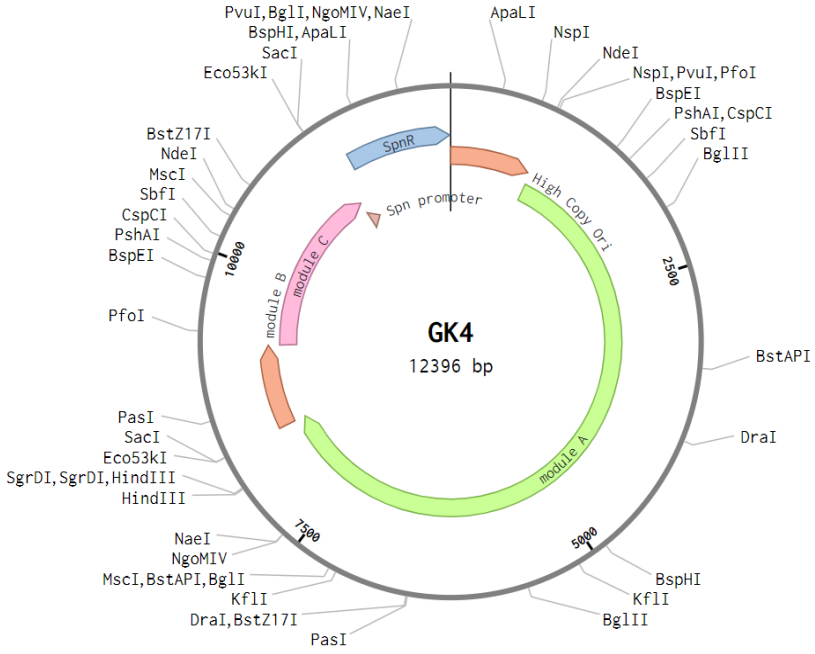


Figure 31. Plasmid map of GK4

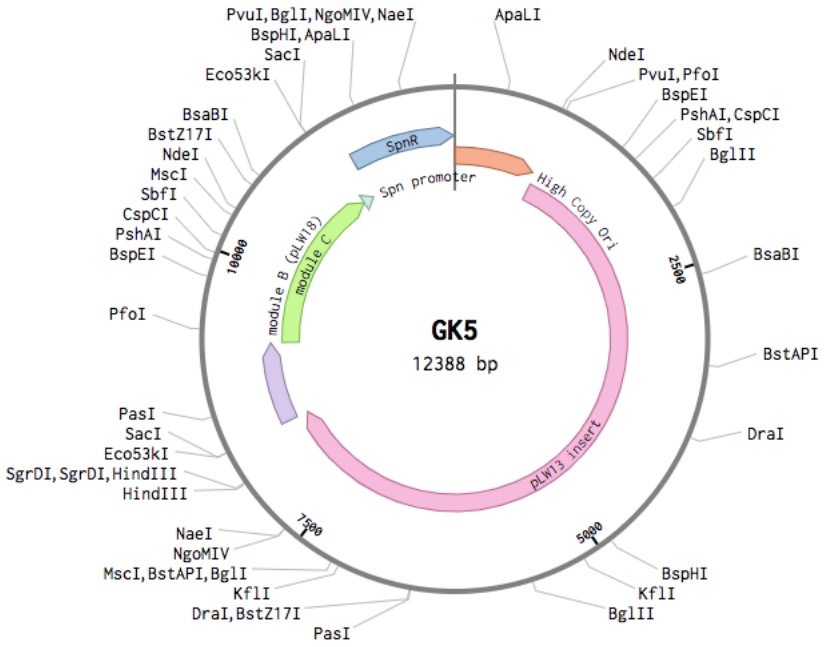


Figure 32. Plasmid map of GK5

A large scale (100 mL) liquid culture of LB medium with the presence of appropriate antibiotic (Spectinomycin) was initiated from confirmed GK colonies to use in protoplast transformation (Figure 33).

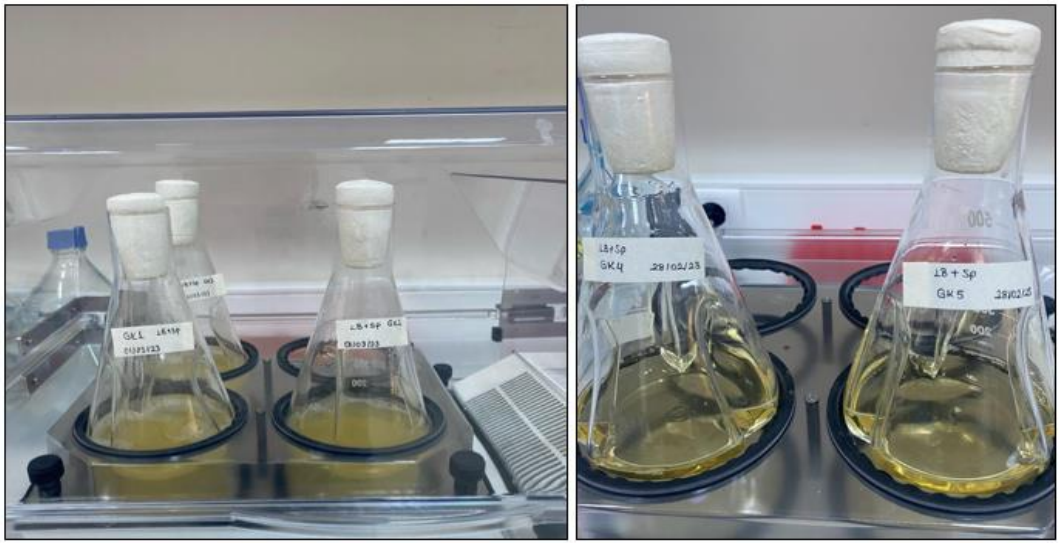


Figure 33. Large-scale liquid cultures of GK samples in 100 mL

Plasmid DNA isolation was performed using the Macherey-Nagel midi prep isolation kit from cultures which was grown over-night at 37^{o}C in a shaker incubator. The steps applied in DNA isolation are given below.

1. After overnight incubation, grown GK cultures were centrifuged at 4100xg for 20 minutes at 4^{o}C. The supernatant was removed, and the cells were precipitated in 50 mL falcons.
2. 8 mL Resuspension Buffer (RES) was added to the precipitated cells and mixing by vortex was performed. At the end of this process, the cells were thawed in RES buffer.
3. 8 mL of Lysis buffer (LYS) was added to the dissolved cells, and they were gently mixed 5 times. This was followed by a 5 min incubation in the presence of LYS buffer at room temperature.
4. After incubation, lysis was stopped by adding 8 mL of Neutralization buffer (NEU) and gently mixed until the cell solution became white.
5. Afterwards, the samples in the falcon were centrifuged at 4100xg for 15 minutes. After centrifugation, the supernatant was transferred to a filter.
6. The filtered DNA samples were then washed in two steps with a 5 mL Equilibration buffer (EQU) and 8 mL wash buffer.
7. After the two-step washing, 5 mL of Elution buffer (ELU) was added to the filter and the DNA samples dissolved in ELU buffer were transferred to a clean falcon.
8. Then, 3.5 mL of room temperature isopropanol was added to precipitate the eluted plasmid DNA. They were gently mixed and centrifuged for 40 minutes at 15,000xg speed and 4^{o}C condition.
9. Supernatant was removed, and 2 mL 70% cold ethanol was added to precipitated DNA and they were centrifuged again for 15 minutes at 15,000xg speed and room temperature.
10. Finally, supernatant was carefully removed, and they were incubated at room temperature to remove ethanol completely. After that plasmid DNAs were dissolved in 120 µL sterile ddH_2O.

After plasmid isolation was performed, DNA concentration of them was measured by Qubit. The concentration results are shown in Table 14. Thus, the DNAs were ready to be used in protoplast transformation.

Table 14. DNA concentration of final plasmids which are used in protoplast transformation.

Targeted Plasmid	DNA concentration (ng/µL)
GK1	1004 ng/µl
GK2	900 ng/µl
GK3	920 ng/µl
GK4	1920 ng/µl
GK5	1000 ng/µl
pMODC-3001	1280 ng/µl

2.4. Obtainment of Chardonnay grapevine plants

Chardonnay cultivars were supplied in steel form by Kavaklıdere A.Ş. and they were preserved in the Manisa Viticulture Research Institute's cold-air storage facilities. In this process, the planting step was carried out (Figure 34) and Chardonnay cultivars were grown in a growth chamber at temperatures 17°C at night and 25°C during the day with the presence of relative humidity between 60-80% (Figure 35).



Figure 34. Planting of Chardonnay cultivars



Figure 35. Chardonnay cultivars in a growth chamber

2.5. Protoplast Isolation

A series of progressive experiments focused on optimizing one element at a time to obtain high number of healthy protoplasts. Optimization of protoplast isolation protocol was performed based on previous studies Yoo et al. (2007), Shan et al. (2014) and Zhao et al. (2015). The key parameters that affect the protoplast isolation were implemented and compared to enhance protoplasts isolation efficiency. Applied and optimized parameters are shown in detail in Table 15.

Table 15. Implemented optimization parameters in protoplast isolation.

Implemented parameters	Description of parameters
Leaf age	Young leaves
	Mature leaves
Leaf amount	20 mg
	40 mg
Sterilization of leaves	Surface of leaves were sterilized in 5.25% sodium hypochlorite for 1 min

	and followed second sterilization step by 70% ethanol for 2 min and they were rinsed 4 times by sterile distilled water.
	Antibiotic addition in enzymatic solution
	Washing by sterile distilled water
Cutting style	Random cutting: All parts of leaves were randomly cut into approximately 0.1-0.5 mm pieces by razor blade
	Tape- Sandwich: Using tape to support the leaf's upper surface and another to remove the lowest layer of epidermis.
	Strip cutting: The leaves without petiole part were gently cut into 0.5-1.0 mm strips on filter paper.
Pretreatment	Before enzymatic digestion, leaf samples were incubated with 0.6M mannitol
	No pretreatment
Enzymatic digestion time	4 hours
	8 hours
	16 hours
	20 hours
Separation of protoplasts from enzymatic solution	Filtration of protoplasts by nylon mesh which has 40 µm pore size
	Filtration of protoplasts by nylon mesh which has 70 µm pore size
Separation of protoplasts after washing with W5	Sucrose gradient
	Ice incubation
	Centrifugation at 150 x g using swinging rotor

Furthermore, certain protocol stages did not change during the isolation experiments. As a result of the implemented parameters, protoplast isolation protocol was optimized. According to optimized protocol, fresh young leaves were used as explants for each protoplast isolation experiment. 1.4 gram of youngest leaves (Figure 36) were weighed by precision scale. For protoplast isolation, three different cutting styles were implemented. While the first cutting style was performed as randomly, harsh and bulk cutting, second cutting style was implemented by tape-sandwich method. In tape-sandwich method, while 3M tape was sticked on the upper epidermis layer of the leaf, clear tape was sticked on the lower epidermis layer of the leaf. The lower epidermal layer was peeled away by removing of tape. In the strip cutting style, leaves were gently cut into strips as 0.5-1.0 mm on the filter paper by razor blade with the removing of petiole part. The three implemented cutting styles are shown in Figure 37. In optimized protocol, leaves were cut by strip cutting style and the strips were transferred into 60 mL enzyme solution without waiting. The enzyme solution content was not changed in protoplast isolation experiments. According to literature work, enzyme content which was shown best result was used. The enzyme solution content is shown in Table 16.

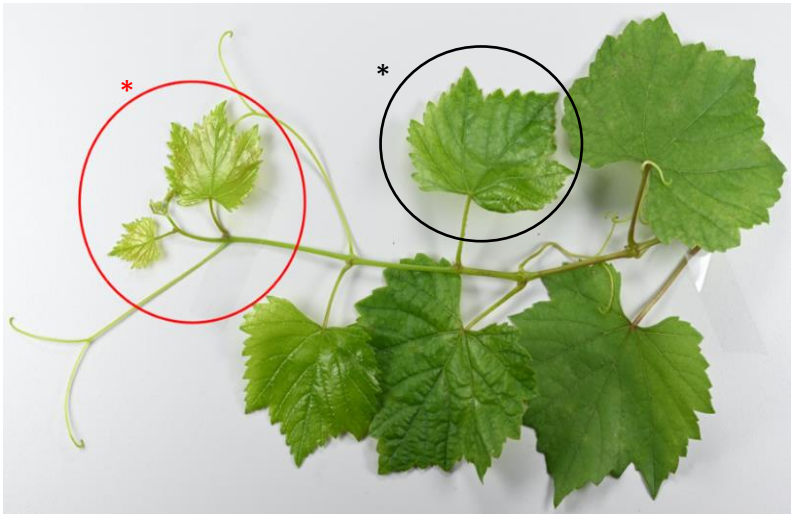


Figure 36. Leaf samples used for protoplast isolation (*: young leaves which are used in the optimized protoplast isolation protocol. *: mature leaf tissue).

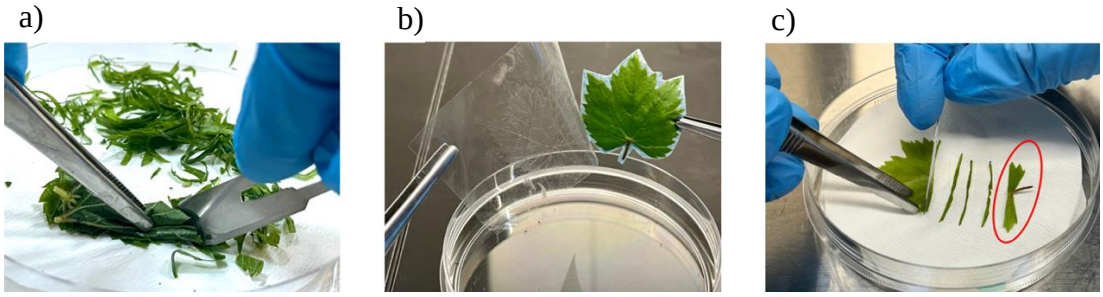


Figure 37. Different cutting styles of leaves which are performed in this study. a) random cutting style, b) tape-sandwich method, and c) strip cutting (petiole part is indicated by red color).

Table 16. Content of enzyme solution and their concentration

Component	Concentration
Cellulase R10 (Yakult, Japan)	1.5 %
Macerozyme R10 (Yakult, Japan)	0.75 %
D (-) Mannitol	0.6 M
$CaCl_2$	10 mM
MES, pH 5.7	10 mM
BSA	0.1 %
ddH_2O	Up to 100 mL

Strip samples in petri dish which includes enzyme solution were placed into desiccator for vacuum infiltration at ~400–500 mmHg for 30 min in the dark with vacuum cycles in every ten minutes as 3 stages. The vacuum was then released, and the strips were incubated with the presence of enzyme solution in the dark with gentle shaking (50 rpm) on a shaker at room temperature for 8 hours. After the digestion was completed, the protoplasts were released, and the digestion was stopped by adding an equal volume of W5 solution and gently mixing for one minute. The content of W5 buffer is shown in Table 17.

Table 17. Content of W5 buffer and their concentration

Component	Concentration
NaCl	154 mM
$CaCl_2$	125 mM
KCl	5 mM

D (+) Glucose	5 mM
MES, pH 5.7	2 mM
ddH_2O	Up to 1000 mL

Subsequently, the protoplasts underwent filtration using a 70 µm nylon mesh and were centrifuged at 150xg in a swinging bucket rotor for 5 minutes at room temperature (RT) with lowest acceleration and deceleration. To maximize the protoplast yield, a second washing and centrifugation step was performed after the removing of supernatant and transferring a clean falcon tube. After centrifugation, settled protoplasts in the bottom of falcon tubes were combined and dissolved in 2 mL of MMG solution. The contents of the MMG solution are detailed in Table 18. The steps which were applied in protoplast isolation protocol are shown in detail in Figure 38.

Table 18. Content of MMG buffer and their concentration

Component	Concentration
D (-) mannitol	0.4 M
$CaCl_2$	100 mM
$MgCl_2$	15 mM
MES, pH 5.7	4 mM
ddH_2O	Up to 1000 mL

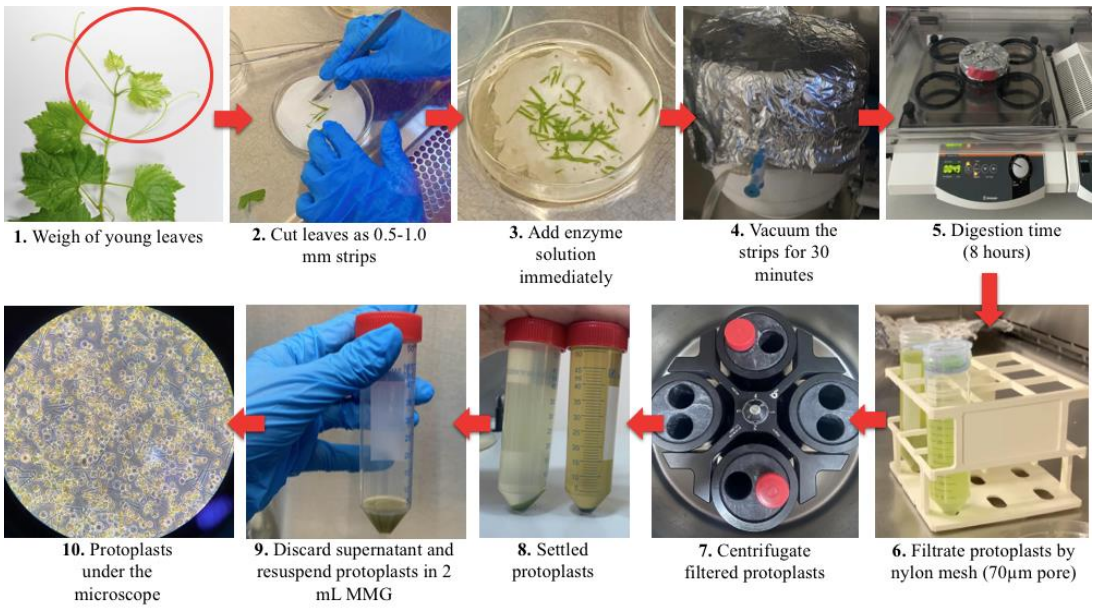


Figure 38. Workflow of optimized protoplast isolation protocol

The protoplasts were counted and observed by using an Olympus CKX53 microscope (Olympus, Tokyo, Japan) with a hemocytometer. Protoplast yield was calculated as the protoplasts number per gram fresh weight (FW) of used leaf tissue. Fluorescein diacetate (FDA) staining was performed to assess the viability of protoplast. Firstly, FDA was dissolved in DMSO (5 mg/ml), and they were added into protoplast solution to reach a final concentration of 0.05%. After that, they were incubated in the dark for 2 minutes. The viable protoplasts which are FDA-stained were observed by using an Olympus IX53 inverted fluorescence microscope (Olympus, Tokyo, Japan). The viable cells fluorescence as green color after staining, whereas the dead cells and cellular debris remained dark. The viability of protoplast was calculated as follows.

$$\text{Viability (\%)} = \left(\frac{\text{Total Fluorescent protoplast number}}{\text{Total protoplast number}}\right) \text{x } 100$$

2.6. PEG mediated transformation for protoplasts

Transformation of grapevine protoplasts was performed using a polyethylene glycol (PEG)–Ca^{2+} transformation method with some modifications (Yoo et al., 2007; Shan et al., 2014; Zhao et al., 2015). Firstly, the procedure was optimized according to the key parameters that affect the transformation efficiency like different protoplast number, different PEG incubation time, incubation time after transformation, and incubation buffer after transformation to increase transformation efficiency. Implemented and optimized parameters in transformation of protoplast are shown in detail in Table 19. Three independent replicates were performed to assess each factor in transformation experiment.

Table 19. Implemented optimization parameters in protoplast transformation.

Implemented parameters	Description of parameters
Protoplast number	$2.5x10^5$
	$5x10^5$
	$1x10^6$
	$2x10^6$
PEG incubation time	2 min
	5 min

	10 min
	15 min
Incubation buffer after transformation	W5
	MMG
Incubation time after transformation	16 h
	48 h

According to implemented parameters, protoplast transformation protocol was optimized. $5x10^5$ protoplast number was used for each transformation set. 10 µg of GKs DNA was used for transformation of protoplasts. Used DNA amount of GK plasmids is shown in Table 20. According to Table 20, total volume of GK plasmids was completed to 15 µL during the transformation. $5x10^5$/200 µL protoplasts were gently mixed with 10 µg GK plasmids in 2 ml round-bottomed centrifuge tubes.

Table 20. Used plasmid DNA amount in transformation of protoplasts.

Plasmid DNA	**Amount**
GK1	9.96 µL
GK2	11.1 µL
GK3	10.86 µL
GK4	5.20 µL
GK5	10 µL
pMODC-3001 (+)	7.81 µL

Then, 10 mL PEG solution was freshly prepared and filtered. Firstly, 4 gr of PEG was weighed by precision scale and added to 15 mL falcon tube. Then, 2 mL ultra-pure water was added to the falcon, and the solution was vortexed. After that, 2.5 mL mannitol from 0.8M mannitol stock and 1 mL CaCl2 from 1M stock were added to the same falcon in respectively. Total volume was filled up to 10 mL and they were vortex until PEG solution was dissolved homogenously. An equal volume of PEG solution was added to 2 ml round-bottomed centrifuge tubes which includes GK plasmids and protoplasts, and they were gently mixed. The content of PEG solution is shown in Table 21. Protoplast-PEG mixture was incubated for 5 minutes in the dark at room temperature. After PEG incubation time, 900 µL W5 solution was added to stop the PEG incubation. Then, the mixture was centrifuged at room temperature and 100xg with the lowest acceleration and deceleration for 5 min to collect protoplasts. After centrifugation, supernatant was poured, and protoplasts were resuspended in 2

mL W5 solution. They were transferred to 6-well plates and incubated in the dark condition for 16 hours. The workflow of applied protoplast transformation protocol is shown in Figure 39.

Table 21. Content of PEG solution

Component	Concentration
Mannitol	0.2 M
$CaCl_2$	0.1 M
PEG-4000	40% (w/v)

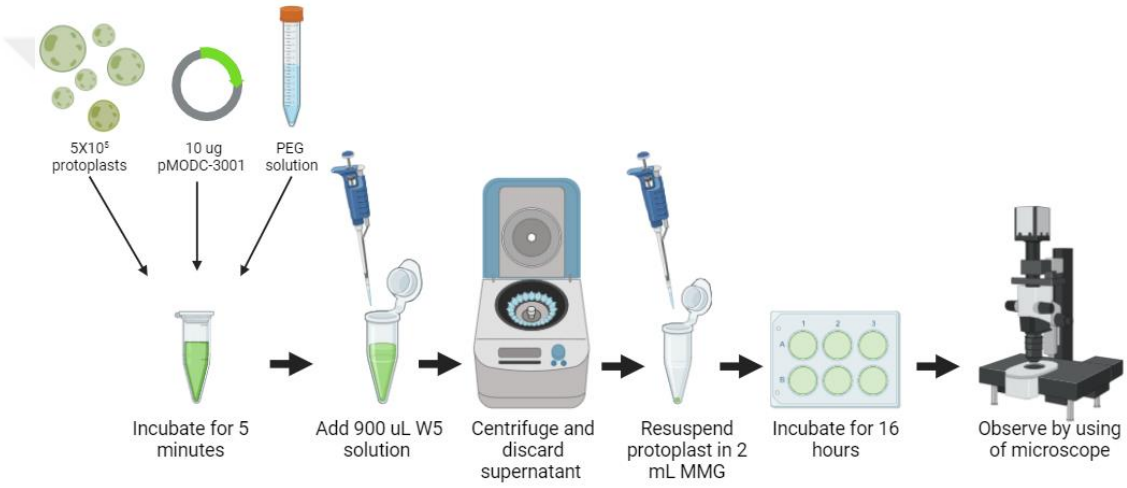


Figure 39. Workflow of applied protoplast transformation protocol (Biorender)

After over-night (16 hours) incubation, protoplasts were observed by using an Olympus IX53 inverted fluorescence microscope (Olympus, Tokyo, Japan) and GFP glowing was observed at 488 nm. Transformation efficiency was calculated by equation as follows.

$$\text{Transformation efficiency (\%)} = \left(\frac{\text{Transformed protoplast number}}{\text{Total protoplast number}}\right) \text{x } 100$$

Three replicates for transformation of each GK plasmids were performed. After the calculation, the transformation efficiencies between all GK constructs were compared and the data was recorded.

2.7. Amplicon Sequencing for transformed protoplast samples

After transformation of protoplasts, genomic DNA was isolated from the protoplasts to send them for amplicon sequencing. Doyle & Doyle (1990) DNA isolation protocol was applied for DNA isolation from protoplasts. The steps of the protocol are given in detail below.

1. Each of the protoplast samples in the well-plate was transferred into 2 mL Eppendorf tubes and centrifuged at 10,000xg for 3 minutes. The supernatant was removed, and the bottom-settled protoplasts were dissolved in 500 µL of CTAB solution.
2. Samples were incubated in CTAB solution at 55^{o}C for 30 minutes. After the incubation period was completed, 500 µL of chloroform was added to each sample and the samples were gently mixed.
3. After addition of chloroform, the samples were centrifuged at 10,000xg for 5 minutes. After centrifugation, the supernatant was transferred to clean Eppendorf tubes and 1 mL of cold isopropanol was added.
4. After the addition of cold isopropanol, the Eppendorf tubes were gently mixed for 50 times and incubated at -20^{o}C for 30 minutes.
5. After 30 minutes of incubation, the samples were centrifuged at 10,000xg for 10 minutes. After centrifugation, the supernatant was removed, and the pellet was washed with 1 mL of cold 70% ethanol.
6. Samples which are washed with ethanol were centrifuged at 10,000xg for 5 minutes. The supernatant was removed, and the pellet was allowed to dry. After the ethanol was evaporated and the pellet was dried, settled DNA of transformed and non-transformed protoplasts were dissolved in 25 µL of sterile ultra-pure water.

Therefore, DNAs both of transformed and non-transformed protoplasts were isolated. DNA concentrations were measured by Qubit (Invitrogen by Thermo Scientific). As a result of the Qubit measurement, the concentrations were recorded as too low. Then, the first round PCR with protoplast DNA samples was performed for the amplicon sequencing. Amplicon sequencing was conducted by Cornell University, Institute of Biotechnology through Prof. Dr. Adam Bogdanove. Since Illumina sequencing gives 2x150bp reads, primers were designed with a maximum DNA fragment size of 150 bp to be amplified by PCR and appropriate adapter sequences were added to these primers and synthesized. Detailed information of primers which

were used in PCR step for amplicon sequencing is given in Table 22. The adapter sequence added to the forward primer is shown in red and the adapter sequence added to the reverse primers is shown in blue.

Table 22. Primer information designed for amplicon sequencing of GK plasmids.

Primer name	Sequence (5'-3')	Length of primer	GC content	T_m temperature	PCR product size
*pLL3*_D131A_ampseq_F	TCGTCGGCAG CGTCAGATGTG TATAAGAGACAG CCACATCCACCA TTGCGTGC	20 bp	60	59	291
*pLL3*_D131A_ampseq_R	GTCTCGTGGGC TCGGAGATGTGTA TAAGAGACAGCAT CGT GATGCGAGAAAAA GTT GTTGG	27 bp	46	59.4	
*pLL3*_R218K_ampseq_F	TCGTCGGCAG CGTCAGATGTG TATAAGAGACAG CTCGCATCACGAT GA GGTGATGC	23 bp	56	60	287
*pLL3*_R218K_ampseq_R	GTCTCGTGGGC TCGGAGATGTGTA TAAGAGACAGCTC CCC TGGGTTGATGGTG G	20 bp	65	59.5	
*pLL13*_D131A_ampseq_F	TCGTCGGCAG CGTCAGATGTG TATAAGAGACAGC AA ATCACGGGCGGTG GCT	19 bp	63	60	286

*pLL13*_D131A_ampseq_R	GTCTCGTGGGCTCGGAGATGTGTATAAGAGACAGGTTGTTTGATAGGGTGATGGCGGT	24 bp	50	59	
*pLL13*_R218K_ampseq_F	TCGTCGGCAGCGTCAGATGTGTATAAGAGACAGCTCGCATCATGACAAAGTGATGCTCC	26 bp	50	60.3	308
*pLL13*_R218K_ampseq_R	GTCTCGTGGGCTCGGAGATGTGTATAAGAGACAGCGGTGGTGCTGTGTAACGGT	20 bp	60	59.4	
*PDS1*_ampseq_For	TCGTCGGCAGCGTCAGATGTGTATAAGAGACAATGACTCAATTCAGATATGTTTCTGCGGTG	30 bp	40	59.4	279
*PDS1*_ampseq_Rev	GTCTCGTGGGCTCGGAGATGTGTATAAGAGACAGGGGCAGAAATCCTTCCTCCGC	21 bp	62	59.6	

The reaction components and their amount used in the PCR for amplicon sequencing are given in Table 23 and the reaction steps and number of cycles are given in Table 24. After PCR step, the samples were run on a 1% gel.

Table 23. Reaction components and quantities used in PCR for amplicon sequencing.

PCR components	Amount
2X Q5 High Fidelity enzyme buffer	12.5 µl
Forward primer	1 µl
Reverse primer	1 µl
ddH_2O	6.5 µl
DNA	4 µl

Total volume	25 µl

Table 24. Temperature, time, and number of cycles applied in the first PCR round for amplicon sequencing.

Temperature	Duration	Cycle
98ºC	30 s	-
98ºC	10 s	30
T_a (Primer binding temperature)	30 s	
72ºC	30 s	
98ºC	10 s	20
T_a (Primer binding temperature)	30 s	
72ºC	1 dk	
72ºC	2 dk	-
+4	∞	

The samples were separated on 1% agarose gel electrophoresis and the target bands were extracted from the gel using the Monarch DNA Gel extraction kit. The steps of gel extraction are given in detail below.

1. Under the transilluminator, agarose gel was observed, and the PCR products (DNA fragments) were sliced by razor blade. All gel slice was weighed in Eppendorf tube by precision scale. Exposure time of UV light was kept as short as possible to minimize.
2. 4 volumes of Monarch Gel Dissolving Buffer per mg gel slice were added to all Eppendorf tube.
3. After addition of Monarch Gel Dissolving Buffer, all samples were incubated in dry bath at 50°C for 10 minutes with the inverting periodically until the gel slice is completely dissolved.
4. Dissolved PCR product samples were loaded through column. They were spin-down for 1 minute at 16,000xg and supernatant was discarded, and DNA remained filter of column (Note: samples which exceed 800 µL volume were spin down at two-stage because column capacity is max 800 µL).

5. After that, columns were re-inserted into collection tubes. 200 µL DNA wash buffer was added to column and the samples spin down again for 1 minute at 16,000xg. Two-stages washing step was performed with DNA wash buffer. Then, supernatant was discarded flow-through.
6. The washed columns were transferred to clean 2 ml round-bottomed centrifuge tubes.
7. In next, 20 µL DNA Elution Buffer was added to filter column of all sample tubes. They were incubated for 2 minutes at room temperature. At the end, they were spin down for 1 minute at 16,000xg.

All obtained extracted PCR product samples were transferred to 200 µL PCR tubes. The collected samples were sent to Cornell University. Amplicon sequencing was performed at Cornell University Institute of Biotechnology Sequencing unit and sequence results were provided as fastq files. Sequencing results were analyzed using the web-based program "Crispresso2" (http://crispresso2.pinellolab.org/submission) to calculate mutation efficiency (editing efficiency).

SECTION THREE

RESULTS AND DISCUSSION

3.1. Confirmation of Prime Editing Designed Constructs

Confirmation of the GK plasmids which is designed by Prime Editing approach was conducted by *Sac*I restriction digestion. DNA band profile which is expected by restriction digestion of GK plasmids with *Sac*I enzyme was obtained in Benchling web tool application as a virtual digest (Figure 40).

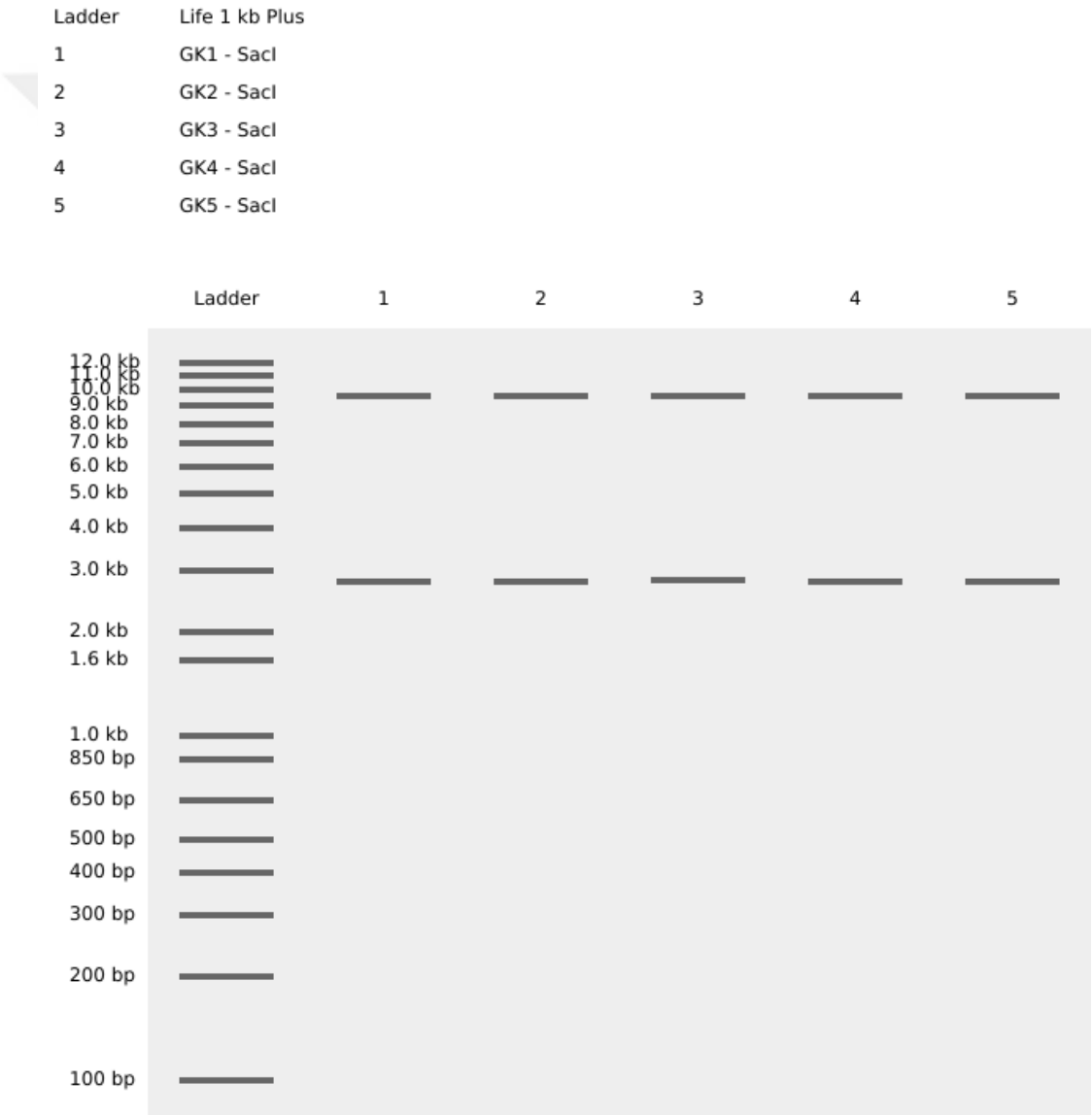


Figure 40. Virtual digest of GK plasmids by *Sac*I enzyme

As a result of the restriction digestion with *Sac*I enzyme, images of GK plasmids which were ran on the 1% agarose gel are shown in Figure 41.

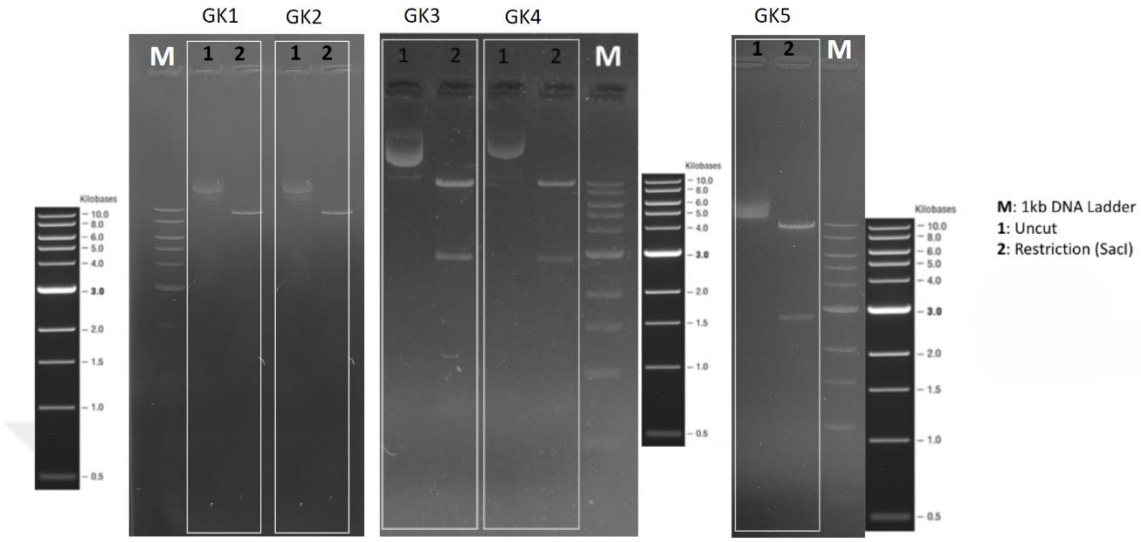


Figure 41. 1% agarose gel images of GK plasmids in terms of restriction digestion

When agarose gel images of GK plasmids (Figure 41) were compared to virtual digestion (Figure 40), they showed that the same DNA fragment sizes with the expected band profile as 9.6 and 2.8 kb. In this way, GK plasmid constructs were confirmed by restriction digestion for protoplast transformation to assess prime editing constructs.

3.2. Protoplast Isolation from Chardonnay leaves

A number of parameters were implemented in the study to optimize an effective protoplast isolation from leaf tissue of grapevine. A series of optimization steps were performed to enhance the yield and viability of protoplast for transformation.

3.2.1. Effect of explant tissue and tissue age in protoplast isolation

Numerous tissue and organ types, such as leaves (Zhao et al., 2015), calli (Scintilla et al., 2022; Tricoli and Debernardi, 2024), stems (Alleweldt, 1988), berries

(Fontes et al., 2010), and roots (Alleweldt, 1988), can be used to isolate grapevine protoplasts. These many sources of tissue have unique properties that require different culture conditions (Fontes et al., 2010; Wang et al., 2015; Zhao et al., 2015). Protocols for grapevine callus, stem, and berry tissues that are currently in use have drawbacks, including low yield and a large time commitment (Fontes et al., 2010; Zhao et al., 2015). These limitations prevent the progressing of genome editing studies. On the other hand, the mesophyll tissues in leaves provide highly useful source of numerous uniform cells to isolate protoplasts (Li et al., 2020).

The tissue age also plays a crucial role in terms of protoplast yield and viability, especially in woody plants (Yohichi Wakita, 1996; Zhao et al., 2015). Selection of proper source is a significant factor at the first stage to obtain a high yield healthy protoplast. Also, reports emphasized that physiological states and leaf age affect the quality of protoplasts during the isolation process (Jiang et al., 2021). Even, Zhao et al. (2015) reported that the significance of using young leaves to isolate highly efficient protoplasts from *V. vinifera* cv. Rizamat and the wild Chinese grapevine (Zhao et al., 2015). They also indicated that using of older leaves decreases the protoplast yield. In the preliminary experiments of this study, using of mature leaves which are shown in Figure 36, caused to obtain lots of debris instead of healthy protoplasts. The use of mature leaves for protoplast isolation was performed in 3 replicates. However, the protoplast number was observed too low to count. Therefore, the data are not shown. Thus, the youngest leaves were used in the progressive set of experiments (Figure 36). In line with our results, it was also seen that obtainment of high yield and viable protoplast from older leaves of various plant species like orchids, maize, and rice is challenging (Ren et al., 2021).

In the next stage, different amounts of young leaves as 20 mg and 40 mg per mL extraction buffer were compared in terms of protoplast yield. While 20 mg young leaves per mL extraction buffer was used $75x10^6$/g weight protoplast yield was obtained, using of 40 mg young leaves per mL extraction buffer caused to obtain more debris instead of healthy protoplasts. Also, the comparison of microscopic imaging of protoplast yield at different concentrations of 20 mg and 40 mg per mL extraction buffer is shown in Figure 42. Also, Figure 42 proved that healthy protoplasts were

obtained with the highest yield by using of 20 mg leaves per mL extraction buffer. However, more debris were obtained instead of healthy protoplasts by using of 40 mg leaves per mL extraction buffer. In this sense, it was observed that using of 40 mg of leaves per 1 mL of extraction buffer was more than sufficient for a good and homogenous digestion. In consequence, inadequate digestion conditions with 40 mg of leaves caused to release of fewer protoplasts and to collect more debris. In addition, Zhao et al. (2015) proved that the using of 20 mg mesophyll leaf tissue of grapevine per mL extraction buffer was sufficient to obtain high yield and healthy protoplasts (Zhao et al., 2015). They obtained the highest yield as approximately $3x10^4$ protoplasts when the using of 20 mg of tissue per mL of extraction solution. However, when 20 mg of tissue per mL of extraction solution was used in this study, the highest yield was obtained as $1.5x10^6$ protoplasts. Therefore, using of 20 mg of young leaves were first optimized parameter in the highly efficient protoplast isolation from Chardonnay mesophyll leaf tissue in this study.

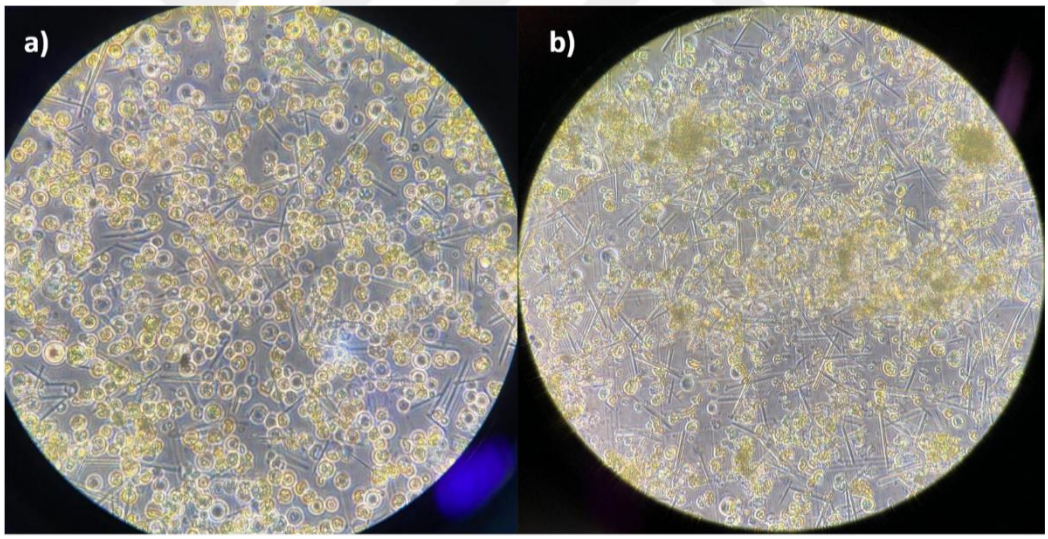


Figure 42. Effects of leaf amount of grapevine on protoplast isolation a) Protoplasts obtained with 20 mg of young leaves b) Protoplasts obtained with 40 mg of young leaves.

3.2.2. Effect of surface sterilization of leaves in protoplast isolation

The effect of surface sterilization on grapevine leaves in terms of protoplast isolation efficiency was also investigated in this study. It was observed that performing

of surface sterilization of leaves by using of Clorox and ethanol decreased the protoplast yield because of damaging the tissue. Additionally, antibiotics were added to enzyme solution for the sterility. However, antibiotics did not show any visible effect to prevent contamination during the protoplast isolation. In this study, when leaves were washed with only water and immediately afterwards experiments were conducted at sterile environments, no contamination was observed. While surface sterilization of grapevine leaves was performed in previous studies of protoplast isolation (Wright, 1985), sterilization process was not effective in this study. In addition, surface sterilization of grapevine leaves were not mentioned in reports of mesophyll protoplast isolation.

3.2.3. Effect of Cutting style in protoplast isolation

Three different cutting style were assessed in this study to determine the most efficient cutting style for protoplast isolation from Chardonnay leaves. Implementation of random cutting in protoplast isolation caused to tissue damaging and this situation resulted in failed to obtain healthy protoplasts. With the application of random cutting style, undigested and damaged protoplasts were obtained as a clump. The microscopic imaging of the protoplast which are obtained by implementation of random cutting is shown in Figure 43a.

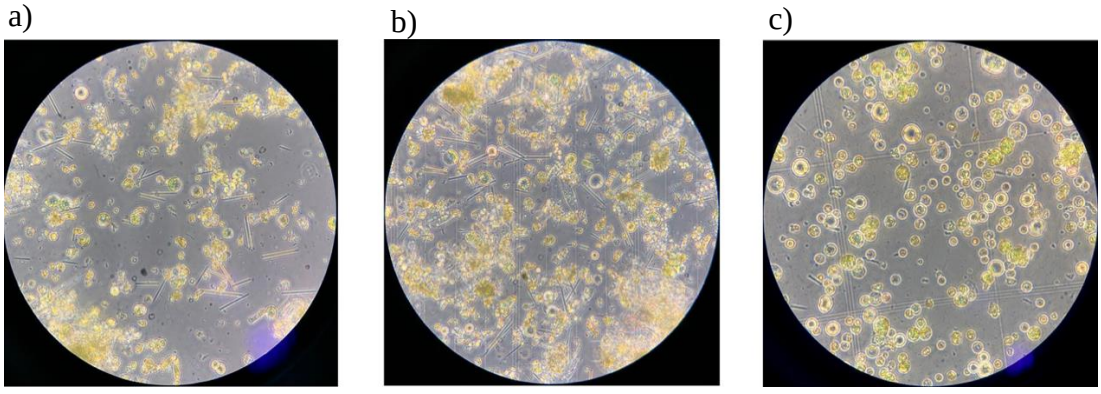


Figure 43. Imaging of protoplasts under the bright- field microscope by the implementation of different cutting styles. a) microscopic imaging of protoplast by application of random cutting, b) microscopic imaging of protoplast by application of tape-sandwich method, c) microscopic imaging of protoplast by application of strip cutting.

Although tape-sandwich method was previously performed in different plant species such as *Arabidopsis*, and *Artemisia japonica* (Wu et al., 2009; Deng et al., 2023), the method was applied for grapevine this study at a first time. The imaging of protoplasts under the bright field microscope by application of tape-sandwich method is shown in Figure 43b. According to microscopic imaging, it was seen that tape-sandwich method was not show effective digestion to obtain healthy protoplasts. The leaf tissues were not digested homogenously by this method. Also, similar results with this study were proved by Moon et al. (2021) in potato protoplasts in terms of ineffective digestion.

In this study, strip cutting by gentle acting provided to obtain high number of protoplasts. The imaging of protoplast under the bright field microscope which are obtained by application of strip cutting is shown in Figure 43c. In contrast with random cutting and tape-sandwich method, health protoplasts were obtained without undigested clumps and debris. Also, the importance of gentle acting in leaf cutting was highlighted in the other studies for obtaining of high number of protoplasts (Wu et al., 2009; Moon et al., 2021; Deng et al., 2023). Correspondingly, Yoo et al. (2007) proved that gentle cutting as a strip which they performed resulted in obtaining of a high number of protoplasts in *Arabidopsis* (Yoo et al., 2007). Moreover, while Zhao et al. (2015) obtained an average protoplast yield as $3.3x10^6$/g from *V. vinifera* cv. Rizamat and the wild Chinese grapevine leaves by the application of gentle cutting strips as 0.5-1.0 mm (Zhao et al., 2015), the highest protoplast yield was obtained as a $75x10^6$/g from *V. vinifera* cv. Chardonnay leaves by the gentle cutting strips as 0.5-1.0 mm with the application of optimized protocol in this study. On the other hand, Malnoy et al. (2016) did not mentioned about the importance of cutting style of grapevine leaves for protoplast isolation in their study. Also, one of the most critical things is to avoid dry conditions of laminar flow cabinet during the strip cutting. Therefore, strips should be transferred into enzyme solution immediately.

3.2.4. Effect of pretreatment in protoplast isolation

In this study, the effect of pretreatment was evaluated in terms of obtaining of high yield protoplasts from Chardonnay leaves. Reports highlighted that the pretreatment applications enable the penetration of enzyme solution through the cell

wall and cell membrane of plant (Reed and Bargmann, 2021; Li et al., 2022b; Chen et al., 2023). In addition, 0.4-0.6M mannitol mediated pretreatment was applied in leaves of different plant species like *Phalaenopsis*, *Brassica*, and *Artemisia japonica* in the previous studies (Li et al., 2018; Sun et al., 2019; Deng et al., 2023). They were indicated that mannitol mediated pretreatment facilitated the penetration of enzyme solution through of plant cells in their protocols. Although the pretreatment for Chardonnay leaf strips was applied in this study with the 0.6M mannitol incubation before the enzymatic digestion, pretreatment was not effective for high yield protoplast isolation. In this study, three independent replicates were performed for pretreatment and non-pretreatment applications. The other variables were kept as constant. The effect of pretreatment was compared in terms of protoplast yield. As a result of the three independent replications, the protoplast yield corresponding of pretreatment and non-pretreatment step is shown in Figure 44a. According to graphical result the highest protoplast yield was obtained by non-pretreatment implementation instead of mannitol (+) mediated pretreatment application. At the same time, the avoidance of pretreatment in protoplast isolation from grapevine leaves and callus in the previous studies proved the results of this study (Zhao et al., 2015; Scintilla et al., 2022). Therefore, pretreatment step was ignored for the progressive protoplast isolation protocol from Chardonnay leaves in this study.

3.2.5. Effect of different digestion time in protoplast isolation

The four various digestion time (4h, 8h, 16h, 20h) were implemented to leaf strips in this study for assessment of protoplast yield. Also, the effect of both extension and shorten of digestion time was evaluated to understand the effect in protoplast isolation efficiency. Three repetitions were performed for each digestion time and protoplast yield corresponding of each digestion time are shown in Figure 44b. According to these results, protoplast yield continued to increase regularly until the 8-hour digestion time. However, when digestion time exceeded 8 hours, the protoplast yield started to decline. The optimal digestion time was proved as 8 hours to obtain high yield protoplasts from Chardonnay leaves. Also, obtained protoplasts after different digestion time were observed under the inverted bright-field microscope. The microscopic imaging of these protoplasts is shown in Figure 45. According to microscopic images, there are undigested clumps of leaf tissue as shown in Figure 45a.

Therefore, it was seen that 4 hours incubation time was not efficient to digest leaf tissue homogenously. According to Figure 45c and Figure 45d, prolonged digestion time like 16 hours and 20 hours caused to rupturing of protoplasts and they lost their characteristic spherical shape. However, healthy and spherical shaped protoplasts were obtained with the implementation of 8 hours digestion time as shown in Figure 45b.

Yoo et al. (2007) also reported that the optimal digestion time can be changed depending on various parameters like material type, purpose of research and outcomes, types and concentrations of enzyme which is used in the protoplast isolation. (Yoo et al., 2007). For instance, the first study on the isolation of protoplasts from grapevine leaf mesophyll tissues found that two to three hours was the ideal incubation time for producing the high yield of viable protoplasts, with two and a half hours being the typical amount of time (Bessis, 1990). Diversly, Malnoy et al. (2016) isolated protoplasts from Chardonnay by incubating the embryogenic calli and leaves for four hours and overnight, respectively (Malnoy et al., 2016).

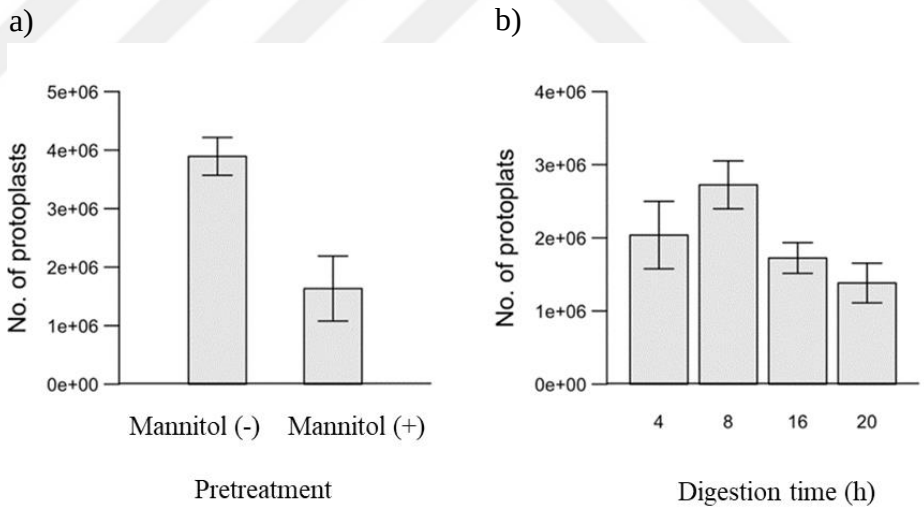


Figure 44. Comparison of protoplast yield depend on a) pretreatment, and b) different digestion time.

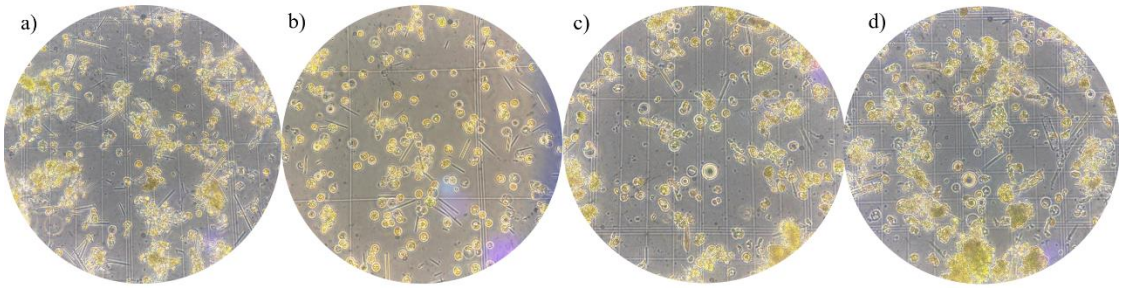


Figure 45. Visualization of obtained protoplasts under the inverted bright field microscope after different digestion time a) after 4 hours, b) after 8 hours, c) 16 hours, and d) after 20 hours.

Other reports mentioned that implementation of 16 hours digestion time was the optimal in protoplast isolation from embryogenic callus of different cultivars like Sugraone, Crimson Seedless, Merlot, and Thompson Seedless (Scintilla et al., 2022; Tricoli and Debernardi, 2024). Corresponding to findings of this study, Zhao et al. (2015) investigated different digestion times (6h, 10h, 14h, and 18h) for the isolation of protoplasts from *V. vinifera* cv. Rizamat leaf mesophyll tissues. They were found that 14 hours was the ideal digestion time for the protoplast isolation (Zhao et al., 2015). Different from all these studies, the optimal digestion time was identified as 8 hours for the protoplast isolation from mesophyll leaf tissue of Chardonnay grapevine cultivars in this study. Incoherence of the results are related to nature of protoplast isolation implementations. Therefore, protoplast isolation protocols need to be optimized depend on different grapevine cultivars and experimental purposes.

3.2.6. Separation of protoplasts from enzymatic solution and after washing with W5 buffer

Following enzymatic digestion, filtration of protoplasts was performed by using of nylon mesh filters with different pore sizes (40 and 70 µm) to separate clumps and debris. The presence of bigger protoplasts above 40 µm resulted in a low yield, even though the 40 µm filter eliminated clumps and huge cell debris effectively. Therefore, the best pore size of mesh was identified as 70 µm to enhance protoplast yield without breaking of large protoplasts. Other grapevine studies also used similar pore sizes with this study (Zhao et al., 2015; Scintilla et al., 2022; Tricoli and

Debernardi, 2024). On the other hand, sucrose cushion method, ice incubation, and centrifugation steps were assessed to eliminate debris and clumps effectively after washing of filtered protoplasts. For the sucrose cushion method, 5 different sucrose concentrations were prepared as 10%, 15%, 20%, 25% and 30%. These concentrations of sucrose were transferred to 15 mL falcon tubes from highest concentration to lowest concentration. After addition of 2 mL protoplasts, phase separation occurred in over time (Figure 46). The phases were observed under the bright field microscope. While sucrose cushion method successfully applied in in potato and *Arabidopsis* protoplasts (Jeong et al., 2021; Moon et al., 2021), the method was not effective in purification of grapevine protoplasts in this study. Out of the sucrose gradient, ice incubation was also applied for 30 minutes in preliminary experiments for obtain protoplast at the supernatant part with settlement of debris. Although ice incubation was successfully applied in purification of *Uncaria rhynchophylla* and banana protoplasts (Wu et al., 2020; Shao et al., 2023), this technique was not effective for purification of grapevine protoplasts in this study. It was concluded that centrifugation was sufficient for protoplast purification out of the sucrose cushion and ice incubation. Therefore, all parameters were optimized to obtain high number of healthy protoplasts. All parameters selected for use with the optimized protocol are given in Table 25.

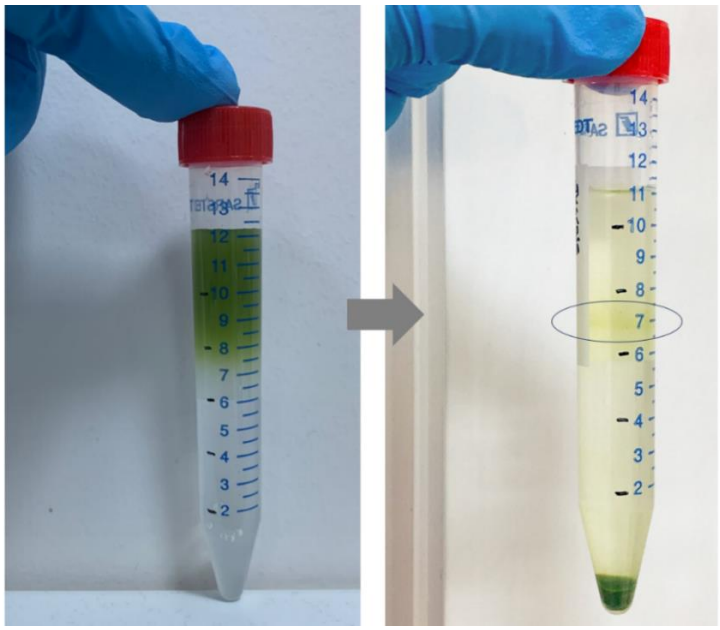


Figure 46. Phase separation after sucrose cushion method

Table 25. Selected application for optimized protoplast isolation protocol

Optimization parameter	Optimized parameter
Leaf age	Young leaves
Leaf amount	20 mg leaf/ mL enzymatic solution
Sterilization of leaves	Only washing with water
Cutting style	Strip cutting
Pretreatment	No pretreatment application
Enzymatic digestion time	8 hours
Separation of protoplast from enzymatic solution	Filtration of protoplasts by nylon mesh with 70 µm pore size
Separation of protoplast after washing with W5	Centrifugation at 150 x g using swinging rotor

3.2.7. Protoplast yield and viability

As a result of the application of optimized protoplast isolation protocol, healthy protoplasts were obtained and microscopic image of them is shown in Figure 47. They were homogenously digested, and healthy protoplasts were got without debris.

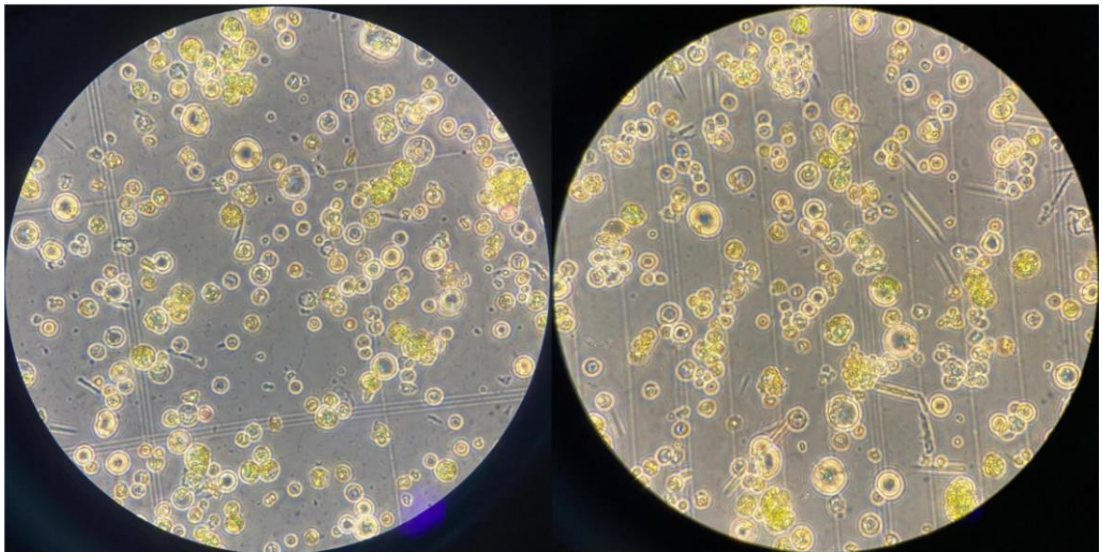


Figure 47. Images of protoplasts in different areas under the inverted bright field microscope

Also, the maximum protoplast yield was counted as $75x10^6$ protoplasts/g leaf weight by using of hemocytometer. The maximum protoplast yield which is obtained in this study was compared with the other grapevine studies. While $40x10^6$ protoplasts/g leaf obtained by Barbier and Bessis (1990), Zhao et al. (2006) obtained yield as $5.7x10^6$ protoplast/g. In addition, Zhao et al. (2015) obtained the highest yield as $3.4x10^5$ protoplasts/g leaf (Bessis, 1990; Zhao et al., 2015). In addition, Malnoy et al. (2016) obtained the highest yield from Chardonnay leaves as $2x10^6$ protoplasts/g leaf (Malnoy et al., 2016). However, it was concluded that the result of this study in terms of obtained protoplast yield from Chardonnay leaves was greater than the result of Malnoy et al. (2016). It was supposed that the reason of the difference between protoplast yield related to concentration of enzyme solution because while Malnoy et al. (2016) used Macerozyme R10–0.1%, Cellulase R10–1% concentration for enzyme solution, the concentration of enzyme solution was used in this study as Macerozyme R10–0.75%, Cellulase R10–1.5%.

After obtaining of protoplasts, their viability was observed and calculated by FDA staining. As a result of the FDA staining, the viability of protoplasts was recorded as 91%. The viable protoplasts were observed under the fluorescence microscope and the microscopic imaging is shown in Figure 48. Furthermore, the viability of the same protoplasts was calculated as 78% one day later by FDA staining.

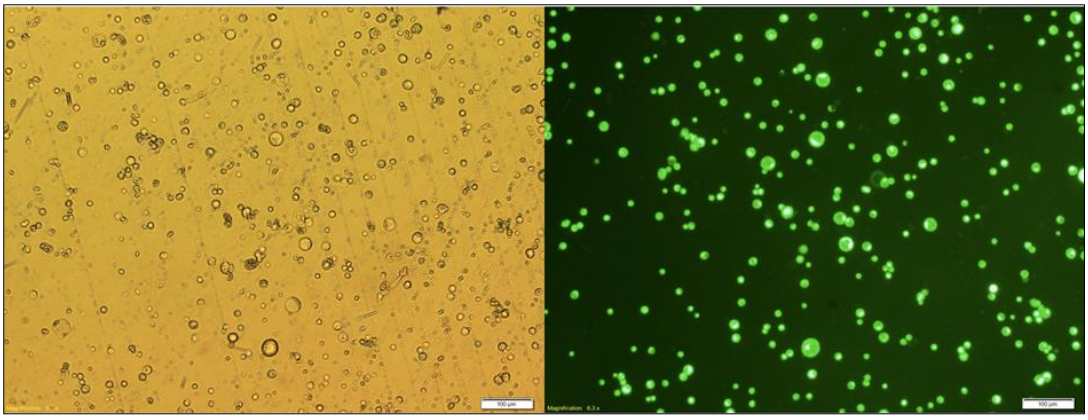


Figure 48. Imaging of viable protoplasts under the bright field and Fluorescence microscope

3.3. Transformation efficiency in protoplasts

Through a series of trials, an effective transformation protocol in grapevine protoplasts was enhanced. This protocol includes several optimization procedures that are applied gradually to improve transformation efficiency. With the optimized transformation protocol, GK plasmids which were designed by prime editing were transferred to obtained protoplasts. The transformation efficiencies of the prime editing constructs were compared between each other.

3.3.1. Effect of protoplast number in transformation efficiencies

In this investigation, the protoplast number was regarded as an important parameter in transformation efficiencies of protoplasts because optimal protoplasts number can be different from one plant species to another. Also, cultivars can also affect the ideal protoplast number for higher transformation efficiency except of plant species. Furthermore, various protoplast numbers were evaluated for effective transformation in various plant species such as *Phalaenopsis*, carnation, grapevine, and passion fruit (Zhao et al., 2015; Li et al., 2018; Adedeji et al., 2022; Wang et al., 2023). According to progressive experiments in this study, four different protoplast numbers as $2.5x10^5$, $5x10^5$, $1x10^6$, and $2x10^6$ were used to evaluate transformation efficiency in Chardonnay mesophyll protoplasts. Three repetition was performed for transformation in each protoplast numbers. The microscopic images which are obtained because of the transformation performed by using 4 different protoplast numbers are given in Figure 49.

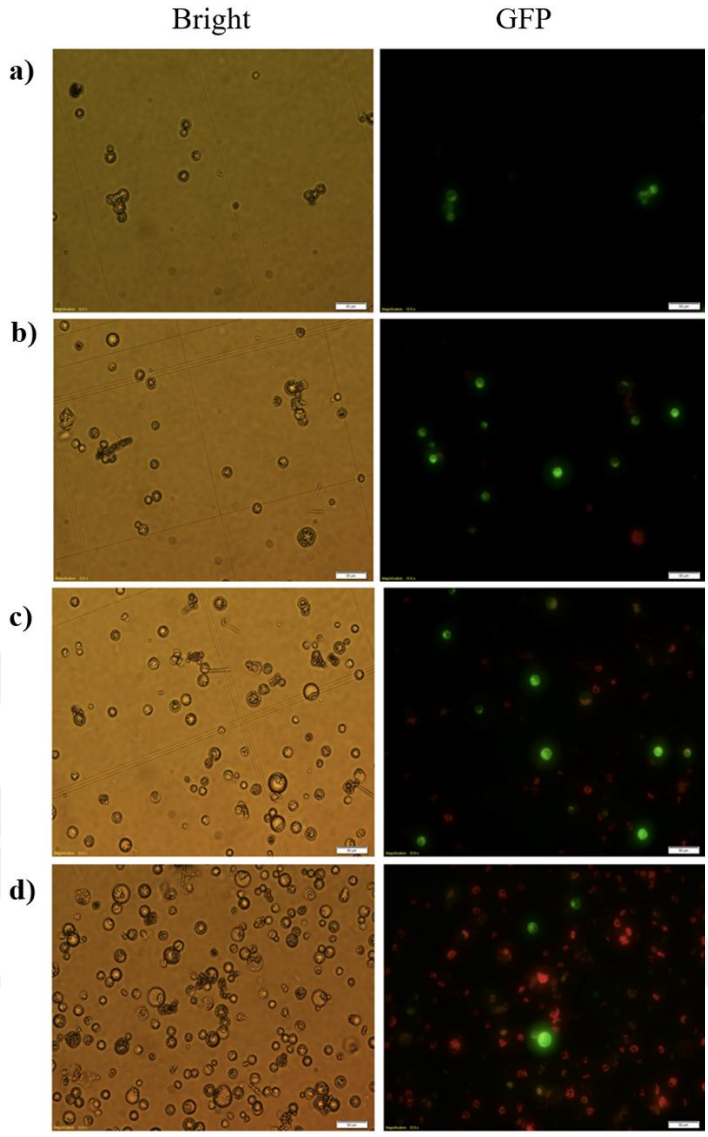


Figure 49. Microscopic imaging of transformed protoplasts under the bright field and fluorescence microscope a) $2.5x10^5$ protoplast number, b) $5x10^5$ protoplast number, c) $1x10^6$ protoplast number, d) $2x10^6$ protoplast number.

The transformation efficiencies of different protoplast numbers were counted and compared between each other. The results of the transformation efficiencies are shown in Figure 50.

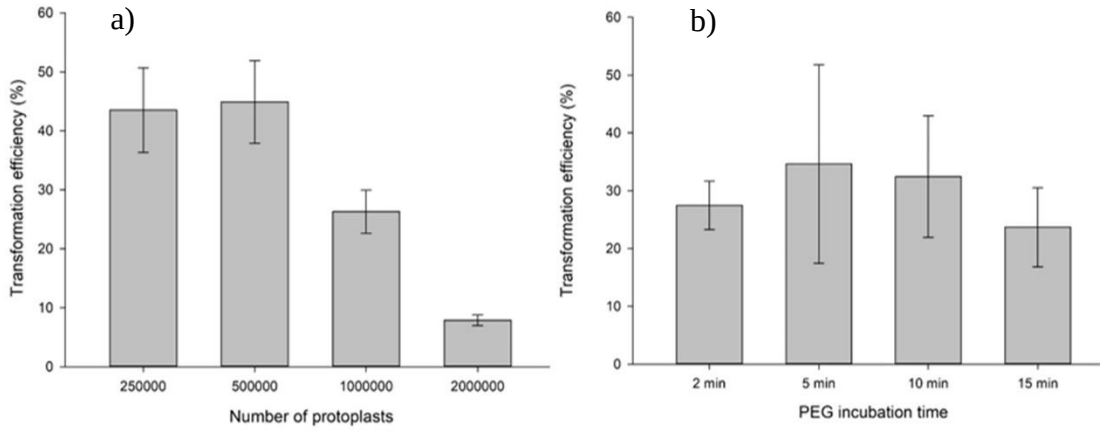


Figure 50. Comparison of transformation efficiency depend on a) protoplast number, and b) PEG incubation time.

According to Figure 50a, the highest transformation efficiency was obtained by using of $5x10^5$ protoplast number. When the protoplast number was exceeded $5x10^5$, transformation efficiency started to dramatically decrease. It was concluded that as the protoplast number increased, transformation efficiency decreased. Therefore, parameter of protoplast number was optimized and $5x10^5$ protoplasts were used for optimized transformation protocol. Although Zhao et al. (2015) found that the ideal protoplast number for effective transformation in wild Chinese and Rizamat grapevine species was $6x10^4$ (Zhao et al., 2015) optimal protoplast number was founded as $5x10^5$ for effective transformation in Chardonnay grapevine cultivars in this study. It can be concluded that the optimal protoplast number for efficient transformation can also be varied depend on the cultivar of plant. In another study, Malnoy et al. (2016) did not compared the protoplast number for the transformation efficiency. However, they used $2x10^5$ protoplast number for the transformation (Malnoy et al., 2016).

3.3.2. Effect of different PEG incubation time in transformation efficiency

In this work, PEG incubation time was regarded as another significant parameter to optimize the transformation protocol. Four different PEG incubation time as 2 minutes, 5 minutes, 10 minutes, and 15 minutes were tested to select the optimal PEG incubation time for high transformation efficiency. Other parameters remained

constant. Three repetition was performed for protoplast transformation with each of the PEG incubation times. The transformation efficiency of four different PEG incubation time was calculated and compared in Figure 50. According to Figure 50b, it was concluded that the highest transformation efficiency was obtained by application of 5 minutes PEG incubation time. Transformation efficiency continued to increase until 5 minutes. However, when the time exceeded 5 minutes, transformation efficiency started to decrease. Therefore, the optimal PEG incubation time was selected as 5 minutes in optimized transformation protocol. Also, different PEG incubation times were evaluated for transformation efficiencies in various plant species such as carnation, *Camellia oleifera*, grapevine, passion fruit, peanut, wishbone flower, *japonica, Uncaria rhynchophylla* (Zhao et al., 2015; Adedeji et al., 2022; Biswas et al., 2022; Li et al., 2022b; Zhang et al., 2022; Deng et al., 2023; Shao et al., 2023; Wang et al., 2023). While grapevine cv. Chardonnay protoplasts showed a better transformation efficiency after 5 minutes of PEG incubation in this study, other plant-derived protoplasts showed a higher transformation efficiency after 15 or 20 minutes. Moreover, Zhao et al. (2015) also tested and compared various PEG incubation time for transformation of wild Chinese and Rizamat grapevine protoplasts. They compared incubation time of 1 min, 2 min, 5 min, 10 min, 20 min, and 40 min. They reported that the highest transformation efficiency was obtained by application of 5 min PEG incubation time. Results of Zhao et al. (2015) shown similarity with results of this study.

In addition, the variations in the graphs may be due to the application, because protoplasts are quite fragile and sensitive, which has caused variations between the experimental sets. Even a slight delay in the addition of the solution that stops the transformation can cause variations.

3.3.3. Effect of incubation time and incubation buffer after transformation

An additional crucial factor in transformation of protoplasts is the incubation buffer. In the preliminary works, protoplasts cultured in MMG after transformation for transient gene expression did not undergo transformation. Moreover, protoplasts also fractured and underwent shape changes because of the using MMG buffer. However, Zhao et al. (2015) and Malnoy et al. (2016) used W5 buffer in their studies for transient

gene expression incubation (Zhao et al., 2015; Malnoy et al., 2016). So that after the failure results with using of MMG buffer, when protoplasts were cultured in W5 for transient gene expression, transformation went smoothly, and the protoplasts maintained their health and viability by maintaining their shape.

While Zhao et al. (2015) incubated wild Chinese and Rizamat grapevine protoplast samples for transient gene expression by GFP for 20-25 hours (Zhao et al., 2015), it has been shown that the ideal incubation period for transient gene expression of Chardonnay protoplasts is 16 hours. Under a fluorescent microscope, protoplasts were seen to be green at the conclusion of the 16-hour period. Nevertheless, the protoplasts did not brighten when the incubation period was extended to 20 hours. Therefore, incubation time after transformation parameter was optimized as 16 hours in this study.

Consequently, all parameters were optimized to obtain high transformation efficiency for prime editing constructs. All parameters selected for use with the optimized protocol are given in Table 26.

Table 26. Selected application for optimized protoplast transformation protocol

Optimization parameter	**Optimized parameter**
Protoplast number	$5x10^5$ protoplasts
PEG incubation time	5 minutes
Incubation buffer after transformation	W5 buffer
Incubation time after transformation	16 hours

3.4. Transformation efficiencies of GK plasmids on Chardonnay mesophyll protoplasts

After optimization of protoplast isolation and protoplast transformation protocols for high efficiency, GK plasmids which were designed by prime editing approach were transferred to protoplasts by application of optimized protocols. The

transformation efficiencies of GK plasmids (GK1-GK2-GK3-GK4-GK5) were calculated and compared between each other. Three independent replication was performed for each prime editing constructs. The same optimized parameters were applied for each sample. The microscopic images of three replication of GK1 plasmid are shown in Figure 51. The overall transformation efficiency of GK1 plasmids was calculated as 25.3 %.

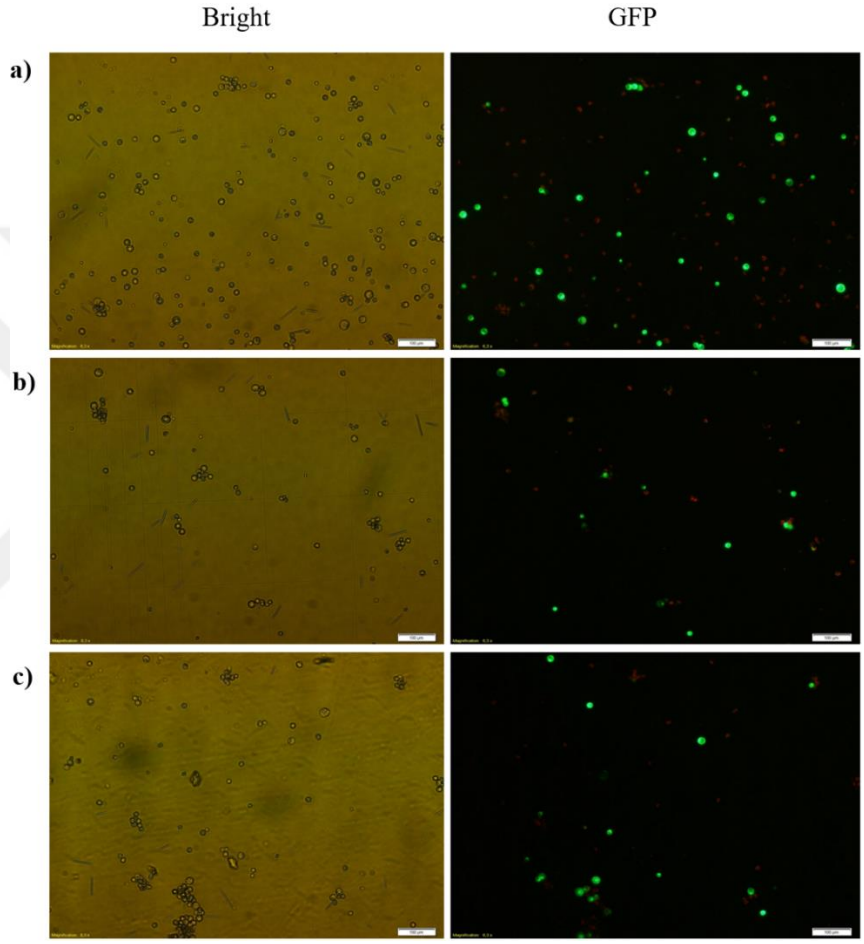


Figure 51. Microscopic images of transformed protoplasts with GK1 plasmids under the bright field and fluorescence microscope a) images from first replication, b) images from second replication, c) images from third replication.

The microscopic images of three replication of GK2 plasmid are shown in Figure 52. The overall transformation efficiency of GK2 plasmids was calculated as 23.43 %. In addition, the microscopic images of three replication of GK3 plasmid are

shown in Figure 53. The overall transformation efficiency of GK3 plasmids was calculated as 21.15 %.

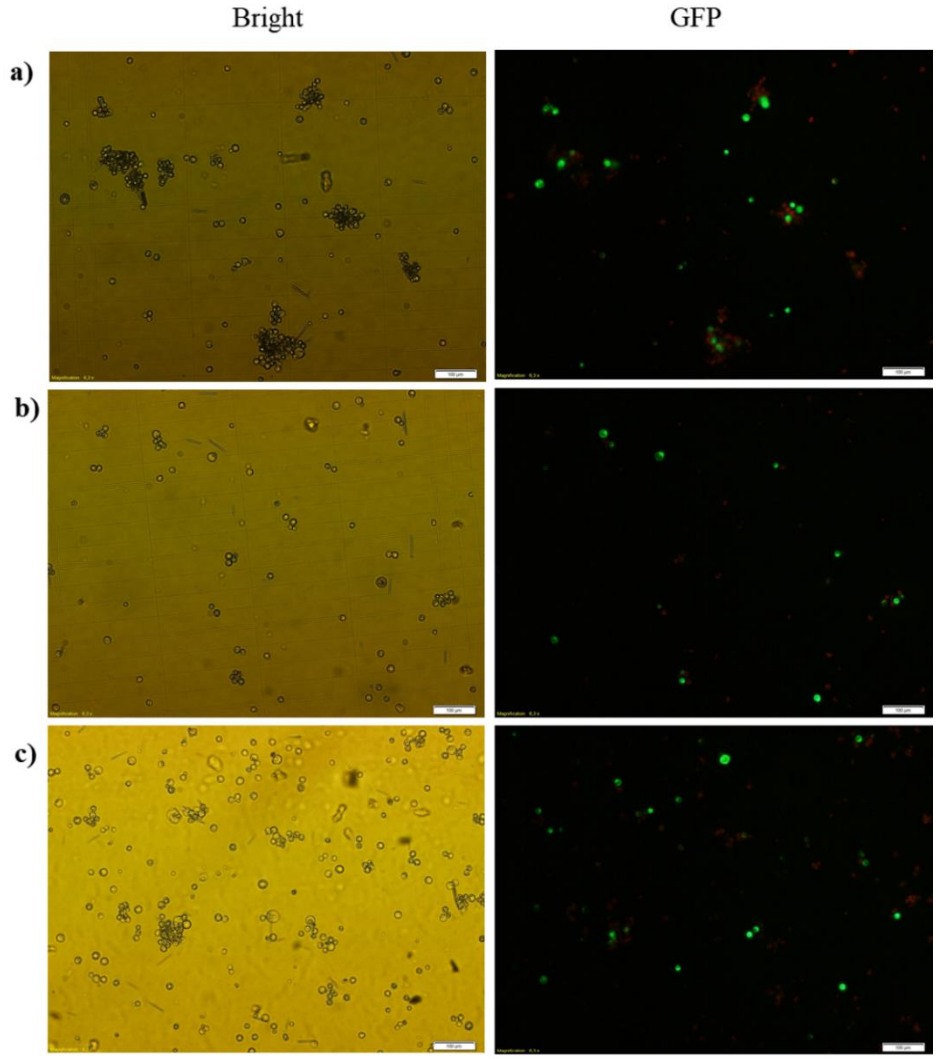


Figure 52. Microscopic images of transformed protoplasts with GK2 plasmids under the bright field and fluorescence microscope a) images from first replication, b) images from second replication, c) images from third replication

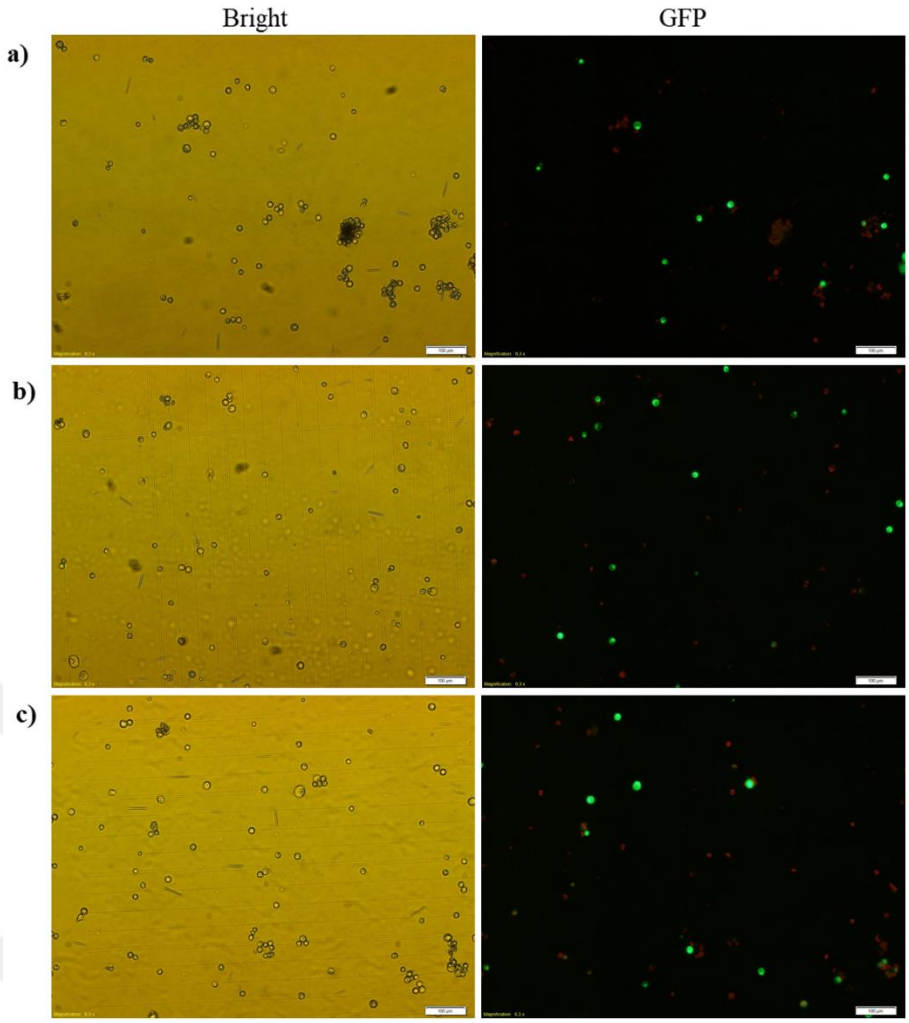


Figure 53. Microscopic images of transformed protoplasts with GK3 plasmids under the bright field and fluorescence microscope a) images from first replication, b) images from second replication, c) images from third replication

While the microscopic images of three replication of GK4 plasmid are shown in Figure 54, the images of GK5 plasmids are shown in Figure 55. The overall transformation efficiency of GK4 and GK5 plasmid were calculated as 27.79 % and 20.25 %, respectively. The microscopic images both (+) control and (-) control are also shown in Figure 56. The transformation efficiencies of all constructs are summarized in detailed in Table 27.

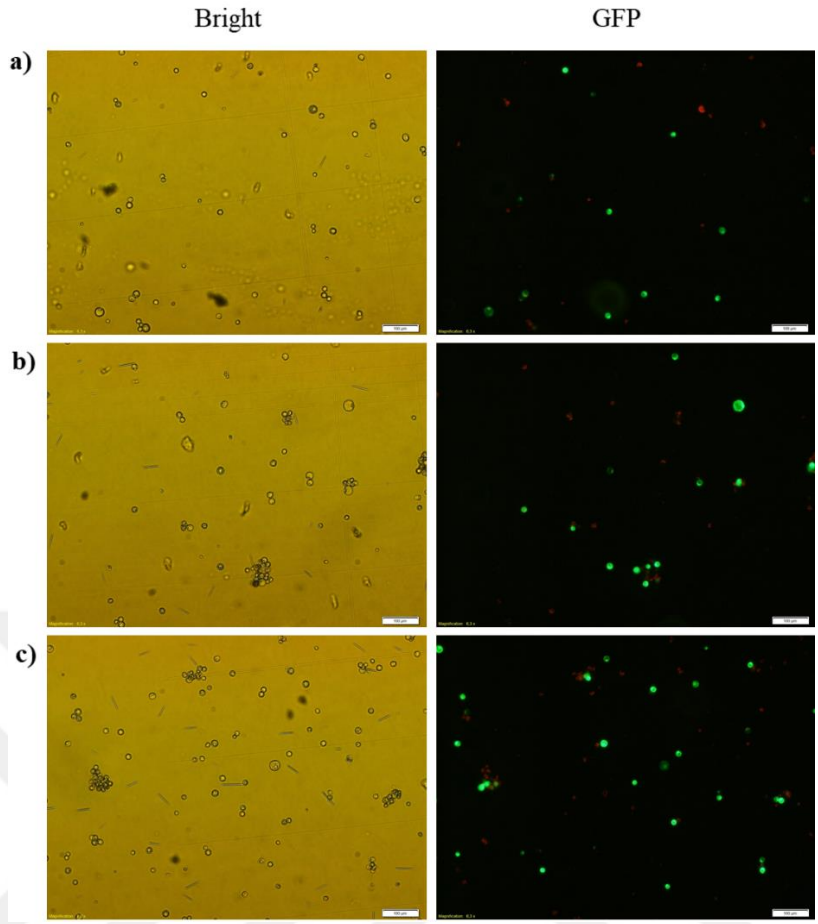


Figure 54. Microscopic images of transformed protoplasts with GK4 plasmids under the bright field and fluorescence microscope a) images from first replication, b) images from second replication, c) images from third replication

Table 27. Comparison of transformation efficiencies of prime editing constructs

Plasmid	Transformation efficiency
GK1 (*pLL3*_R218K)	25.3 %
GK2 (*pLL13*_R218K)	23.43 %
GK3 (*pLL3*_D131A)	21.15 %
GK4 (*pLL13*_D131A)	27.79 %
GK5 (*PDS1*)	20.25 %
pMODC-3001 (+) control	23 %

According to Table 27, transformation efficiencies of all constructs are similar each other. When they were compared between them, the highest transformation efficiency was obtained with GK4 plasmid.

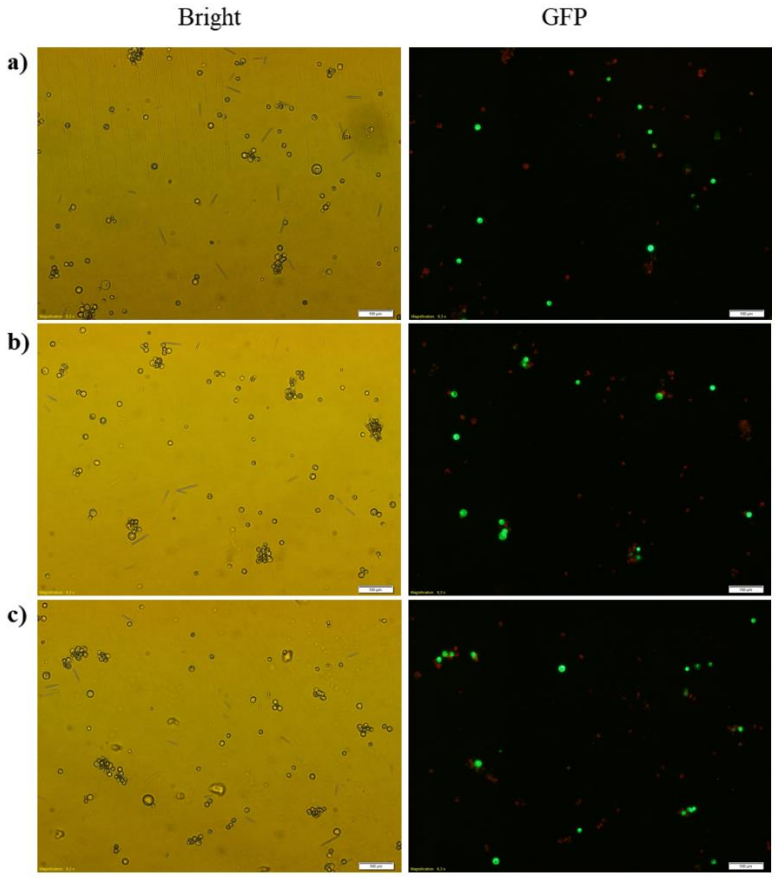


Figure 55. Microscopic images of transformed protoplasts with GK5 plasmids under the bright field and fluorescence microscope a) images from first replication, b) images from second replication, c) images from third replication

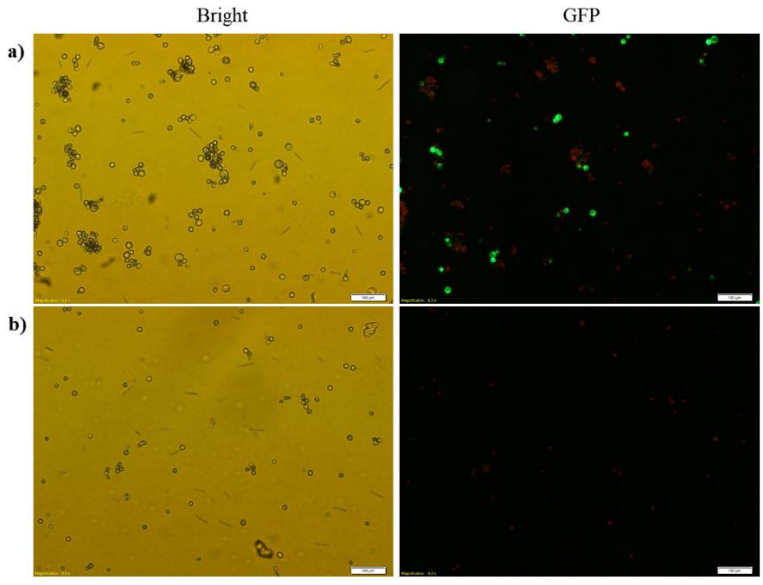


Figure 56. Microscopic images of transformed protoplasts a) (+) control, b) (-) control

3.5. The PCR analysis for Amplicon sequencing of the prime editing constructs

After transformation of protoplasts, obtained gel image of PCR which is conducted by DNAs of protoplasts for amplicon sequencing is shown in Figure 57. In addition, gel image of PCR which is conducted by pMODC-3001, and non-transformed protoplast DNAs is shown in Figure 58.

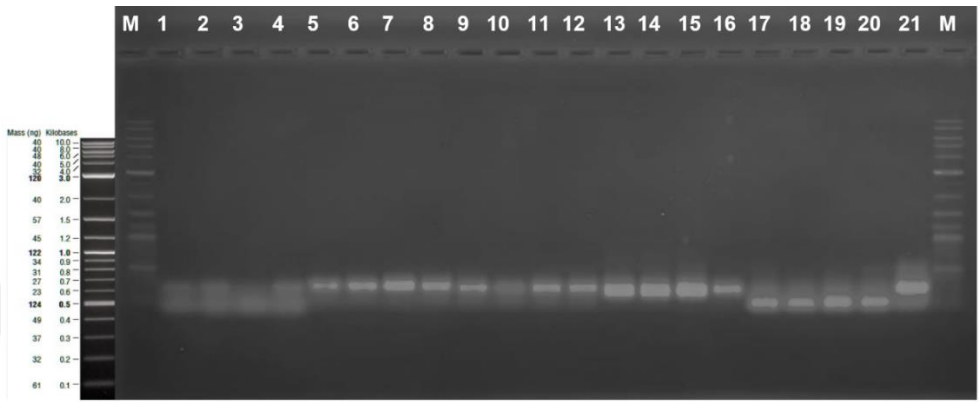


Figure 57. Obtained gel image of protoplast GK samples as a result of PCR.

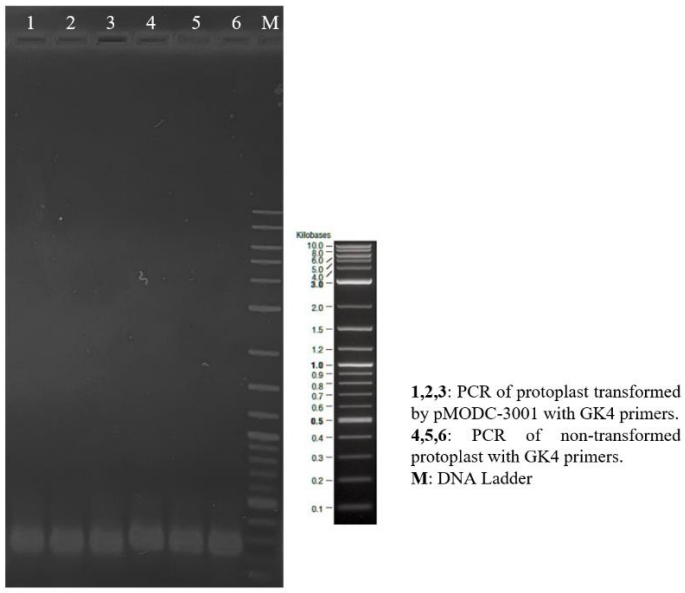


Figure 58. Obtained gel image of protoplast samples as a result of PCR with pMODC-3001 and non-transformed.

In the Figure 57, PCR product fragments were obtained with desired small sizes. However, the exact length of the fragments was unknown because the small sizes was hard to distinguish by gel electrophoresis. Therefore, PCR with gel electrophoresis was not reliable process to observe and prove desired editing. So that, PCR product samples were isolated from 1% agarose gel, and they were sent to amplicon sequencing. Also, both PCR products of pMODC-3001 and non-transformed protoplast samples were sent for amplicon sequencing as control groups.

3.6. The Amplicon sequencing analysis of prime editing constructs

Amplicon sequencing results of prime editing constructs were recorded to observe editing efficiencies. The amplicon sequencing results of GK1 construct are shown in Figure 59.

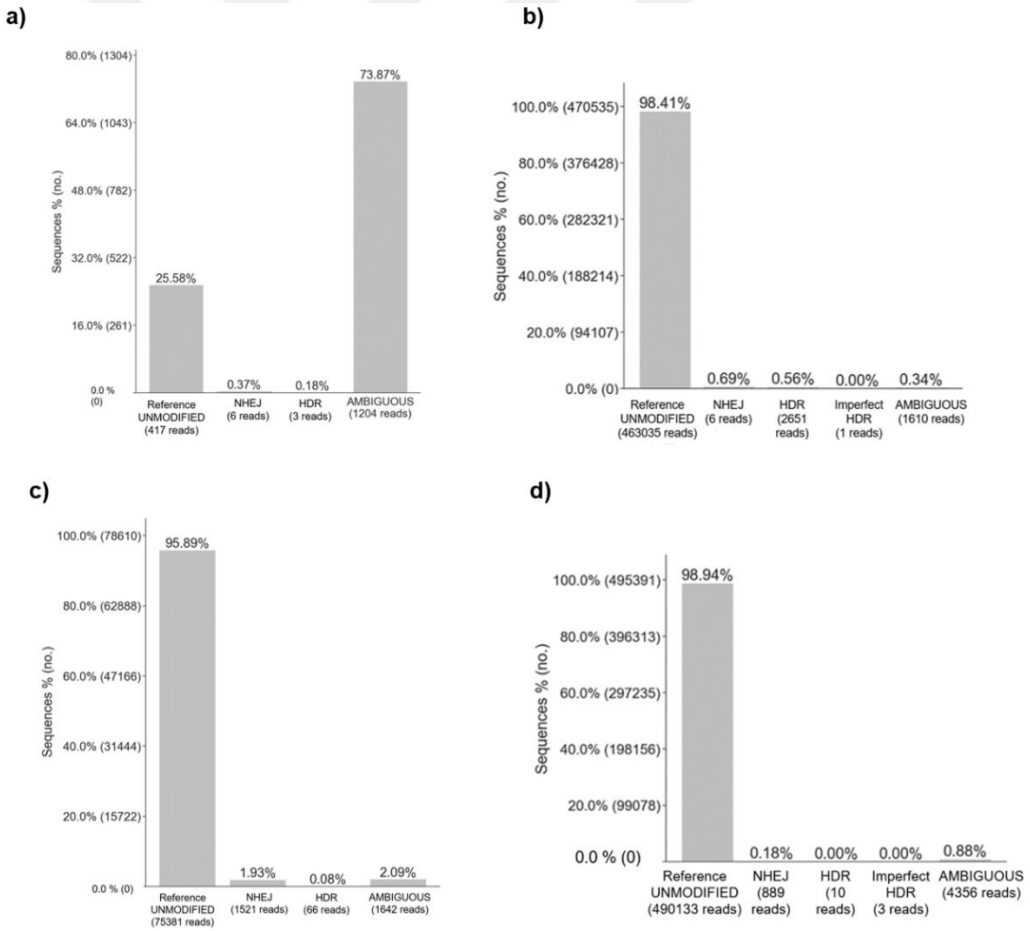


Figure 59. Amplicon sequencing results of GK1 construct. a) first replication of GK1, b) second replication of GK1, c) third replication of GK1, d) (-) control of GK1

The amplicon sequencing results of GK2 construct are shown in Figure 60. While amplicon sequencing results of GK3 construct are shown in Figure 61, results of GK4 construct are shown in Figure 62. The results of the final GK5 construct are shown in Figure 63, respectively.

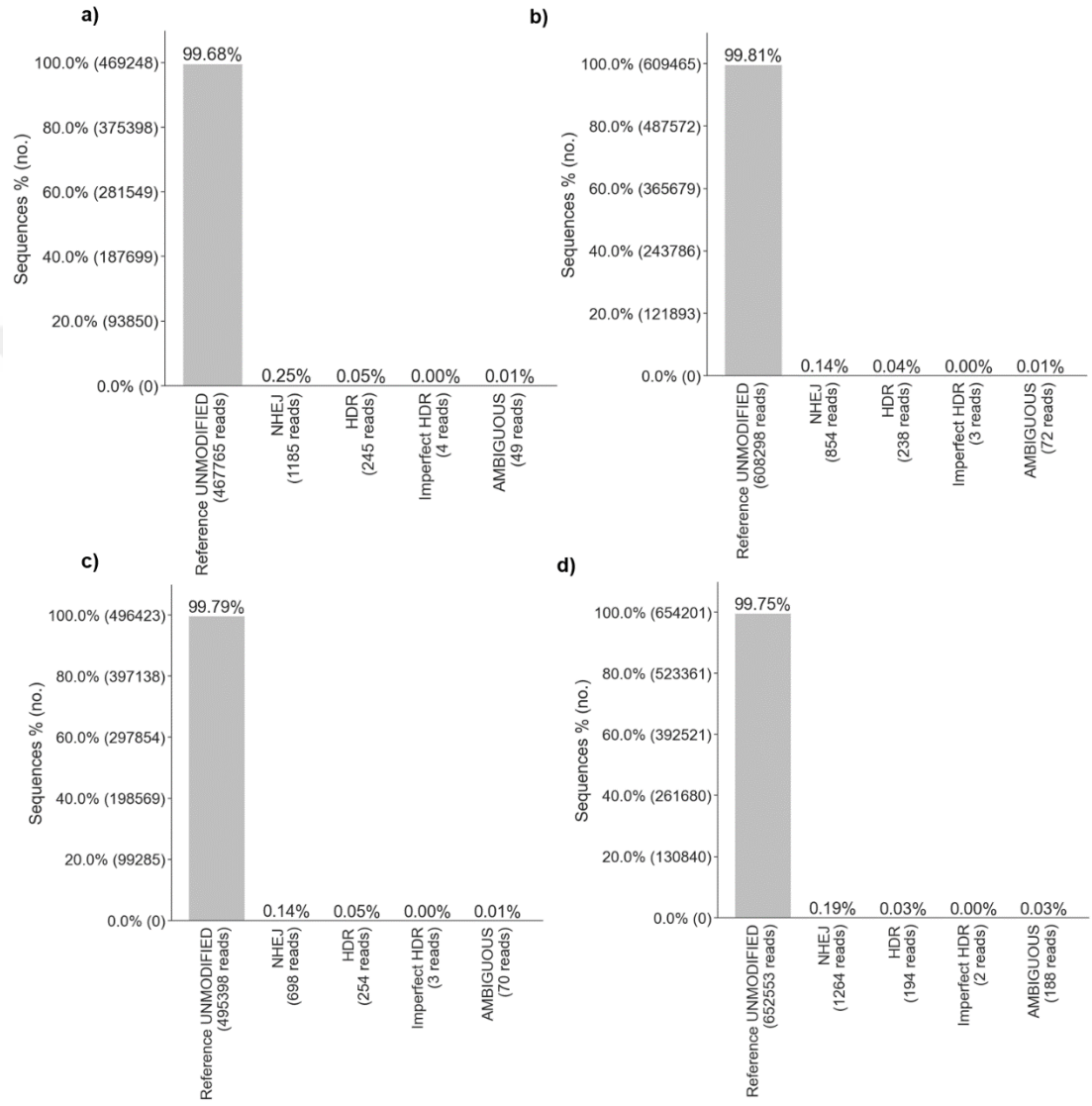


Figure 60. Amplicon sequencing results of GK2 construct. a) first replication of GK2, b) second replication of GK2, c) third replication of GK2, d) (-) control of GK2

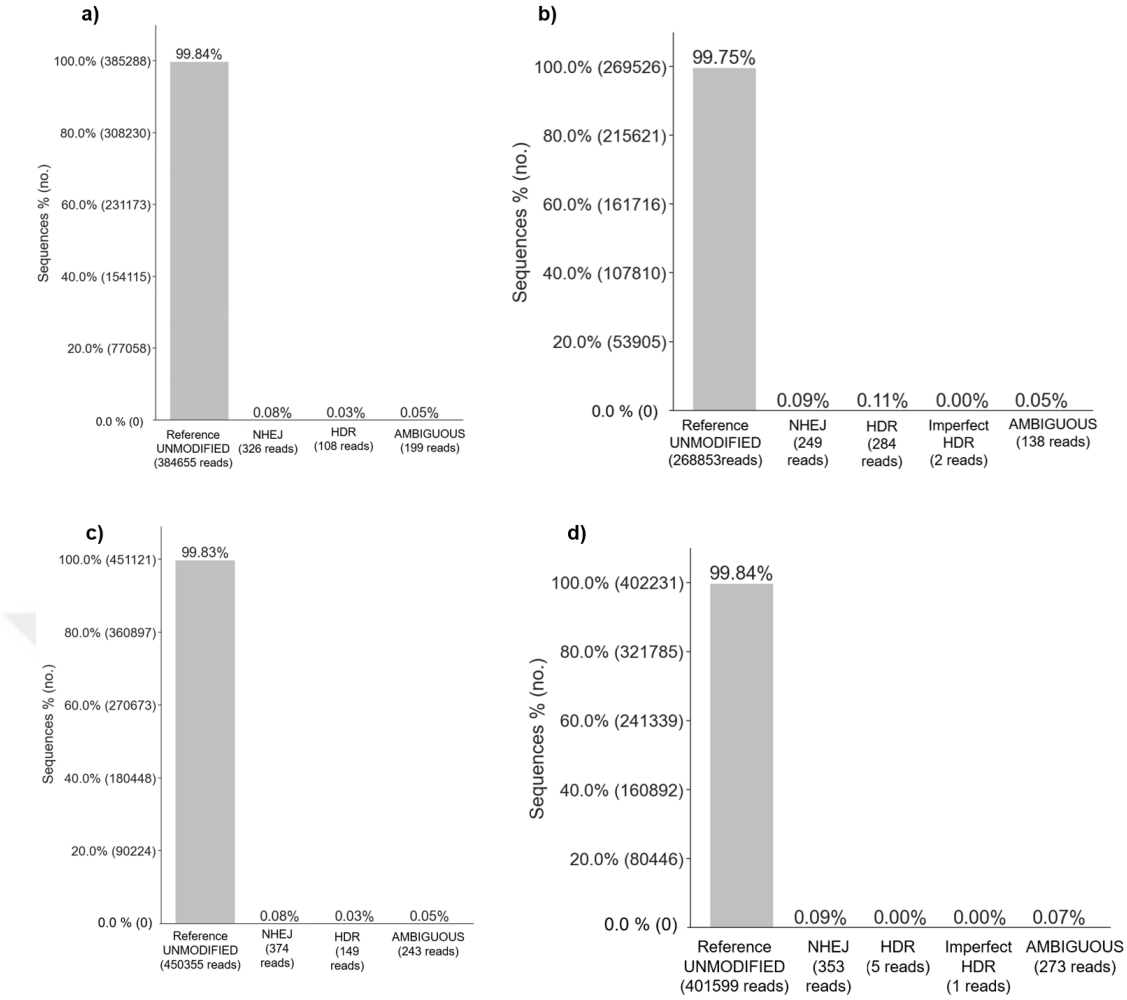


Figure 61. Amplicon sequencing results of GK3 construct. a) first replication of GK3, b) second replication of GK3, c) third replication of GK3, d) (-) control of GK3

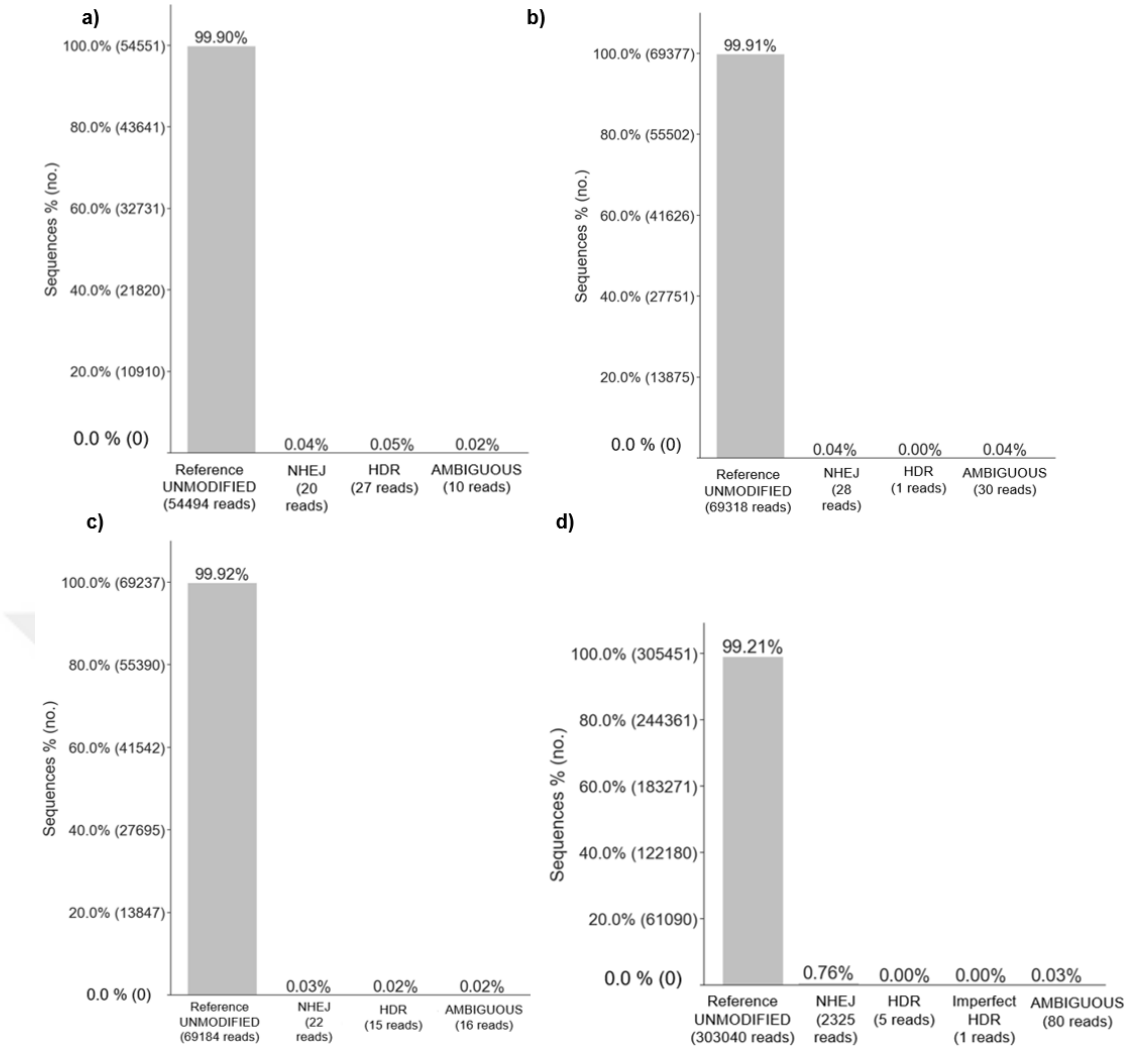


Figure 62. Amplicon sequencing results of GK4 construct. a) first replication of GK4, b) second replication of GK4, c) third replication of GK4, d) (-) control of GK4

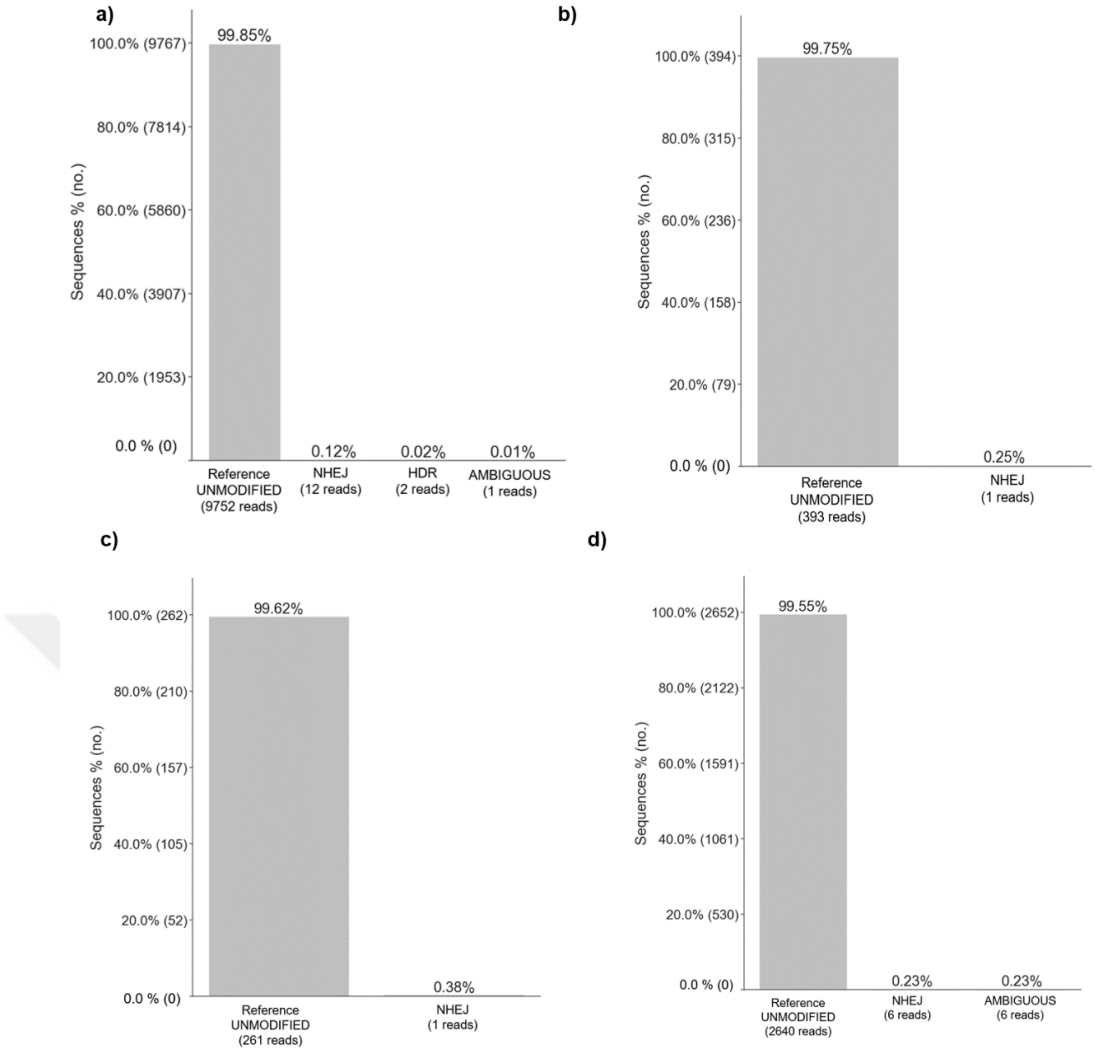


Figure 63. Amplicon sequencing results of GK5 construct. a) first replication of GK5, b) second replication of GK5, c) third replication of GK5, d) (-) control of GK4

After obtaining of amplicon sequencing results, the editing efficiencies of prime editing constructs were calculated and shown in Table 28.

Table 28. Editing efficiencies (%) of GK plasmids.

Plasmid	Editing efficiency (%)
GK1 (*pLL3*_R218K)	%0.76
GK2 (*pLL13*_R218K)	%0.16
GK3 (*pLL3*_D131A)	%0.18
GK4 (*pLL13*_D131A)	%0.04
GK5 (*PDS1*)	%0.19

According to Table 28, the highest editing efficiency was obtained with transformation of GK1 plasmid with *PLL3*-R218K mutation. The transformation of GK2 showed the lowest editing efficiency. The editing efficiency results obtained in the range of 0.16%-0.76% by amplicon sequencing have shown that prime editing dual-epegRNA approach works successfully in Chardonnay grapevine protoplasts. Although the highest transformation efficiency was obtained with the GK4 plasmid, the highest editing efficiency was demonstrated by the GK1 plasmid. Transformation efficiency does not have to be directly proportional to editing efficiency, as not every transformed protoplast may contain the target editing. Target editing efficiency is screening by sequencing. Low editing efficiencies do not negatively affect our results. On the contrary, even with low efficiency, it has been shown that constructs designed for prime editing work successfully in grape protoplasts, achieving the desired outcome.

There are studies evaluating prime editing in different plant protoplasts. For instance, Tang et al. (2020) assessed prime editing in rice protoplasts with the 0.05%-0.15% editing efficiency. In addition, Biswas et al. (2022) performed assessment of mutant GFP which are designed by prime editing in protoplasts of chickpea, cowpea, and rice. They evaluated single-peg and dual-peg RNA for the higher prime editing efficiency. It was highlighted that higher editing efficiency was achieved by using of dual-peg RNA. On the other hand, their editing efficiency results were recorded as between 0.2–0.5% in chickpea, cowpea, and rice protoplasts. In addition, they mentioned that position of sgRNA for nCas9, and length of reverse transcriptase (RT) and primer binding site (PBS) are the crucial factor in prime editing efficiency (Biswas et al.,2022). The editing efficiencies obtained in prime editing studies conducted in protoplasts are consistent with the editing efficiencies obtained in grapevine protoplasts within the scope of this thesis study. Additionally, Huang, T. K., and Puchta, H. (2021) noted that many independent studies have shown that PE can modify the genomes of plant protoplasts even with low editing efficiency (Huang and Puchta, 2021).

Also, the first prime editing study in grapevine was carried out by Yang et al. (2024), they assessed the dual-epegRNA approach in grapevine calli of Scarlet Royal

grapevine cultivar (Yang et al., 2024). They reported editing efficiencies between 0.65 % and 2.33% were obtained with the designed prime editing constructs tested in transgenic callus as a results of amplicon sequencing performed. On the other hand, higher editing efficiency (~%86) was obtained in *in vitro* propagated clones of transgenic grapevine plants which is obtained from these calli. Their evaluation of prime editing in grapevine calla instead of grapevine protoplasts still preserves the originality of this thesis study.

CONCLUSION & RECOMMENDATIONS

Grapevine, one of the plants with the most significant economic and cultural value, faces substantial yield loss due to powdery mildew disease caused by the fungus *Uncinula necator*. With the increasing world population and changing climate conditions, it is predicted that traditional plant breeding methods will be insufficient for the production of agricultural products. This situation has led to the development and use of transgene-free genome editing tools, such as CRISPR, which achieve targeted modifications using nucleases. Genome editing studies in plants are successfully continuing with Prime editing, a new adaptation of CRISPR technology, using the dual-epegRNA approach. One of the most crucial steps in conducting genome editing studies in agricultural plant products is evaluating the activity of genome editing reagents before directly transferring them to plants. Using plant tissue culture for this purpose requires intensive effort, time, and cost. To minimize these drawbacks, protoplast technology, a faster alternative to plant tissue culture, is used for the evaluation of genome editing reagents.

Within the scope of this thesis, the highest protoplast yield of $75x10^6$/g leaf was obtained using the optimized protoplast isolation protocol. The viability of the obtained protoplasts was calculated to be 91%. With the optimization of the protoplast transformation protocol carried out within the scope of the thesis, the highest transformation efficiency was determined to be 45%. Detailed research and experiments resulted in obtaining target plasmids GK1, GK2, GK3, GK4, and GK5 using prime editing and the dual-epegRNA approach, targeting the *pLL3* and *pLL13*, pectate lyase-like genes, and the *PDS* gene related to resistance to powdery mildew disease. These plasmids were evaluated in terms of transformation and editing efficiency in Chardonnay grapevine protoplasts, which are of commercial importance in viticulture. The average transformation efficiency was obtained range between 20.25%-27.79% with the transformation of GK plasmid DNAs into grapevine protoplasts, while the editing efficiency was recorded in the range of 0.16-0.76% in the samples sent for amplicon sequencing after transformation. Consequently, it was observed that the dual-epeg prime editing technique used successfully achieved target mutations in Chardonnay grapevine protoplasts. It is also considered that the results

obtained within the scope of this thesis provide an important resource for studies to be conducted in this field.

REFERENCES

A. Mliki, R.J., G. M. Reustle, A. Ghorbel (2003). Isolation and culture of leaf protoplasts from Tunisian grapes. *Vigne et Vin Publications Internationales* 37**,** 145-153.

Adedeji, O.S., Naing, A.H., Kang, H., Chung, M.Y., Lim, K.B., and Kim, C.K. (2022). Optimization of protocol for efficient protoplast isolation and transient gene expression in carnation. *Scientia Horticulturae* 299.

Ainley, W. M., Sastry-Dent, L., Welter, M. E., Murray, M. G., Zeitler, B., Amora, R., ... & Carroll, D. (2013). Trait stacking via targeted genome editing. *Plant Biotechnology Journal*, 11(9), 1126-1134.

Andersson, M., Turesson, H., Nicolia, A., Falt, A.S., Samuelsson, M., and Hofvander, P. (2017). Efficient targeted multiallelic mutagenesis in tetraploid potato (Solanum tuberosum) by transient CRISPR-Cas9 expression in protoplasts. *Plant Cell Rep* 36(1)**,** 117-128.

Anzalone, A.V., Randolph, P.B., Davis, J.R., Sousa, A.A., Koblan, L.W., Levy, J.M., et al. (2019). Search-and-replace genome editing without double-strand breaks or donor DNA. *Nature* 576(7785)**,** 149-157.

Arif SEMERCİ, T.K., Ahmet Duran ÇELİK, Mehmet Ali KİRACI (2015). Türkiye Bağcılığının Genel Durumu. *Journal of Agricultural Faculty of Mustafa Kemal University*.

Armijo, G., Schlechter, R., Agurto, M., Munoz, D., Nunez, C., and Arce-Johnson, P. (2016). Grapevine pathogenic microorganisms: Understanding infection strategies and host response scenarios. *Front Plant Sci* 7**,** 382.

Bailey-Serres, J., Parker, J.E., Ainsworth, E.A., Oldroyd, G.E.D., and Schroeder, J.I. (2019). Genetic strategies for improving crop yields. *Nature* 575(7781)**,** 109-118.

Bertini, E., Tornielli, G.B., Pezzotti, M., and Zenoni, S. (2019). Regeneration of plants from embryogenic callus-derived protoplasts of Garganega and Sangiovese grapevine (Vitis vinifera L.) cultivars. *Plant Cell, Tissue and Organ Culture (PCTOC)* 138(2)**,** 239-246.

Bessis, M.B.a.R. (1990). Isolation and culture of grape vine cv. Chardonnay leaf protoplasts. *Euphytica* 47**,** 39-44.

Bishnoi, R., Kaur, S., Sandhu, J.S., and Singla, D. (2023). Genome engineering of disease susceptibility genes for enhancing resistance in plants. *Funct Integr Genomics* 23(3)**,** 207.

Biswas, S., Bridgeland, A., Irum, S., Thomson, M. J., & Septiningsih, E. M. (2022). Optimization of prime editing in rice, peanut, chickpea, and cowpea protoplasts by restoration of GFP activity. *International Journal of Molecular Sciences*, 23(17), 9809.

Brookes, G., and Barfoot, P. (2020). Environmental impacts of genetically modified (GM) crop use 1996-2018: impacts on pesticide use and carbon emissions. *GM Crops Food* 11(4)**,** 215-241.

Butt, H., Rao, G.S., Sedeek, K., Aman, R., Kamel, R., and Mahfouz, M. (2020). Engineering herbicide resistance via prime editing in rice. *Plant Biotechnol J* 18(12)**,** 2370-2372.

Caffall, K.H., and Mohnen, D. (2009). The structure, function, and biosynthesis of plant cell wall pectic polysaccharides. *Carbohydr Res* 344(14)**,** 1879-1900.

Cai, Y., Chen, L., Liu, X., Guo, C., Sun, S., Wu, C., et al. (2018). CRISPR/Cas9-mediated targeted mutagenesis of GmFT2a delays flowering time in soya bean. *Plant Biotechnol J* 16(1)**,** 176-185.

Cermak, T., Curtin, S.J., Gil-Humanes, J., Cegan, R., Kono, T.J.Y., Konecna, E., et al. (2017). A Multipurpose Toolkit to Enable Advanced Genome Engineering in Plants. *Plant Cell* 29(6)**,** 1196-1217.

Čermák, T., Baltes, N. J., Čegan, R., Zhang, Y., & Voytas, D. F. (2015). High-frequency, precise modification of the tomato genome. *Genome Biology*, 16(1), 232.

Chandrasekaran, J., Brumin, M., Wolf, D., Leibman, D., Klap, C., Pearlsman, M., et al. (2016). Development of broad virus resistance in non-transgenic cucumber using CRISPR/Cas9 technology. *Mol Plant Pathol* 17(7)**,** 1140-1153.

Char, S.N., Neelakandan, A.K., Nahampun, H., Frame, B., Main, M., Spalding, M.H., et al. (2017). An Agrobacterium-delivered CRISPR/Cas9 system for high-frequency targeted mutagenesis in maize. *Plant Biotechnol J* 15(2)**,** 257-268.

Custodio, L., Charles, G., Magne, C., Barba-Espin, G., Piqueras, A., Hernandez, J.A., et al. (2022). Application of in vitro plant tissue culture techniques to halophyte species: a review. *Plants (Basel)* 12(1).

D'Ambrosio, C., Stigliani, A.L., and Giorio, G. (2018). CRISPR/Cas9 editing of carotenoid genes in tomato. *Transgenic Res* 27(4)**,** 367-378.

Dangl, J., Jones, J. (2001). Plant pathogens and integrated defence responses to infection. *Nature* 411**,** 826–833.

Derman, S.S., and Vivier, M.A. (2022). The promise of using protoplasts in grapevine research. *South African Journal of Enology and Viticulture* 43(2).

Djennane, S., Gersch, S., Le-Bohec, F., Piron, M. C., Baltenweck, R., Lemaire, O., ... & Mestre, P. (2024). CRISPR/Cas9 editing of Downy mildew resistant 6 (DMR6-1) in grapevine leads to reduced susceptibility to Plasmopara viticola. *Journal of Experimental Botany*, *75*(7), 2100-2112.

Doyle, J. J. (1990). Isolation of plant DNA from fresh tissue. *Focus*, *12*, 13-15.

El-Mounadi, K., Morales-Floriano, M.L., and Garcia-Ruiz, H. (2020). Principles, applications, and biosafety of plant genome editing using CRISPR-Cas9. *Front Plant Sci* 11**,** 56.

Endo, M., Mikami, M., and Toki, S. (2016). Biallelic gene targeting in rice. *Plant Physiol* 170(2)**,** 667-677.

Feechan, A., Jermakow, A.M., and Dry, I.B. (2009). Grapevine MLO candidates required for powdery mildew pathogenicity? *Plant Signal Behav* 4(6)**,** 522-523.

Feng, Z., Xue, F., Xu, M., Chen, X., Zhao, W., Garcia-Murria, M.J., et al. (2016). The ER-membrane transport system is critical for intercellular trafficking of the NSm movement protein and tomato spotted wilt tospovirus. *PLoS Pathog* 12(2)**,** e1005443.

Fontes, N., Gerós, H., Papadakis, A. K., Delrot, S., & Roubelakis-Angelakis, K. A. (2010). Isolation and use of protoplasts from grapevine tissues. *Methodologies and Results in Grapevine Research*, 277-293.

Fouillet, E., Delière, L., Chartier, N., Munier-Jolain, N., Cortel, S., Rapidel, B., & Merot, A. (2022). Reducing pesticide use in vineyards. Evidence from the analysis of the French DEPHY network. *European Journal of Agronomy*, *136*, 126503.

Gaj, T., Sirk, S.J., Shui, S.L., and Liu, J. (2016). Genome-editing technologies: principles and applications. *Cold Spring Harb Perspect Biol* 8(12).

Gao, H., Smith, J., Yang, M., Jones, S., Djukanovic, V., Nicholson, M. G., ... & Zhang, Y. (2010). Heritable targeted mutagenesis in maize using a designed endonuclease. *The Plant Journal*, 61(1), 176-187.

Gao, H., Gadlage, M. J., Lafitte, H. R., Lenderts, B., Yang, M., Schroder, M., ... & Voytas, D. F. (2014). Superior field performance of waxy corn hybrids produced through an edited gene conversion approach. *Plant Biotechnology Journal*, 12(8), 1096-1105.

Gao, C. (2020). Genome engineering for crop improvement and future agriculture. *Cell*, 184(6), 1436-1451.

Garcia-Ruiz, H. (2018). Susceptibility genes to plant viruses. *Viruses* 10(9).

Garcia-Ruiz, H., Szurek, B., and Van den Ackerveken, G. (2021). Stop helping pathogens: engineering plant susceptibility genes for durable resistance. *Curr Opin Biotechnol* 70**,** 187-195.

Giacomelli, L., Zeilmaker, T., Giovannini, O., Salvagnin, U., Masuero, D., Franceschi, P., et al. (2023). Simultaneous editing of two DMR6 genes in grapevine results in reduced susceptibility to downy mildew. *Front Plant Sci* 14**,** 1242240.

Gilliard, G., Huby, E., Cordelier, S., Ongena, M., Dhondt-Cordelier, S., and Deleu, M. (2021). Protoplast: a valuable toolbox to investigate plant stress perception and response. *Front Plant Sci* 12**,** 749581.

Glawe, D. A. (2008). The powdery mildews: a review of the world's most familiar (yet poorly known) plant pathogens. *Annu. Rev. Phytopathol.*, *46*(1), 27-51.

Gökhan Söylemezoglu, A.A., Yılmaz Boz, Akay Unal and Mehmet Saglam (2016). Viticulture in Turkey. *Chronica Horticulturae* 56(2)**,** 26-31.

Grizot, S., Epinat, J. C., Thomas, S., Duclert, A., Rolland, S., Paques, F., & Duchateau, P. (2009). Generation of redesigned homing endonucleases comprising DNA-binding domains derived from two different scaffolds. *Nucleic Acids Research* 37(8), 2620-2630.

Herron, S.R., Benen, J.A., Scavetta, R.D., Visser, J., and Jurnak, F. (2000). Structure and function of pectic enzymes: virulence factors of plant pathogens. *Proc Natl Acad Sci U S A* 97(16)**,** 8762-8769.

Herron, S.R., Scavetta, R.D., Garrett, M., Legner, M., and Jurnak, F. (2003). Characterization and implications of Ca2+ binding to pectate lyase C. *J Biol Chem* 278(14)**,** 12271-12277.

Hua, K., Jiang, Y., Tao, X., and Zhu, J.K. (2020). Precision genome engineering in rice using prime editing system. *Plant Biotechnol J* 18(11)**,** 2167-2169.

Huang, T.K., and Puchta, H. (2021). Novel CRISPR/Cas applications in plants: from prime editing to chromosome engineering. *Transgenic Res* 30(4)**,** 529-549.

Jaiswal, S., Singh, D.K., and Shukla, P. (2019). Gene editing and systems biology tools for pesticide bioremediation: a review. *Front Microbiol* 10**,** 87.

Jia, H., Zhang, Y., Orbovic, V., Xu, J., White, F.F., Jones, J.B., et al. (2017). Genome editing of the disease susceptibility gene CsLOB1 in citrus confers resistance to citrus canker. *Plant Biotechnol J* 15(7)**,** 817-823.

Jia, Y., Ding, Y., Shi, Y., Zhang, X., Gong, Z., and Yang, S. (2016). The cbfs triple mutants reveal the essential functions of CBFs in cold acclimation and allow the definition of CBF regulons in Arabidopsis. *New Phytol* 212(2)**,** 345-353.

Jiang, F., and Doudna, J.A. (2017). CRISPR-Cas9 Structures and Mechanisms. *Annu Rev Biophys* 46**,** 505-529.

Jiang, W., Bush, J., and Sheen, J. (2021). A versatile and efficient plant protoplast platform for genome editing by Cas9 RNPs. *Front Genome Ed* 3**,** 719190.

Jiang, W.Z., Henry, I.M., Lynagh, P.G., Comai, L., Cahoon, E.B., and Weeks, D.P. (2017). Significant enhancement of fatty acid composition in seeds of the allohexaploid, Camelina sativa, using CRISPR/Cas9 gene editing. *Plant Biotechnol J* 15(5)**,** 648-657.

Jiang, Y.Y., Chai, Y.P., Lu, M.H., Han, X.L., Lin, Q., Zhang, Y., et al. (2020). Prime editing efficiently generates W542L and S621I double mutations in two ALS genes in maize. *Genome Biol* 21(1)**,** 257.

Jorgensen, J.H. (1992). Discovery, characterization and exploitation of MLO powdery mildew resistance in barley. *Euphytica* 63**,** 141-152.

Jung, H.I., Yan, J., Zhai, Z., and Vatamaniuk, O.K. (2015). Gene functional analysis using protoplast transient assays. *Methods Mol Biol* 1284**,** 433-452.

Kaya, H. B. (2023). Base Editing and Prime Editing. In *A Roadmap for Plant Genome Editing* (pp. 17-39). Cham: Springer Nature Switzerland.

Kaya, H.B., Dilli, Y., Oncu-Oner, T., and Unal, A. (2023). Exploring genetic diversity and population structure of a large grapevine (Vitis vinifera L.) germplasm collection in Turkiye. *Front Plant Sci* 14**,** 1121811.

Kayin, N., and Turan, F. (2023). Bitki doku kültürünün biyoteknolojik olarak kullanımı. *Journal of Agricultural Biotechnology* 4(1)**,** 1-10.

Klap, C., Yeshayahou, E., Bolger, A. M., Arazi, T., Gupta, S. K., Shabtai, S., ... & Barg, R. (2017). Tomato facultative parthenocarpy results from Sl AGAMOUS-LIKE 6 loss of function. *Plant Biotechnology Journal*, *15*(5), 634-647.

Kocsisova, Z., and Coneva, V. (2023). Strategies for delivery of CRISPR/Cas-mediated genome editing to obtain edited plants directly without transgene integration. *Front Genome Ed* 5**,** 1209586.

Kunova, A., Pizzatti, C., Saracchi, M., Pasquali, M., & Cortesi, P. (2021). Grapevine powdery mildew: fungicides for its management and advances in molecular detection of markers associated with resistance. *Microorganisms*, *9*(7), 1541.

Kusch, S., & Panstruga, R. (2017). mlo-based resistance: an apparently universal "weapon" to defeat powdery mildew disease. *Molecular Plant-Microbe Interactions*, *30*(3), 179-189.

Laforest, L.C., and Nadakuduti, S.S. (2022). Advances in delivery mechanisms of CRISPR gene-editing reagents in plants. *Front Genome Ed* 4**,** 830178.

Li, A., Jia, S., Yobi, A., Ge, Z., Sato, S.J., Zhang, C., et al. (2018). Editing of an alpha-kafirin gene family increases, digestibility and protein quality in sorghum. *Plant Physiol* 177(4)**,** 1425-1438.

Li, H., Li, J., Chen, J., Yan, L., and Xia, L. (2020). Precise modifications of both exogenous and endogenous genes in rice by prime editing. *Mol Plant* 13(5)**,** 671-674.

Li, H., Xu, D., Liu, Y., Tan, X., Qiao, J., Li, Z., et al. (2022). Preventing mycolic acid reduction in Corynebacterium glutamicum can efficiently increase L-glutamate production. *Biochemical Engineering Journal* 177.

Li, J., Zhang, H., Si, X., Tian, Y., Chen, K., Liu, J., et al. (2017). Generation of thermosensitive male-sterile maize by targeted knockout of the ZmTMS5 gene. *J Genet Genomics* 44(9)**,** 465-468.

Li, M., Li, X., Zhou, Z., Wu, P., Fang, M., Pan, X., et al. (2016). Reassessment of the four yield-related genes Gn1a, DEP1, GS3, and IPA1 in rice using a CRISPR/Cas9 system. *Front Plant Sci* 7**,** 377.

Li, T., Liu, B., Spalding, M.H., Weeks, D.P., and Yang, B. (2012). High-efficiency TALEN-based gene editing produces disease-resistant rice. *Nat Biotechnol* 30(5)**,** 390-392.

Li, Z.H., Wang, J., Xu, J.P., Wang, J., and Yang, X. (2023). Recent advances in CRISPR-based genome editing technology and its applications in cardiovascular research. *Mil Med Res* 10(1)**,** 12.

Liang, Z., Wu, Y., Guo, Y., and Wei, S. (2023). Addition of the T5 exonuclease increases the prime editing efficiency in plants. *J Genet Genomics*.

Lin, C. S., Hsu, C. T., Yang, L. H., Lee, L. Y., Fu, J. Y., Cheng, Q. W., ... & Shih, M. C. (2018). Application of protoplast technology to CRISPR/Cas9 mutagenesis: from single-cell mutation detection to mutant plant regeneration. *Plant biotechnology journal*, *16*(7), 1295-1310.

Lin, Q., Jin, S., Zong, Y., Yu, H., Zhu, Z., Liu, G., et al. (2021). High-efficiency prime editing with optimized, paired pegRNAs in plants. *Nat Biotechnol* 39(8)**,** 923-927.

Lin, Q., Zong, Y., Xue, C., Wang, S., Jin, S., Zhu, Z., et al. (2020). Prime genome editing in rice and wheat. *Nat Biotechnol* 38(5)**,** 582-585.

Lu, C., Kuang, J., Shao, T., Xie, S., Li, M., Zhu, L., & Zhu, L. (2022). Prime editing: An all-rounder for genome editing. *International Journal of Molecular Sciences*, *23*(17), 9862.

Lu, Y., Tian, Y., Shen, R., Yao, Q., Zhong, D., Zhang, X., et al. (2021). Precise genome modification in tomato using an improved prime editing system. *Plant Biotechnol J* 19(3)**,** 415-417.

Malnoy, M., Viola, R., Jung, M. H., Koo, O. J., Kim, S., Kim, J. S., ... & Nagamangala Kanchiswamy, C. (2016). DNA-free genetically edited grapevine and apple protoplast using CRISPR/Cas9 ribonucleoproteins. *Frontiers in plant science*, *7*, 1904.

Miao, J., Guo, D., Zhang, J., Huang, Q., Qin, G., Zhang, X., et al. (2013). Targeted mutagenesis in rice using CRISPR-Cas system. *Cell Res* 23(10)**,** 1233-1236.

Nadakuduti, S.S., Starker, C.G., Ko, D.K., Jayakody, T.B., Buell, C.R., Voytas, D.F., et al. (2019). Evaluation of methods to assess in vivo activity of engineered genome-editing nucleases in protoplasts. *Front Plant Sci* 10**,** 110.

Naim, F., Dugdale, B., Kleidon, J., Brinin, A., Shand, K., Waterhouse, P., et al. (2018). Gene editing the phytoene desaturase alleles of Cavendish banana using CRISPR/Cas9. *Transgenic Res* 27(5)**,** 451-460.

Najafi, S., Bertini, E., D'Inca, E., Fasoli, M., and Zenoni, S. (2023). DNA-free genome editing in grapevine using CRISPR/Cas9 ribonucleoprotein complexes followed by protoplast regeneration. *Hortic Res* 10(1)**,** uhac240.

Nakajima, I., Ban, Y., Azuma, A., Onoue, N., Moriguchi, T., Yamamoto, T., ... & Endo, M. (2017). CRISPR/Cas9-mediated targeted mutagenesis in grape. *PLoS One*, *12*(5), e0177966.

Nekrasov, V., Wang, C., Win, J., Lanz, C., Weigel, D., and Kamoun, S. (2017). Rapid generation of a transgene-free powdery mildew resistant tomato by genome deletion. *Sci Rep* 7(1)**,** 482.

Nelson, J.W., Randolph, P.B., Shen, S.P., Everette, K.A., Chen, P.J., Anzalone, A.V., et al. (2022). Engineered pegRNAs improve prime editing efficiency. *Nat Biotechnol* 40(3)**,** 402-410.

Okada, A., Arndell, T., Borisjuk, N., Sharma, N., Watson-Haigh, N.S., Tucker, E.J., et al. (2019). CRISPR/Cas9-mediated knockout of Ms1 enables the rapid

generation of male-sterile hexaploid wheat lines for use in hybrid seed production. *Plant Biotechnol J* 17(10)**,** 1905-1913.

Ortigosa, A., Gimenez-Ibanez, S., Leonhardt, N., and Solano, R. (2019). Design of a bacterial speck resistant tomato by CRISPR/Cas9-mediated editing of SlJAZ2. *Plant Biotechnol J* 17(3)**,** 665-673.

Papikian, A., Liu, W., Gallego-Bartolome, J., and Jacobsen, S.E. (2019). Site-specific manipulation of Arabidopsis loci using CRISPR-Cas9 SunTag systems. *Nat Commun* 10(1)**,** 729.

Paula de Toledo Thomazella, D., Brail, Q., Dahlbeck, D., & Staskawicz, B. (2016). CRISPR-Cas9 mediated mutagenesis of a DMR6 ortholog in tomato confers broad-spectrum disease resistance. *BioRxiv*, 064824.

Peng, A., Chen, S., Lei, T., Xu, L., He, Y., Wu, L., et al. (2017). Engineering canker-resistant plants through CRISPR/Cas9-targeted editing of the susceptibility gene CsLOB1 promoter in citrus. *Plant Biotechnol J* 15(12)**,** 1509-1519.

Perroud, P. F., Guyon-Debast, A., Veillet, F., Kermarrec, M. P., Chauvin, L., Chauvin, J. E., ... & Nogué, F. (2022). Prime Editing in the model plant Physcomitrium patens and its potential in the tetraploid potato. *Plant Science*, *316*, 111162.

Pessina, S., Lenzi, L., Perazzolli, M., Campa, M., Dalla Costa, L., Urso, S., ... & Malnoy, M. (2016). Knockdown of MLO genes reduce susceptibility to powdery mildew in grapevine. *Horticulture research*, *3*.

Petrova, I.O., and Smirnikhina, S.A. (2023). The development, optimization and future of prime editing. *Int J Mol Sci* 24(23).

Qiu, W., Feechan, A., and Dry, I. (2015). Current understanding of grapevine defense mechanisms against the biotrophic fungus (Erysiphe necator), the causal agent of powdery mildew disease. *Hortic Res* 2**,** 15020.

Raj Majumdar, S.M., Jacquelyn Lillis, Michael Osier, Bruce Reisch, Lance Cadle-Davidson (2015). Silencing of grapevine pectate lyase-like genes VvPLL2 and VvPLL3 confers resistance against Erysiphe necator and differentially modulates gene expression.

Ren, C., Guo, Y., Kong, J., Lecourieux, F., Dai, Z., Li, S., et al. (2020). Knockout of VvCCD8 gene in grapevine affects shoot branching. *BMC Plant Biol* 20(1)**,** 47.

Ren, C., Lin, Y., and Liang, Z. (2022). CRISPR/Cas genome editing in grapevine: recent advances, challenges and future prospects. *Fruit Research* 2(1)**,** 1-9.

Ren, C., Liu, X., Zhang, Z., Wang, Y., Duan, W., Li, S., et al. (2016). CRISPR/Cas9-mediated efficient targeted mutagenesis in Chardonnay (Vitis vinifera L.). *Sci Rep* 6**,** 32289.

Ren, C., Liu, Y., Guo, Y., Duan, W., Fan, P., Li, S., et al. (2021a). Optimizing the CRISPR/Cas9 system for genome editing in grape by using grape promoters. *Hortic Res* 8(1)**,** 52.

Ren, F., Ren, C., Zhang, Z., Duan, W., Lecourieux, D., Li, S., et al. (2019). Efficiency optimization of CRISPR/Cas9-mediated targeted mutagenesis in grape. *Front Plant Sci* 10**,** 612.

Ren, R., Gao, J., Yin, D., Li, K., Lu, C., Ahmad, S., ... & Yang, F. (2021). Highly efficient leaf base protoplast isolation and transient expression systems for orchids and other important monocot crops. *Frontiers in plant science*, *12*, 626015.

Sağlam, Ö. Ç., & Sağlam, H. (2018). İnsanlik tarihinde üzümün önemi. *Journal of Agriculture*, *1*(2), 1-10.

Saini, H., Thakur, R., Gill, R., Tyagi, K., and Goswami, M. (2023). CRISPR/Cas9-gene editing approaches in plant breeding. *GM Crops Food* 14(1)**,** 1-17.

Scintilla, S., Salvagnin, U., Giacomelli, L., Zeilmaker, T., Malnoy, M. A., Rouppe van der Voort, J., & Moser, C. (2022). Regeneration of non-chimeric plants from DNA-free edited grapevine protoplasts. *Frontiers in Plant Science*, *13*, 1078931.

Son, S., and Park, S.R. (2022). Challenges Facing CRISPR/Cas9-Based Genome Editing in Plants. *Front Plant Sci* 13**,** 902413.

Soyk, S., Müller, N. A., Park, S. J., Schmalenbach, I., Jiang, K., Hayama, R., ... & Lippman, Z. B. (2017). Variation in the flowering gene SELF PRUNING 5G promotes day-neutrality and early yield in tomato. *Nature Genetics*, *49*(1), 162-168.

Sun, Y., Jiao, G., Liu, Z., Zhang, X., Li, J., Guo, X., ... & Xia, L. (2017). Generation of high-amylose rice through CRISPR/Cas9-mediated targeted mutagenesis of starch branching enzymes. *Frontiers in plant science*, *8*, 298.

Sun, Y., Zhang, X., Wu, C., He, Y., Ma, Y., Hou, H., ... & Xia, L. (2016). Engineering herbicide-resistant rice plants through CRISPR/Cas9-mediated homologous recombination of acetolactate synthase. *Molecular plant*, *9*(4), 628-631.

van Schie, C. C., & Takken, F. L. (2014). Susceptibility genes 101: how to be a good host. *Annual review of phytopathology*, *52*(1), 551-581.

Tanabe, Y., Nomura, N., Minami, M., Takaya, J., Okamoto, N., Yanagi, K., ... & Kaneko, K. (2023). HIST1H1E syndrome with deficiency in multiple pituitary hormones. *Clinical Pediatric Endocrinology*, *32*(3), 195-198.

Tenkumo, T., Aobulikasimu, A., Asou, Y., Shirato, M., Shishido, S., Kanno, T., ... & Nakamura, K. (2020). Proanthocyanidin-rich grape seed extract improves bone loss, bone healing, and implant osseointegration in ovariectomized animals. *Scientific Reports*, *10*(1), 8812.

Tricoli, D.M., and Debernardi, J.M. (2024). An efficient protoplast-based genome editing protocol for Vitis species. *Horticulture Research* 11(1).

Tucker, S., Dumitriu Gabur, G.D., and Teodosiu, C. (2022). Pesticides Identification and Sustainable Viticulture Practices to Reduce Their Use: An Overview. *Molecules* 27(23).

Tyagi, A., Agarwal, R., and Agarwal, C. (2003). Grape seed extract inhibits EGF-induced and constitutively active mitogenic signaling but activates JNK in human prostate carcinoma DU145 cells: possible role in antiproliferation and apoptosis. *Oncogene* 22(9)**,** 1302-1316.

Ueta, R., Abe, C., Watanabe, T., Sugano, S. S., Ishihara, R., Ezura, H., ... & Osakabe, K. (2017). Rapid breeding of parthenocarpic tomato plants using CRISPR/Cas9. *Scientific reports*, *7*(1), 507.

Vogel, J.P., Raab, T.K., Schiff, C., and Somerville, S.C. (2002). PMR6, a pectate lyase-like gene required for powdery mildew susceptibility in Arabidopsis. *Plant Cell* 14(9)**,** 2095-2106.

Vogel, J.P., Raab, T.K., Somerville, C.R., and Somerville, S.C. (2004). Mutations in PMR5 result in powdery mildew resistance and altered cell wall composition. *Plant J* 40(6)**,** 968-978.

Vogel, P.S.-L.a.J. (2000). Closing the ranks to attack by powdery mildew. *Trends in Plant Science* 5(8)**,** 343-348.

Voytas, D. F., & Gao, C. (2014). Precision genome engineering and agriculture: opportunities and regulatory challenges. *PLoS Biology*, 12(6), e1001877.

Wada, N., Ueta, R., Osakabe, Y., and Osakabe, K. (2020). Precision genome editing in plants: state-of-the-art in CRISPR/Cas9-based genome engineering. *BMC Plant Biol* 20(1)**,** 234.

Wan, D. Y., Guo, Y., Cheng, Y., Hu, Y., Xiao, S., Wang, Y., & Wen, Y. Q. (2020). CRISPR/Cas9-mediated mutagenesis of VvMLO3 results in enhanced resistance to powdery mildew in grapevine (Vitis vinifera). *Horticulture research*, *7*.

Wang, F., Wang, C., Liu, P., Lei, C., Hao, W., Gao, Y., ... & Zhao, K. (2016). Enhanced rice blast resistance by CRISPR/Cas9-targeted mutagenesis of the ERF transcription factor gene OsERF922. *PloS one*, *11*(4), e0154027.

Wang, L., Kaya, H. B., Zhang, N., Rai, R., Willmann, M. R., Carpenter, S. C., ... & Bogdanove, A. J. (2021). Spelling changes and fluorescent tagging with prime editing vectors for plants. *Frontiers in Genome Editing*, *3*, 617553.

Wang, X., Tu, M., Wang, D., Liu, J., Li, Y., Li, Z., ... & Wang, X. (2018). CRISPR/Cas9-mediated efficient targeted mutagenesis in grape in the first generation. *Plant biotechnology journal*, *16*(4), 844-855.

Wright, D.C. (1985). Factors affecting isolation of protoplasts from leaves of grape (Vitis vinifera). Journal of Plant Biotechnology Plant Cell Tiss Organ Cult 4, 95-100.

Xu, X. F., Zhu, H. Y., Ren, Y. F., Feng, C., Ye, Z. H., Cai, H. M., ... & Peng, C. Y. (2021). Efficient isolation and purification of tissue-specific protoplasts from tea plants (Camellia sinensis (L.) O. Kuntze). *Plant methods*, *17*, 1-12.

Yang, Y., Wheatley, M., Meakem, V., Galarneau, E., Gutierrez, B., and Zhong, G.Y. (2024). Editing VvDXS1 for the creation of muscat flavour in Vitis vinifera cv. Scarlet Royal. *Plant Biotechnol J*.

Yao, L., Zhang, Y., Liu, C., Liu, Y., Wang, Y., Liang, D., ... & Kelliher, T. (2018). OsMATL mutation induces haploid seed formation in indica rice. *Nature plants*, *4*(8), 530-533.

Yin, K., Gao, C., and Qiu, J.L. (2017). Progress and prospects in plant genome editing. *Nat Plants* 3**,** 17107.

Yoo, S. D., Cho, Y. H., & Sheen, J. (2007). Arabidopsis mesophyll protoplasts: a versatile cell system for transient gene expression analysis. Nature protocols, 2(7), 1565-1572.

Yue, J. J., Yuan, J. L., Wu, F. H., Yuan, Y. H., Cheng, Q. W., Hsu, C. T., & Lin, C. S. (2021). Protoplasts: from isolation to CRISPR/Cas genome editing application. *Frontiers in Genome Editing*, *3*, 717017.

Zhang, F., Wen, Y., & Guo, X. (2014). CRISPR/Cas9 for genome editing: progress, implications and challenges. *Human molecular genetics*, *23*(R1), R40-R46.

Zhang, A., Liu, Y., Wang, F., Li, T., Chen, Z., Kong, D., ... & Luo, L. (2019). Enhanced rice salinity tolerance via CRISPR/Cas9-targeted mutagenesis of the OsRR22 gene. *Molecular breeding*, *39*, 1-10.

Zhang, D., Zhang, Z., Unver, T., and Zhang, B. (2021). CRISPR/Cas: A powerful tool for gene function study and crop improvement. *J Adv Res* 29**,** 207-221.

Zhang, Y., Bai, Y., Wu, G., Zou, S., Chen, Y., Gao, C., & Tang, D. (2017). Simultaneous modification of three homoeologs of Ta EDR 1 by genome editing enhances powdery mildew resistance in wheat. *The Plant Journal*, *91*(4), 714-724.

Zhang, Y., Li, D., Zhang, D., Zhao, X., Cao, X., Dong, L., ... & Wang, D. (2018). Analysis of the functions of Ta GW 2 homoeologs in wheat grain weight and protein content traits. *The Plant Journal*, *94*(5), 857-866.

Zhang, Y., Malzahn, A. A., Sretenovic, S., & Qi, Y. (2019). The emerging and uncultivated potential of CRISPR technology in plant science. *Nature Plants*, *5*(8), 778-794.

Zhao, F. L., Li, Y. J., Hu, Y., Gao, Y. R., Zang, X. W., Ding, Q., ... & Wen, Y. Q. (2016). A highly efficient grapevine mesophyll protoplast system for transient gene expression and the study of disease resistance proteins. *Plant Cell, Tissue and Organ Culture (PCTOC)*, *125*, 43-57.

Zhou, H., He, M., Li, J., Chen, L., Huang, Z., Zheng, S., ... & Zhuang, C. (2016). Development of commercial thermo-sensitive genic male sterile rice accelerates hybrid rice breeding using the CRISPR/Cas9-mediated TMS5 editing system. *Scientific reports*, *6*(1), 37395.

Zhou, J., Peng, Z., Long, J., Sosso, D., Liu, B. O., Eom, J. S., ... & Yang, B. (2015). Gene targeting by the TAL effector PthXo2 reveals cryptic resistance gene for bacterial blight of rice. *The Plant Journal*, *82*(4), 632-643.

Zhuang, Y., Liu, J., Wu, H., Zhu, Q., Yan, Y., Meng, H., ... & Yi, C. (2022). Increasing the efficiency and precision of prime editing with guide RNA pairs. Nature chemical biology, 18(1), 29-37.